University of Stavanger

Faculty of Science and Technology

MASTER THESIS

Study program/ Specialization: Biological Chemistry	Spring semester, 2011 Open access
Author: Yongshun Huang	…… (Author's signature)
Faculty supervisor: Professor Peter Ruoff External supervisor(s):	
Title of thesis: Negative feedback loops leading to nitrate homeostasis and oscillatory nitrate assimilation in plants and fungi.	
Credits (ECTS): 60	
Key words: Nitrate Homeostasis Controller Oscillation *Neurospora crassa*	Pages: …… + enclosure: …… Stavanger,……

University of Stavanger

Department of Mathematics and Natural Science

MASTER THESIS

Negative feedback loops leading to
nitrate homeostasis
and
oscillatory nitrate assimilation
in plants and fungi

Biological Chemistry

Yongshun Huang

Acknowledgements

First and foremost, I want to thank my supervisor Professor Peter Ruoff for favoring me with a lot of instructions and advice. Without his support, it is impossible for me to complete my thesis.
His incredible understanding of research, his rigorous way of thinking as well as his human qualities have benefited me a great deal.

Secondly, I would like to extend my heartfelt gratitude to Professor Cathrine Lillo who kindly provided me a lot of expremental results which were invaluable to the completion of this work.

I also take this chance to thank the PhD fellows Ingunn Westvik Jolma and Xiao-Yu (Eric) Ni for helping me solve some technical problems selflessly.

Finally, I am grateful to to my friends and family, especially my parents for their support and encouragement, It is they who instill in me the understanding of the importance of education and respect for the academic process.

You raise me up, so I can stand on mountains;
You raise me up, to walk on stormy seas;
I am strong, when I am on your shoulder;
You raise me up… To more than I can be

Brendan Graham

Abstract

Nitrate is an important nutrient for plants and fungi. For plants it has been shown that cytosolic nitrate levels are under homeostatic control. Here we describe two networks that can obtain robust, i.e. perturbation independent, homeostatic behavior in cytosolic nitrate concentration. One of the networks, a member in the family of outflow controllers, is based on a negative feedback loop containing a nitrate-induced activation of a controller molecule which removes nitrate. In plants this control structure appears to have at least two representations, one where the controller molecule is nitrate reductase removing nitrate for assimilation, while the other controller molecule takes part in the efflux of nitrate out of the cell. The second homeostatic network, a member in the family of inflow controllers, appears to be associated with the uptake of nitrate into the cell, the translocation of cytosolic nitrate into the vacuole for nitrate storage and the transport of nitrate from the vacuole into the cytosol. Interestingly, this control structure automatically adjusts the flux of nitrate uptake into the cytosol by the extent of how much cytosolic nitrate is removed. After the depletion of environmental nitrate, the vacuolar nitrate is sustained by the remobilization of vacuolar nitrate. In lower eukaryotes which lack nitrate storage in the vacuole and a nitrate efflux system, uptake of nitrate by such a controller depends therefore on the nitrate assimilation rate in the cell. Thus, practically no nitrate uptake should occur in lower eukaryotes when nitrate reductase is not functional, a behavior that was previously observed in fungi. Another interesting aspect is that outflow controller can oscillate and generate limit cycle oscillations in the assimilation of nitrate, thus making a link between circadian oscillations in nitrate assimilation and cytosolic nitrate homeostasis.

Key words: Nitrate; Homeostasis; Controller; Oscillation; *Neurospora crassa*

Contents

1. Introduction

1.1 The homeostasis of cytosolic nitrate concentration

Nitrate is one of the major forms of assimilable nitrogen in the biosphere. Both plants and fungi can utilize nitrate. Apart from being an important nutrient, nitrate also serves as an important signal for growth as plants or fungi respond to nitrate by altering their metabolism and by inducing genes in the nitrate assimilation pathway. These genes encode transporters that take up nitrate from the environment and the enzymes nitrate reductase (*NR*) and nitrite reductase (*NiR*), which convert nitrate into ammonium within the cell (1-7).

By using a combination of pH and nitrate-ion selective microelectrodes (8), Miller and his colleagues have established that in plants cytosolic nitrate concentration is in a clear homeostatic control both under high external nitrate concentration (9) and during the remobilization of nitrate from the vacuole into the cytosol when no external nitrate is available (10-12).

When considering the regulation of cytosolic nitrate in plant cells five major processes are found to be involved (Fig. 1.1). One is the uptake of nitrate by plant roots. It has been found that there are at least three, kinetically distinct, nitrate transport systems for plant roots. Constitutive high affinity transport systems (CHATS) are characterized by low values of both K_m and V_{max}. High affinity transporters (IHATS) with higher K_m and V_{max} values are induced within hours to days of exposure to nitrate. Finally, constitutive low affinity transports (LATS), which can significantly contribute to nitrate uptake at concentrations above 250 μM, fail to saturate at nitrate concentrations as high as 50 mM (4).

The second process is by the nitrate-inducible efflux system, which removes cytosolic nitrate out of the cell (3, 13). An efflux transporter, *NAXT1*, was recently identified belonging to the *NRT1/PTR* family of transporters (14). The efflux system has a much slower turnover rate than the uptake system (13).

The third process consists of two parts, one contributing to cytosolic nitrate homeostasis by storing nitrate in the vacuole when there is a high influx of nitrate into the cell/cytosol (9) and the other by remobilizing nitrate from the vacuole into the cytoplasm when no or no sufficient extracellular nitrate is available (10–12). Early evidence suggested a nitrate/proton transporter in the tonoplast (15, 16). Recent findings show that these nitrate transporters belong to the family of *CLC* transport proteins (7, 17–19) and are connected to the activity of vacuolar H^+-ATPase. H^+-ATPases are irreversible, rotational pumps (20) transporting protons into the vacuole maintaining a proton gradient between cytosol and vacuole that enables to transport nitrate from the cytosol into the vacuole against its concentration gradient (21).

The fourth process participating to cytosolic nitrate homeostasis is nitrate assimilation, where nitrate reductase (*NR*) catalyzes the first step in which nitrate is converted to nitrite. The nitrite is taken up by the chloroplast and further reduced to ammonium by nitrite reductase and subsequently incorporated into the amino acids through the action of glutamine synthetase and glutamate synthase. (2, 22, 23)

Finally, in the fifth process nitrate is transported either from the vacuole or from the cytosol into the symplasm, where it is further transported to the xylem (1, 24).

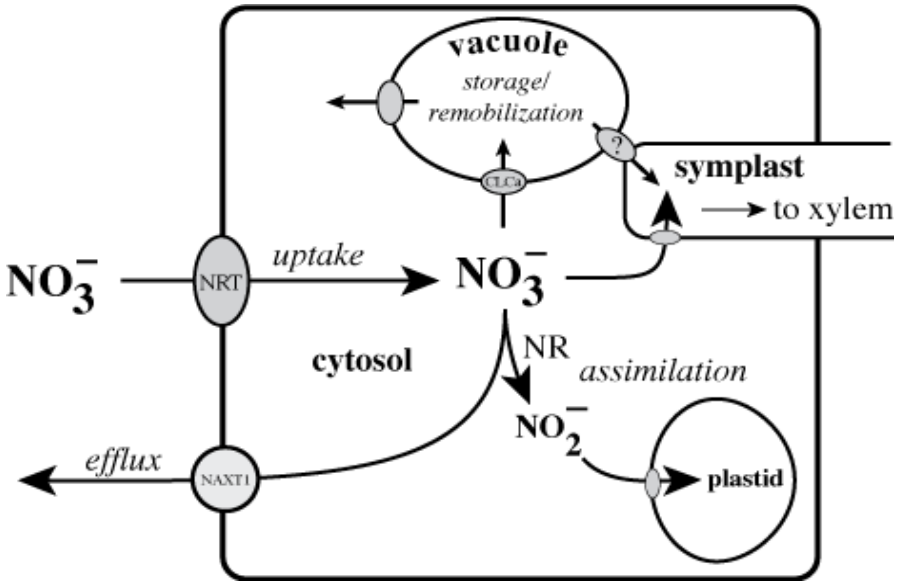

Figure 1.1: Schematic overview on nitrate transport and mechanisms maintaining nitrate homeostasis in a root epidermal cell (1, 24).

As for fungi, their nitrate regulation appears to be less complex than plants. Fungi and other lower eukaryotes appear to lack a nitrate store in the vacuole (25) and no nitrate efflux mechanism has been reported.

1.2 Circadian Oscillations in Expression and Activity of Nitrate Reductase

To avoid the accumulation of nitrite and other side-reaction products, higher plants have developed a complex and redundant control of *NR* activity at multiple levels. In response to the diurnal changes in photosynthesis, *NR* expression and activity vary between day and night (26, 27). During a diurnal cycle, *NR* mRNA level usually peaks at the end of the night or in the early part of the day, then declines and starts to increase towards the end of the night (28, 29). *NR* activity generally rises to a maximum during the first part of the day and declines during the latter part of the day and night. For a number of plant species, when placed in constant light conditions and, thus, deprived of external time cues, circadian oscillations in *NR* expression and activity persist with periods of approximately 24 hours (30). This indicates that these rhythms are endogenous. The pathway by which these circadian rhythms are generated remains to be elucidated. It is widely assumed that a central circadian clock provides metabolic readiness in advance to changing conditions of day and night. An alternative interpretation is that as the result of an autonomous negative feedback loop in which probably glutamine, a product in the reaction chain initialized by *NR*, inhibits transcription of the *NR* gene (26). Higher plant and *Neuropora NR*s show similar features, including negative feedback inhibition by glutamine (31).It has been found when nitrate ion is the only nitrogen source, the nitrate assimilation pathway also shows oscillations in *NR* activity with a period length of approximately 24 hours. These oscillations can be observed both in darkness and under continuous light conditions (32, 33).

1.3 Nitrate metabolism repression for fungi (focusing on *Neurospora crassa*)

The study of nitrate regulation in fungi has led to the identification of regulatory genes that are responsible for both nitrate induction and ammonia repression. The genes mediating the nitrate induction (*NIRA* of *Aspergillus* and *NIT-4* of *Neurospora*) encode positive regulators with zinc finger DNA binding domain similar to *GAL4* from yeast (34-36). The genes mediating ammonia repression (*AREA* of *Aspergillus* and *NIT-2* of *Neurospora*) also encode positive regulators with zinc finger DNA binding motifs that are distinct from *NIRA* and *NIT-4* (37-39).

In *Neurospora crassa*, several lines of evidence indicate that the *NMR* protein functions as a negative regulator by binding to the *NIT2* protein and somehow modulating the *trans*-activation function of the latter, possibly by interfering with DNA binding. Direct interactions between the *NMR* and *NIT2* proteins have been demonstrated by two different experimental approaches and by genetic analysis. Use of the yeast two-hybrid system showed that a specific interaction occurs between *NIT2* and *NMR*. Two distinct short regions of the *NIT2* protein, both predicted to exist as α-helices, appear to be recognized by the *NMR* protein. In vitro mobility shift assays suggested that *NMR* may interfere with *NIT2* DNA binding (40, 41). As yet, no transcriptional factor which functions as *NMR* for regulating nitrate reductase expression has been identified in higher plants.

2. Computational methods

The rate equations were solved using the Fortran subroutine LSODE with ABSOFT's Pro Fortran compiler ver. 10.0.6 (absoft.com). Plots were generated by GNUPLOT. A combined shell and Perl script allowed the automated generation of the numerical and graphical output. GNUPLOT (www.gnuplot.info) and Perl (www.perl.org) are free software.

3. Theoretical background

3.1 The concept of (robust) homeostasis

Many physiologically important compounds are under tight homeostatic regulation, where internal concentrations are adapted at certain levels, despite environmental disturbances. Two concepts have developed to understand homeostasis: one is related to the intrinsic properties of the network showing that the adaptation response is independent of (most but not all) rate constant values (referred to here as robust (42, 43) adaptation/homeostasis), whereas the other concept looks at the homeostasis due to a fine-tuning between rate constants. Perfect adaptation describes an organism's response to an external stepwise perturbation by regulating some of its variables/components precisely to their original preperturbation values. In this respect, perfect adaptation and homeostasis are closely related and we look at homeostasis as a perfectly adapted process.

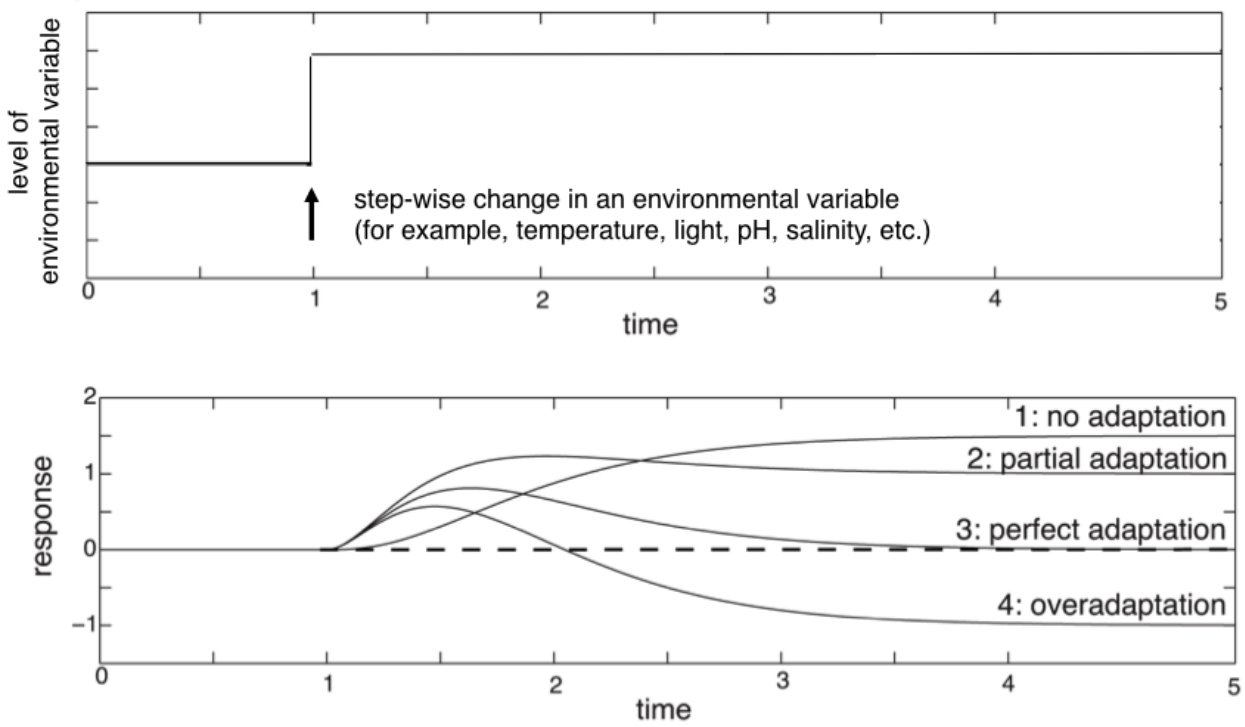

Figure 3.1: The relationship between homeostasis and perfect adaptation. "Perfect adaptation" describes an organism's response to an external stepwise perturbation by regulating some of its variables/components precisely to their original preperturbation values.

Robust perfect adaptation/homeostasis of a perturbed system can be related to the concept of integral control or intergral feedback (44, 45). In the following we will show how this concept can be applied to biochemical systems and how robust homeostasis can emerge from a set of homeostatic network motifs.

The following is a very simple scheme of a feedback system:

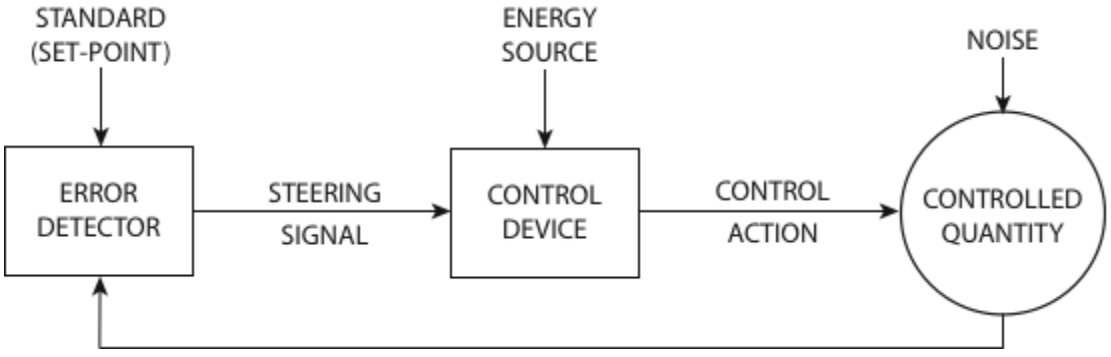

Figure 3.2: Homeostatic Mechanisms with Control Engineering (Cybernetic) Approach. It consists of two "black boxes" (meaning objects of unspecified nature which perform certain stated functions) and a circle indicating an object or property; they are connected by arrows. We have some controlled quantity the level of which depends on some control action and on some unspecified perturbations lumped together under the name "noise".

Figure 3.3 shows a basic feedback control scheme how robust homeostasis in a controlled variable (CV) can be obtained by means of integral control. The controlled variable is compared with the homeostatic set point and the error between the controlled variable and the set point is determined. From this error a signal from the integral controller is generated which, due to a controlling device, leads to an adjustment in the output. It is the presence of the integral controller which assures that robust homeostasis can be obtained (46, 47).

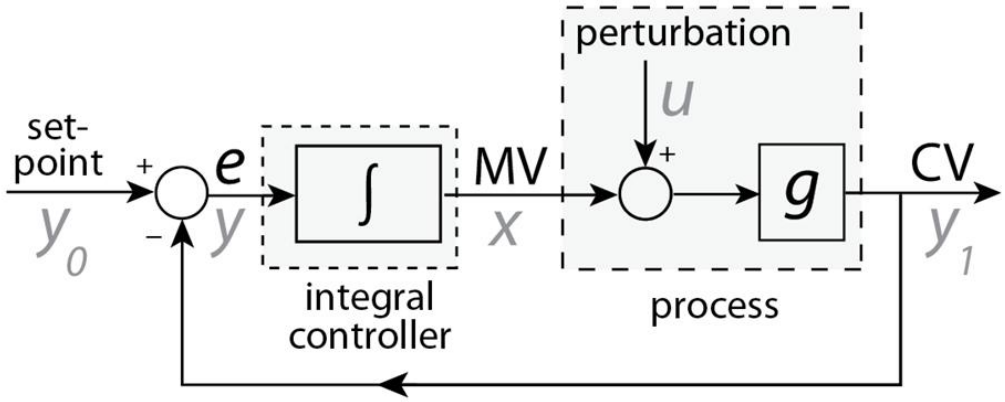

Figure 3.3: Scheme of integral control/feedback of a perturbed system, where the system output is perfectly adapted to the set point and due to the integral controller the error e is robustly controlled to zero. MV and CV are the manipulated and controlled variables, respectively. Symbols in gray denote the notation for integral feedback by Yi et al. (46).

In Figure 3.4(a) we show a simplified version of a feedback loop in which *NR* is induced by nitrate while *NR* removes nitrate as the first step in nitrate assimilation. This feedback motif can lead to robust homeostatic behavior (46, 47). The controller mechanism is based on the removal of excess nitrate by *NR*. We have termed this type of controller for outflow controller (47) because the controller adjusts high inflow rates in the homeostatic controlled variable by removing a necessary amount to maintain homeostasis.

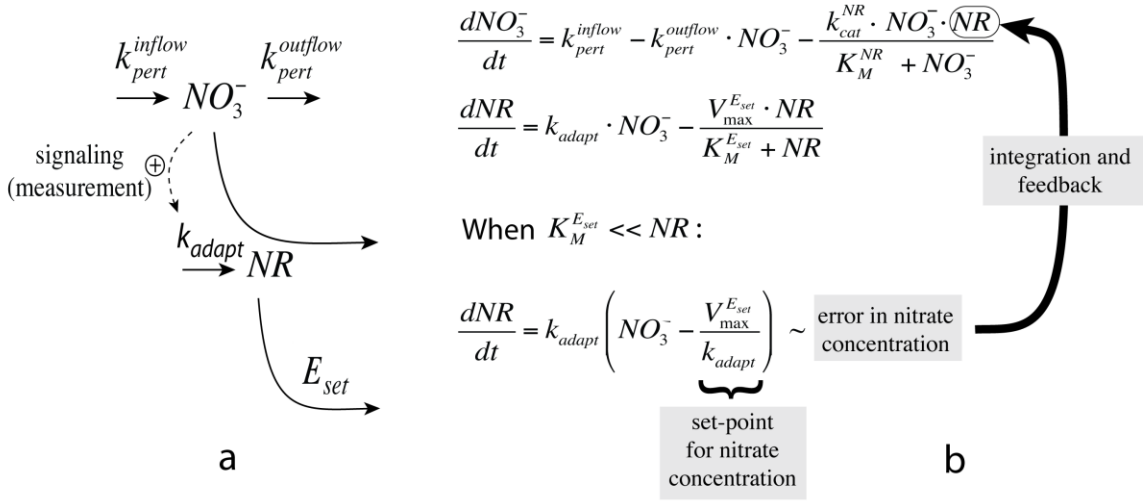

Figure 3.4: (a) Homeostasis control motif whose differential equations are shown in (b) is based on the removal of excess nitrate by *NR*. k_{pert}^{inflow} and $k_{pert}^{outflow}$ are rate constants for perturbation. *NR* and NO_3^- are the

manipulated and controlled variables, respectively. To get robust adaptation in NO_3^- independent of k_{pert}^{inflow} and $k_{pert}^{outflow}$, *NR* is removed through a zero-order flux $V_{max}^{E_{set}}$ by E_{set}. (b) The difference between the actual output NO_3^- and its set point $\frac{V_{max}^{E_{set}}}{k_{adapt}}$ represents the error. Integral control arises through the feedback loop in which the time integral of this error is fed back into the system. As a result, $NO_3^- - \frac{V_{max}^{E_{set}}}{k_{adapt}} \rightarrow 0$ as $t \rightarrow \infty$. When it happens, NO_3^- reaches to a steady state that is determined by the set point.

3.2 A complete set of two-component homeostatic netwroks

We consider two molecular components, *A* and E_{adapt}, which mutually affect each other's synthesis or degradation by either activating them (indicated by a dashed arrow with a positive sign) or by inhibiting them (indicated by a dashed negative inhibition sign). E_{adapt} represents the controller which is responsible for regulating the concentration of *A* whose homeostasis should be kept in a certain level despite of environmental disturbance. The type of feedback (i.e., positive or negative) for a particular motif can be determined as illustrated in Figure 3.5 (48).

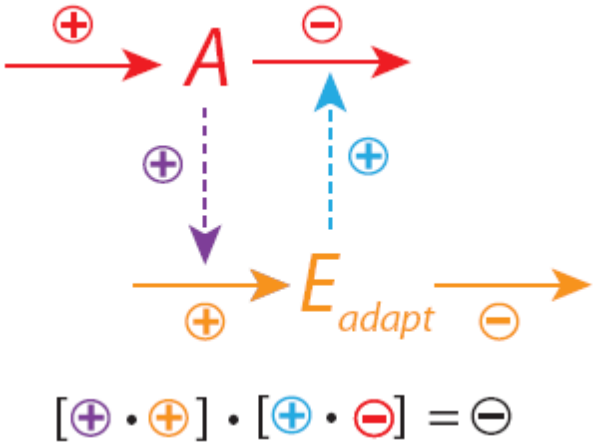

Figure 3.5: Illustrating how to determine the type of feedback (see main text below for details)

Starting from component *A* and moving along the loop while multiplying the plus/minus signs of the activation/inhibition steps with the positive/negative signs of the synthesis /degradation reaction of the other component leads to the sign of the feedback loop, which in case of Figure 3.5 is negative. As we only consider single interactions from *A* to E_{adapt} and from E_{adapt} to *A*, sixteen possible network motifs can be created totally, half of them containing a negative feedback (Figure 3.6) and half of them containing a positive feedback (Figure 3.7). Only the motifs I-VIII with a negative feedback loop are considered here (48).

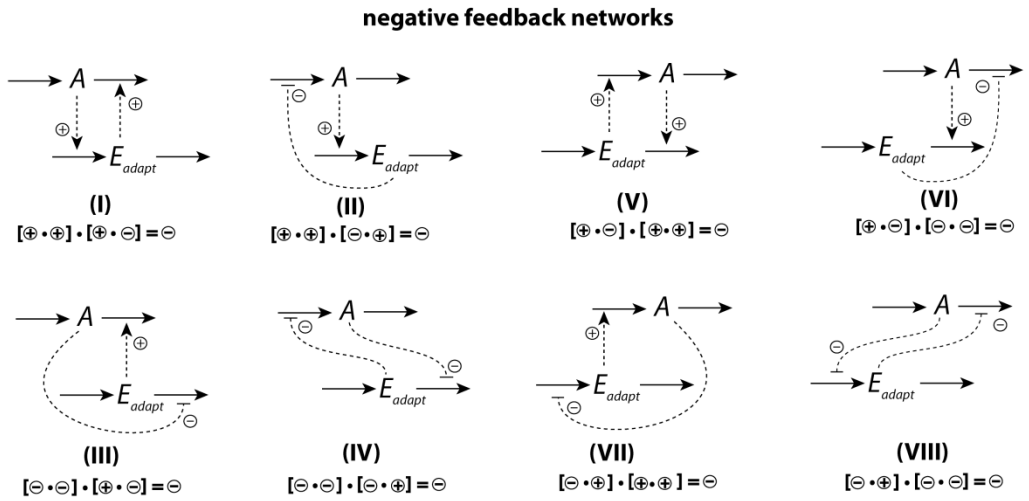

Figure 3.6: Network motifs with negative feedback

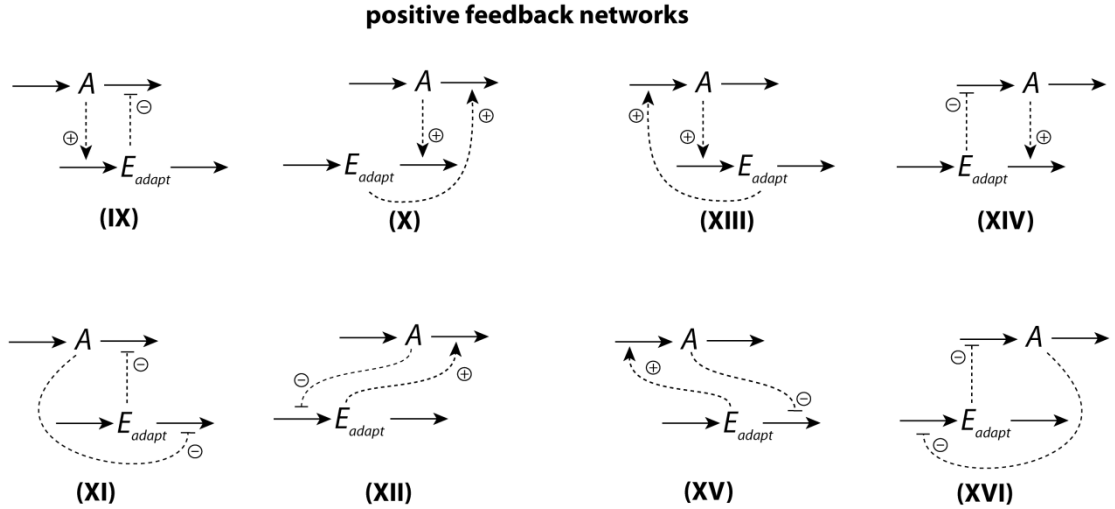

Figure 3.7: Network motifs with positive feedback

The motifs in Figure 3.8 (below) fall into two distinct functional classes, which we named outflow and inflow controllers. In terms of their operation, outflow controllers, compensate for inflow perturbations by removing excess of *A*, while inflow controllers compensate perturbations in the outflow of *A* by adding more *A*.

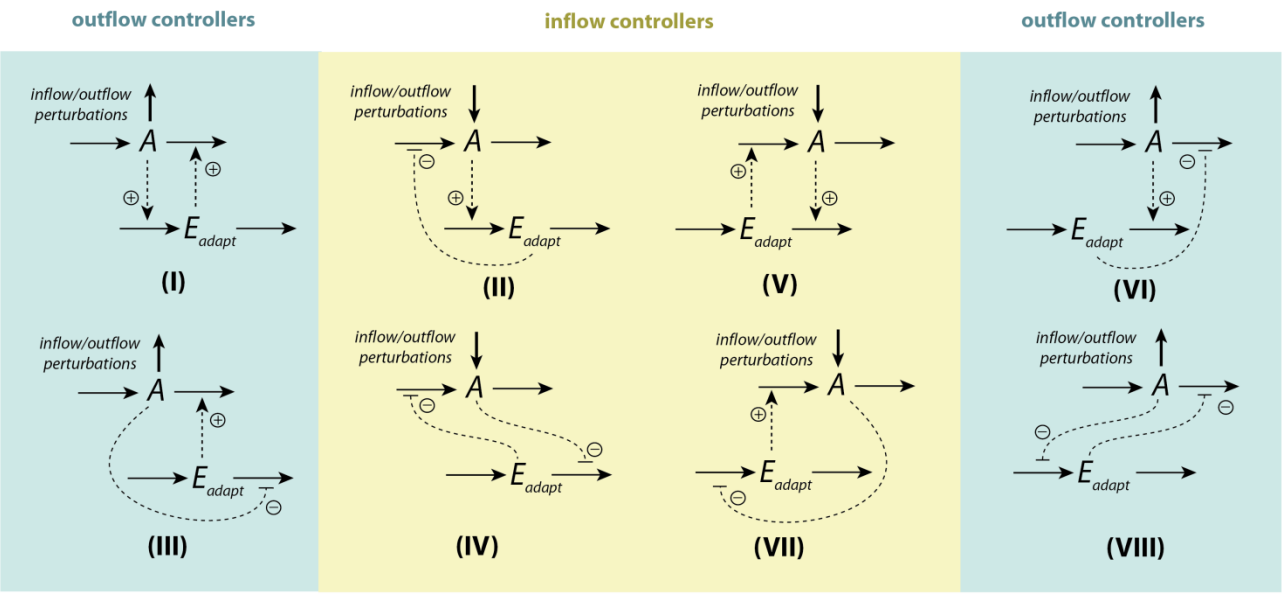

Figure 3.8: A complete set of negative feedback networks from Figure 3.6 which falls into two distinct groups termed as inflow and outflow controller feecback loops.

3.3 The character of inflow/outflow network

The network motifs in Figure 3.8 can be considered as "homeostatic core modules" occurring in various physiological situations. Next I will illustrate the character of outflow network I and inflow network V, respectively.

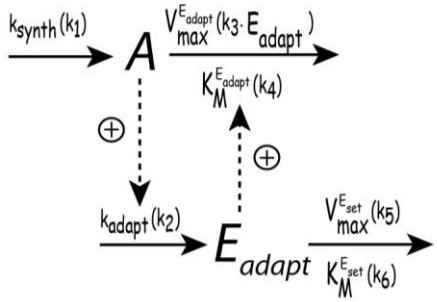

Figure 3.9: The outflow network I with rate constants where E_{set} removes E_{adapt} under zero-order condition.

The differential equation for network I (Figure 3.9) is as follows:

$$\frac{d[A]}{dt} = k_{synth} - \frac{k_{cat}^{E_{adapt}} \cdot [E_{adapt}] \cdot [A]}{K_M^{E_{adapt}} + [A]}$$

$$\frac{d[E_{adapt}]}{dt} = k_{adapt} \cdot [A] - \frac{V_{\max}^{E_{set}} \cdot [E_{adapt}]}{K_M^{E_{set}} + [E_{adapt}]}$$

When $K_M^{E_{set}} << [E_{adapt}]$,

$$\frac{d[E_{adapt}]}{dt} = k_{adapt}([A] - \frac{V_{max}^{E_{set}}}{k_{adapt}})$$

With a rising inflow, E_{adapt} will automatically increase its concentration to remove more A so as to avoid the rise of its level.

Table 3.1 The variation of [A] and [E_{adapt}] when inflow increases ($K_M^{E_{set}} = 1\times 10^{-6}$)

Inflow rate, a.u.	[A], a.u.	[E_{adapt}], a.u.
1.0000×10^{-4}	9.9669×10^{-1}	3.0067×10^{-4}
1.0000×10^{-3}	9.9967×10^{-1}	3.0007×10^{-3}
1.0000×10^{-2}	9.9997×10^{-1}	3.0001×10^{-2}
1.0000×10^{-1}	1.0000×10^{0}	3.0000×10^{-1}
1.0000×10^{0}	1.0000×10^{0}	3.0000×10^{0}
$1.0000\times 10^{+1}$	1.0000×10^{0}	$3.0000\times 10^{+1}$
$1.0000\times 10^{+2}$	1.0000×10^{0}	$3.0000\times 10^{+2}$
$1.0000\times 10^{+3}$	1.0000×10^{0}	$3.0000\times 10^{+3}$

(In this thesis, all the concentrations and timescales are in arbitrary units)

In Table 3.1, both [A] and [E_{adapt}] are given when they reach the steady state.

Plotting [A] and [E_{adapt}] against inflow rate:

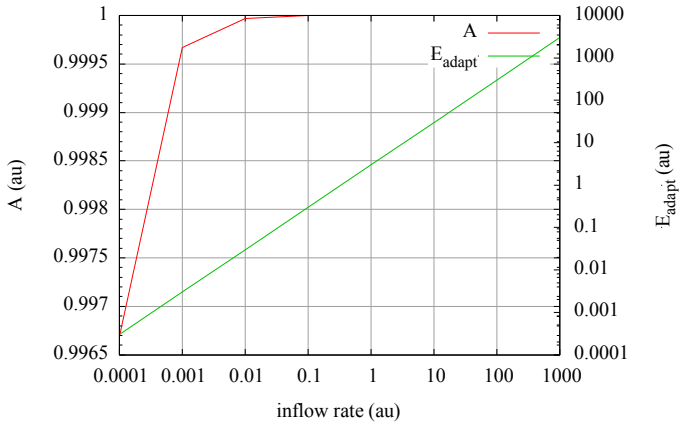

Figure 3.10: The variation of [A] and [E_{adapt}] with the increase of inflow rate ($K_M^{E_{set}} = 1\times 10^{-6}$).

The concentration of E_{adapt} increases by the same order of magnitude with inflow rate, and the concentration of A is maintained in the same level. This type of controller network is suitable for high inflow condition. When it comes to low inflow, a slight decrease in the concentration of A is observed.

A relatively high $K_M^{E_{set}}$ weakens the ability for the outflow controller to keep the homeostasis especially when inflow rate is low.

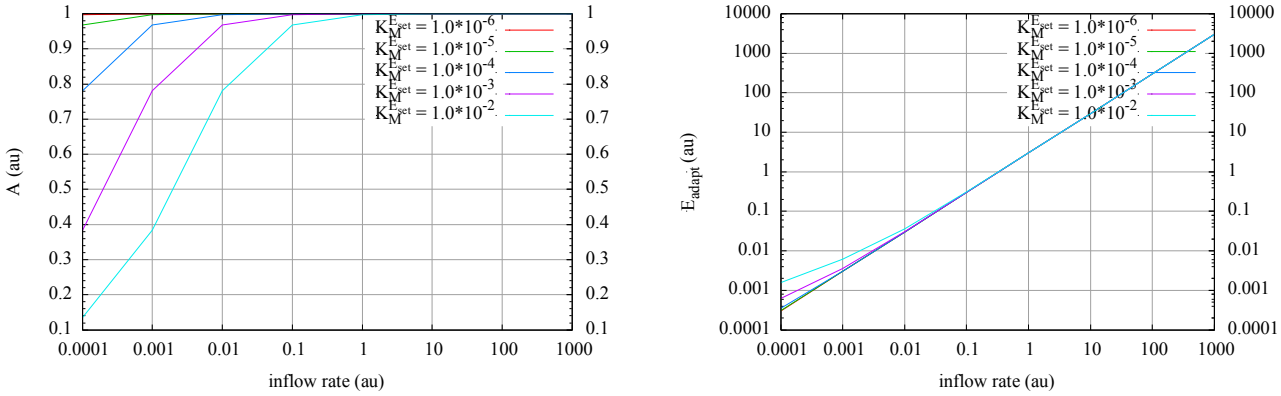

(a) (b)

Figure 3.11: Graph a gives the variation of [*A*] with divergent $K_M^{E_{set}}$ values when inflow rate increases while Graph b is created under all the same condition with Graph a but it shows the variation of [E_{adapt}]. Both [*A*] and [E_{adapt}] are given when they reach the steady state. With the same inflow rate, the rise of $K_M^{E_{set}}$ corresponds to a lower [*A*]. Distinct from [*A*], [E_{adapt}] increases with a higher $K_M^{E_{set}}$. With the increase of inflow rate, its change is much more violent than [*A*].With the growth of inflow rate, the differences of [*A*] and [E_{adapt}] under varied $K_M^{E_{set}}$ become little and little.

From $\frac{d[E_{adapt}]}{dt}=0$, we have

$$[A]=\frac{\frac{V_{\max}^{E_{set}}\cdot[E_{adapt}]}{K_M^{E_{set}}+[E_{adapt}]}}{k_{adapt}}=\frac{V_{\max}^{E_{set}}}{k_{adapt}}\cdot\frac{[E_{adapt}]}{K_M^{E_{set}}+[E_{adapt}]}$$

We assume $K_M^{E_{set}} << [E_{adapt}]$ and $[A]\approx\frac{V_{\max}^{E_{set}}}{k_{adapt}}$, which is called defining concentration (In Figure 3.9, $\frac{V_{\max}^{E_{set}}}{k_{adapt}}$=1). Due to the fact that $\frac{[E_{adapt}]}{K_M^{E_{set}}+[E_{adapt}]}<1$, [*A*] must be lower than $\frac{V_{\max}^{E_{set}}}{k_{adapt}}$. The smaller $K_M^{E_{set}}$ is, the closer [*A*] to its defining concentration.

A high inflow rate corresponds to a high [E_{adapt}] such that the requirement $K_M^{E_{set}} << [E_{adapt}]$ is met, which is the reason why in Figure 3.11(a) the inflow is higher the concentration of *A* is closer to 1.

From $\frac{d[A]}{dt}=0$, we have:

$$\frac{k_{cat}^{E_{adapt}}\cdot[E_{adapt}]\cdot[A]}{K_M^{E_{adapt}}+[A]}=\frac{k_{cat}^{E_{adapt}}\cdot[E_{adapt}]}{\frac{K_M^{E_{adapt}}}{[A]}+1}=k_{synth}$$

On the condition that k_{synth} is constant, the increase of [A] inevitably leads to the fall of $\frac{K_M^{E_{adapt}}}{[A]}+1$, so that [$E_{adapt}$] also decreases, vice versa, which is the reason why in Figure 3.11 [A] and [E_{adapt}] change in the opposite direction with the increase or decrease of $K_M^{E_{set}}$.

As to the inflow controller motif, it is used to keep the homeostasis at the expense of depleting a reservoir.

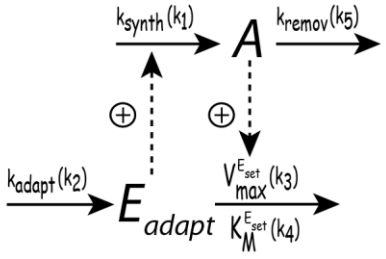

Figure 3.12: The inflow network V with rate constants where E_{set} removes E_{adapt} under zero-order condition.

The differential equation for network V (Figure 3.12) is as follows:

$$\frac{d[A]}{dt} = k_{synth} \cdot [E_{adapt}] - k_{remov} \cdot [A]$$

$$\frac{d[E_{adapt}]}{dt} = k_{adapt} - \frac{V_{max}^{E_{set}} \cdot [A] \cdot [E_{adapt}]}{K_M^{E_{set}} + [E_{adapt}]}$$

When $K_M^{E_{set}} << [E_{adapt}]$,

$$\frac{d[E_{adapt}]}{dt} = -V_{max}^{E_{set}} ([A] - \frac{k_{adapt}}{V_{max}^{E_{set}}})$$

When the depletion rate in A grows, the controller E_{adapt} has to increase its concentration in order to transport more to counterbalance the loss.

Table 3.2. The variation of [A] and [E_{adapt}] when removal rate increases ($K_M^{E_{set}} = 1 \times 10^{-6}$)

Removal rate	[A]	[E_{adapt}]
1.0000×10^{-4}	1.00990	1.00990×10^{-4}
1.0000×10^{-3}	1.00100	1.00100×10^{-3}
1.0000×10^{-2}	1.00010	1.00010×10^{-2}
1.0000×10^{-1}	1.00001	1.00001×10^{-1}
1.0000×10^{0}	1.00000	1.00000×10^{0}
$1.0000\times10^{+1}$	1.00000	$1.00000\times10^{+1}$
$1.0000\times10^{+2}$	1.00000	$1.00000\times10^{+2}$
$1.0000\times10^{+3}$	1.00000	$1.00000\times10^{+3}$

In Table 3.2, both [A] and [E_{adapt}] are given when they reach the steady state.

Plotting [A] and [E_{adapt}] against removal rate:

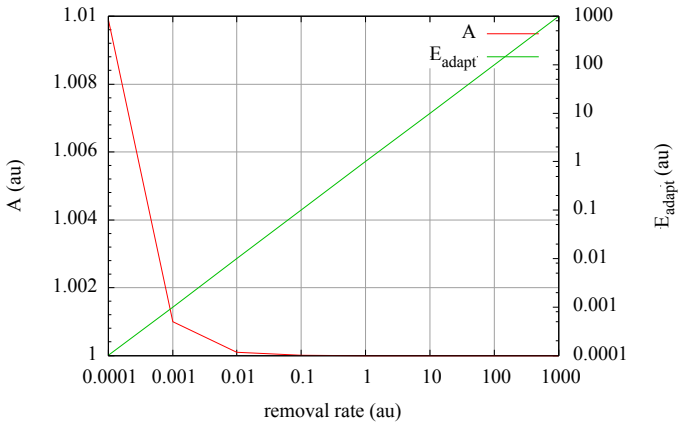

Figure 3.13: The variation of [A] and [E_{adapt}] with the rise of demand in A ($K_M^{E_{set}}$ =1×10^{-6}).

Such a kind of inflow controller functions well on the condition that there is a relatively high removal of A. However, it appears that this controller is not good at keeping the homeostasis when there is little demand of A.

With the rise of $K_M^{E_{set}}$, both [A] and [E_{adapt}] grow, which is more obvious when removal rate is relatively low.

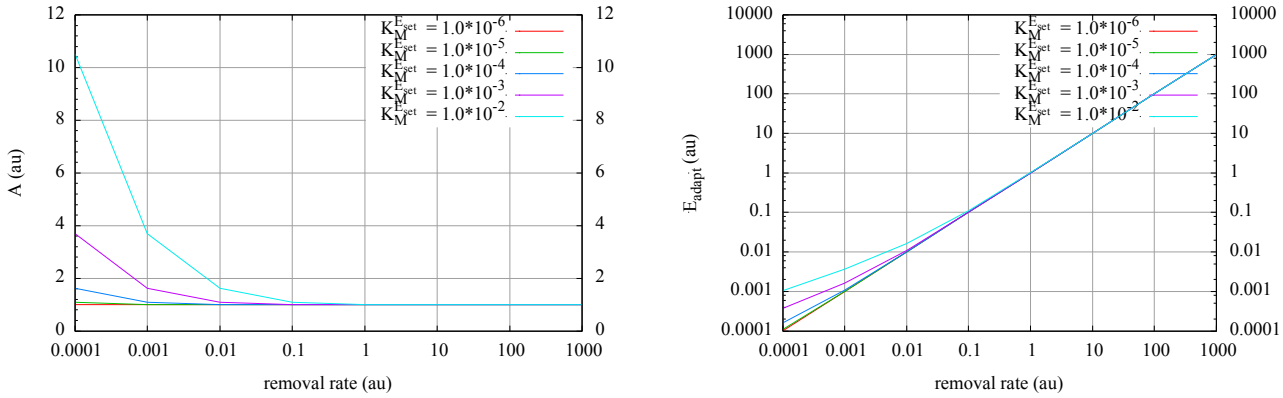

(a) (b)

Figure 3.14: Graph a and b are generated under all the same condition and Graph a demonstrates the variation of [A] with divergent $K_M^{E_{set}}$ values when removal rate increases while Graph b is for the change of [E_{adapt}]. Both [A] and [E_{adapt}] are given when they reach the steady state. Compared to [A], [E_{adapt}] is much more sensitive to the growth of removal rate. Among different $K_M^{E_{set}}$ values, the gap of both [A] and [E_{adapt}] becomes smaller and smaller when it comes to high removal rate.

From $\frac{d[E_{adapt}]}{dt} = 0$

$$[A] = \frac{k_{adapt}}{\frac{V_{\max}^{E_{set}} \cdot [E_{adapt}]}{K_M^{E_{set}} + [E_{adapt}]}} = \frac{k_{adapt}}{V_{\max}^{E_{set}}} \cdot \frac{K_M^{E_{set}} + [E_{adapt}]}{[E_{adapt}]}$$

Assuming $K_M^{E_{set}} << [E_{adapt}]$, $[A] \approx \frac{k_{adapt}}{V_{\max}^{E_{set}}}$, which is called defining concentration (In Figure 3.12, $\frac{k_{adapt}}{V_{\max}^{E_{set}}} = 1$). No matter how low $K_M^{E_{set}}$ is, $\frac{K_M^{E_{set}} + [E_{adapt}]}{[E_{adapt}]} > 1$ always stands, so $[A] > \frac{k_{adapt}}{V_{\max}^{E_{set}}}$.

$[E_{adapt}]$ increases with the rise of demand in *A*, and a high $[E_{adapt}]$ satisfies the requirement $K_M^{E_{set}} << [E_{adapt}]$ better, which is the reason that under a higher removal rate, it is easy for [*A*] to reach its defining concentration.

Dealing with the same $[E_{adapt}]$, the lower $K_M^{E_{set}}$, the closer $\frac{K_M^{E_{set}} + [E_{adapt}]}{[E_{adapt}]}$ to 1, which gives the phenomenon shown in Figure 3.14(a) that under the same removal rate, [*A*] has a closer value to defining concentration if $K_M^{E_{set}}$ is low.

From $\frac{d[A]}{dt} = 0$, we have the relationship:

$$k_{synth} \cdot [E_{adapt}] = k_{remov} \cdot [A]$$

With the same k_{synth} and k_{remov}, [*A*] and $[E_{adapt}]$ will always change in the same direction, as shown in Figure 3.14 that both of them increase with the rise of $K_M^{E_{set}}$.

4. Results and Discussion

4.1 The modeling of fungal nitrate transport and assimilation

In the model, we express nitrogen metabolite repression assuming that the research object is *Neurospora crassa*. Two distinct protein-protein interactions between the *NIT2* and *NMR* regulatory proteins are required to establish nitrogen metabolite repression in *Neurospora crass*. *NIT2* is a member of the *GATA* family of regulatory proteins. It acts to turn on the expression of *nit-3*, which encodes *NR*, as well as many other related structural genes under nitrogen-limited conditions (40, 41). A pathway-specific factor, *NIT4*, is also required for any expression of *nit-3* (34). *NMR* interacts in protein-protein binding with two short regions of the *NIT2* protein. This interaction plays a significant regulatory function in nitrogen repression in *Neurospora crassa*. We try to show the nitrogen metabolite repression of *Neurospora crassa* based on the hypothesis that after binding with *NMR*, *NIT24* will lose its ability to activate the expression of *nit-3*.

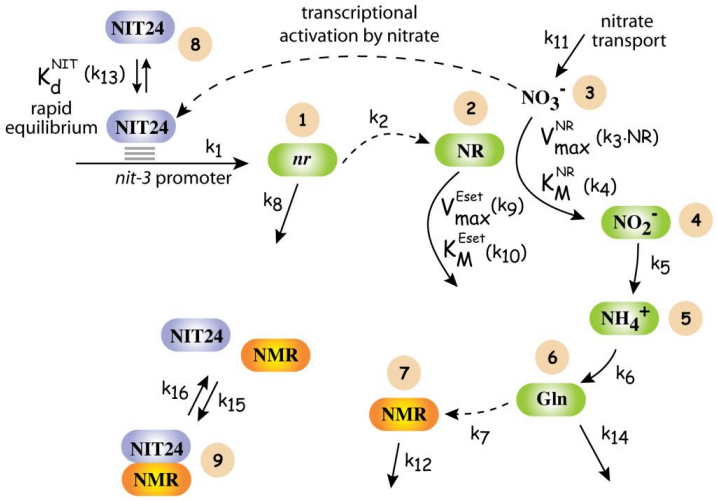

Figure 4.1: *Neurospora crassa*'s nitrate assimilation pathway. In this scheme we only focus on the reduction of nitrate to nitrite catalyzed by *NR* and for the sake of simplicity a simple first-order kinetic is used to express the process of nitrite conversion to ammonium and further incorporation into glutamine. Solid arrows represent input or output flows, and dashed arrows represent induction. Here we use *NIT24* to stand for the complex of *NIT2* and *NIT4* and their synergy is not discussed. The annotation *nr* refers to *nr*-mRNA and *NR* refers to the enzyme of nitrate reductase. The combination of *NTI24* and *nit-3* promoter is assumed to be a rapid equilibrium process while the formation and dissociation of the complex *NIT24*· *NMR* are offered a rate constant individually.

4.1.1 The determination of nitrate concentration by *NR* feedback loop

As I mentioned above, the reduction of cytosolic nitrate by *NR* is a feedback loop based on an outflow controller. The nitrate steady-state concentration of this loop is determined by the removal step of *NR*.

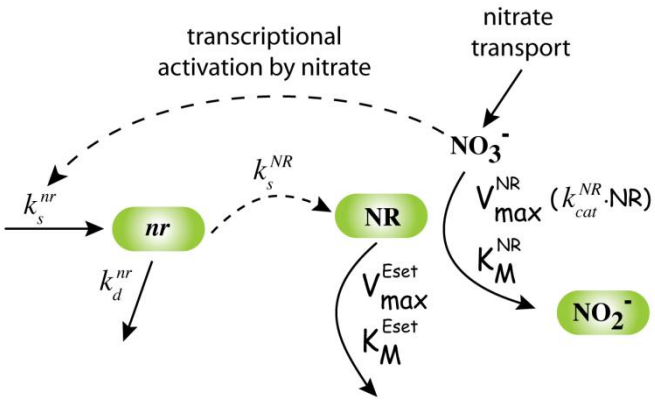

Figure 4.2: Scheme of *NR* removal step by E_{set} in which case Michaelis-Menten kinetics is not expanded.

In Figure 4.2, a single fundamental equation of enzyme kinetics expression $\frac{V_{\max} \cdot [S]}{K_M + [S]}$ is used to stand for the removal of *NR*.

$$\frac{d[nr]}{dt} = k_s^{nr} \cdot [NO_3^-] - k_d^{nr} \cdot [nr] \tag{4.1}$$

$$\frac{d[NR]}{dt} = k_s^{NR} \cdot [nr] - \frac{V_{\max}^{E_{set}} \cdot [NR]}{K_M^{E_{set}} + [NR]} \tag{4.2}$$

when $K_M^{E_{set}} << NR$:

$$[NO_3^-] = \frac{k_d^{nr} \cdot V_{max}^{E_{set}}}{k_s^{nr} \cdot k_s^{NR}} \tag{4.3}$$

When $K_M^{E_{set}} << [NR]$, $\frac{V_{\max}^{E_{set}} \cdot [NR]}{K_M^{E_{set}} + [NR]} \approx V_{\max}^{E_{set}}$. This zero-order flux can cause negative values of *NR*, as will be shown in Figure 4.5. The introduction of a fully expanded Michaelis-Menten kinetics can solve this problem.

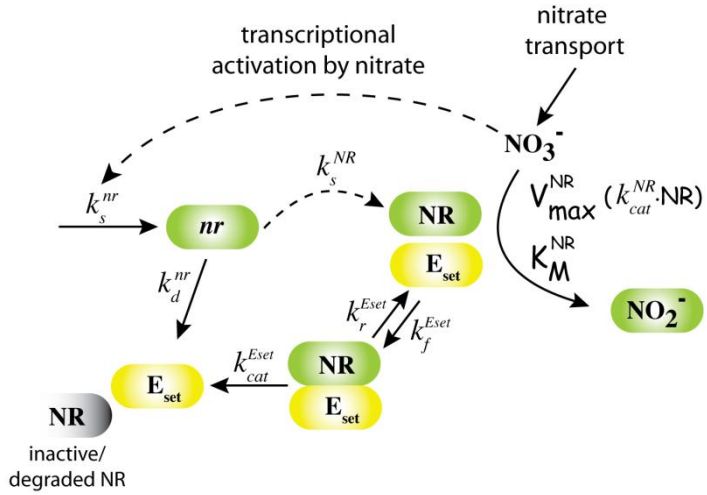

Figure 4.3: Scheme of *NR* removal step by E_{set} in which case Michaelis-Menten kinetics is fully expanded.

In Figure 4.3, E_{set} is treated as a separated variable, and its total amount contains two types of forms: free from (E_{set}) and bound form ($NR{\cdot}E_{set}$).

$$\frac{d[nr]}{dt} = k_s^{nr} \cdot [NO_3^-] - k_d^{nr} \cdot [nr] \tag{4.4}$$

$$\frac{d[NR]}{dt} = k_s^{NR} \cdot [nr] - k_f^{E_{set}} \cdot [NR] \cdot [E_{set}] + k_r^{E_{set}} \cdot [NR \cdot E_{set}] \tag{4.5}$$

From these two equations the expression of $[NO_3^-]$ is determined:

$$[NO_3^-] = \frac{k_d^{nr} \cdot (k_f^{E_{set}} \cdot [NR] \cdot [E_{set}] - k_r^{E_{set}} \cdot [NR \cdot E_{set}])}{k_s^{nr} \cdot k_s^{NR}} \tag{4.6}$$

Expansion of Michaelis-Menten kinetics avoids the negative value of [NR], but it causes the difficulty to calculate a definite value of $[NO_3^-]$. Some attempts have been made to reduce the expression of $[NO_3^-]$.

According to the differential equations of $[E_{set}]$ and $[NR{\cdot}E_{set}]$:

$$\frac{d[E_{set}]}{dt} = (k_r^{E_{set}} + k_{cat}^{E_{set}}) \cdot [NR \cdot E_{set}] - k_f^{E_{set}} \cdot [NR] \cdot [E_{set}] \tag{4.7}$$

$$\frac{d[NR \cdot E_{set}]}{dt} = k_f^{E_{set}} \cdot [NR] \cdot [E_{set}] - (k_r^{E_{set}} + k_{cat}^{E_{set}}) \cdot [NR \cdot E_{set}] \tag{4.8}$$

From $\frac{d[E_{set}]}{dt} = 0$ or $\frac{d[NR \cdot E_{set}]}{dt} = 0$ we can deduce this relationship:

$$k_f^{E_{set}} \cdot [NR] \cdot [E_{set}] - k_r^{E_{set}} \cdot [NR \cdot E_{set}] = k_{cat}^{E_{set}} \cdot [NR \cdot E_{set}] \tag{4.9}$$

Substituting Equation 4.9 to 4.6 gives:

$$[NO_3^-] = \frac{k_d^{nr} \cdot k_{cat}^{E_{set}} \cdot [NR \cdot E_{set}]}{k_s^{nr} \cdot k_s^{NR}} \tag{4.10}$$

In principle, when all the molecules E_{set} are complexed with NR as ($NR{\cdot}E_{set}$), the initial rate of NR removal must be at its maximum value, so that

$$V_{max}^{E_{set}} = k_{cat}^{E_{set}} \cdot [E_{set}]_{tot} = k_{cat}^{E_{set}} \cdot ([E_{set}] + [NR \cdot E_{set}]) \tag{4.11}$$

Substituting Equation 4.11 to 4.3 gives:

$$[NO_3^-] = \frac{k_d^{nr} \cdot k_{cat}^{E_{set}} \cdot ([E_{set}] + [NR \cdot E_{set}])}{k_s^{nr} \cdot k_s^{NR}} \tag{4.12}$$

Because of the unpredictability of the variation of $[NR{\cdot}E_{set}]$, we can only assign the value of $[E_{set}]_{tot}$. But when it comes to design the calculation program, we need to use Equation 4.10 to calculate nitrate steady-state concentration. We call $[NO_3^-]$ determined by Equation 4.10 steady-state concentration or set point while that by Equation 4.12 defining concentration.

If $k_f^{E_{set}} >> k_r^{E_{set}} + k_{cat}^{E_{set}}$, $[E_{set}]+[NR \cdot E_{set}] \approx [NR \cdot E_{set}]$, which means nitrate steady-state concentration equals approximately defining one. When there is no nitrate to activate the transcription of *NR*, $NR \cdot E_{set}$ will also disappear. But $[E_{set}]_{tot}$ is still constant. At this moment, nitrate steady-state concentration should go to zero, while defining concentration does not change.

The value of $[NO_3^-]$ is inversely proportional to the generation of *NR* (the denominator of Equation 4.3 or 4.10 is $k_s^{nr} \cdot k_s^{NR}$) and proportional to the removal of *NR* (the numerator $k_d^{nr} \cdot V_{\max}^{E_{set}}$).

When dealing with the case with an extremely low $K_M^{E_{set}}$, the model in which *NR* removal step by E_{set} is expanded by Michaelis-Menten kinetics should be used.

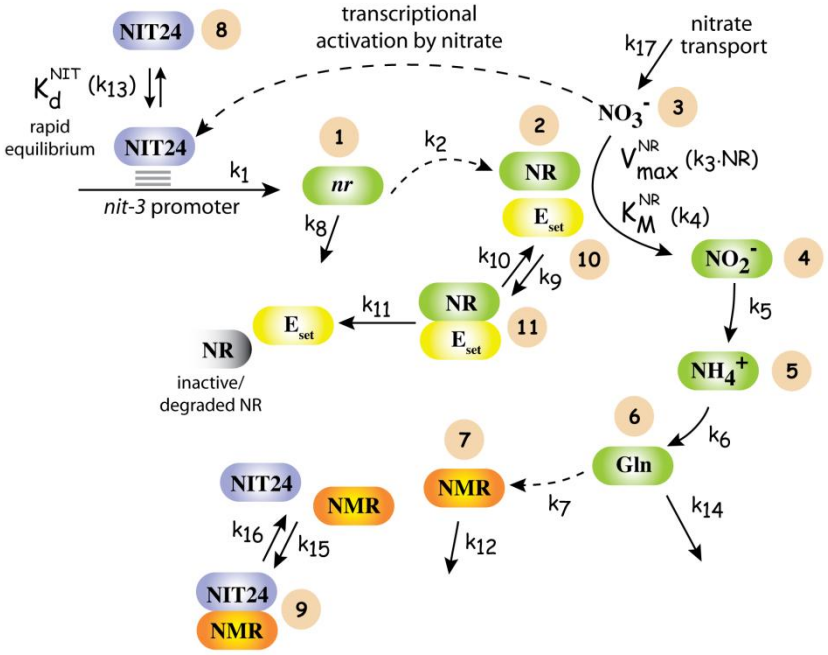

Figure 4.4: Based on Figure 4.1, *NR* removal by E_{set} is expanded with Michaelis-Menten kinetics.

Next I will use an example to show the effect of avoiding the negative value of concentration through this expansion method.

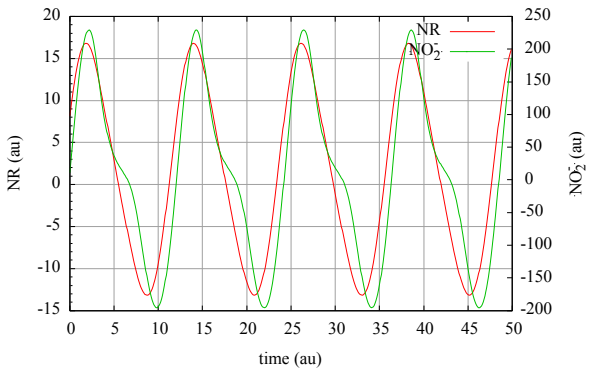

(a)

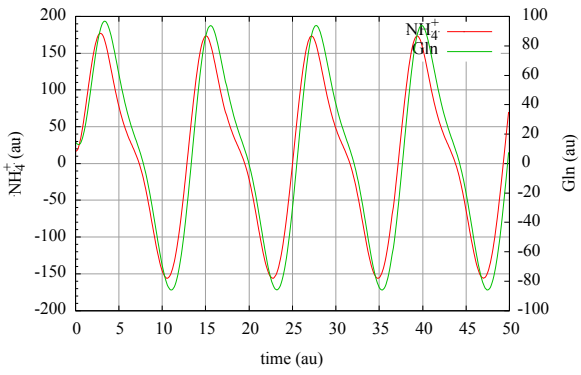

(b)

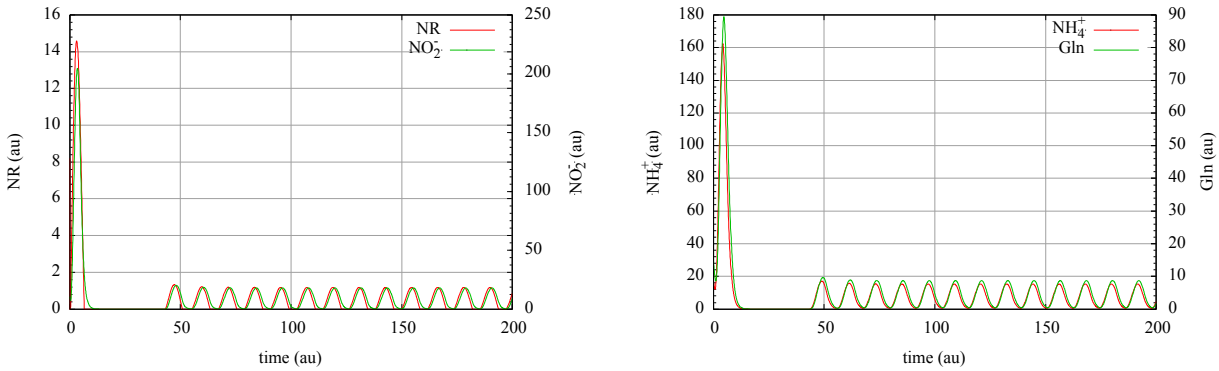

(c) (d)

Figure 4.5: Graph a and b are generated from Figure 4.1 where k_{10} ($K_M^{E_{set}}$) = 1×10^{-8}. On top of *NR*, the concentrations of NO_2^- , NH_4^+ and *Gln* also show negative values. Graph c and d are generated from Figure 4.4 where $k_{10} = 1\times10^{8}$, $k_{10} = k_{11} = 0.5$ so that $K_M^{E_{set}} = \frac{k_{10} + k_{11}}{k_9}$ is also 1×10^{-8}. With the help of Michaelis-Menten kinetics, there is no negative concentration for these four variables. In both cases, $k_7 = 0$. If we assign a value to k_7, negative [*NMR*] will also be observed when $K_M^{E_{set}}$ is too low. But no matter how small $K_M^{E_{set}}$ is, I never observed negative [*nr*] and $[NO_3^-]$.

In addition to avoid negative concentration, another outstanding advantage of this expansion method is to reflect nitrate level more accurately.

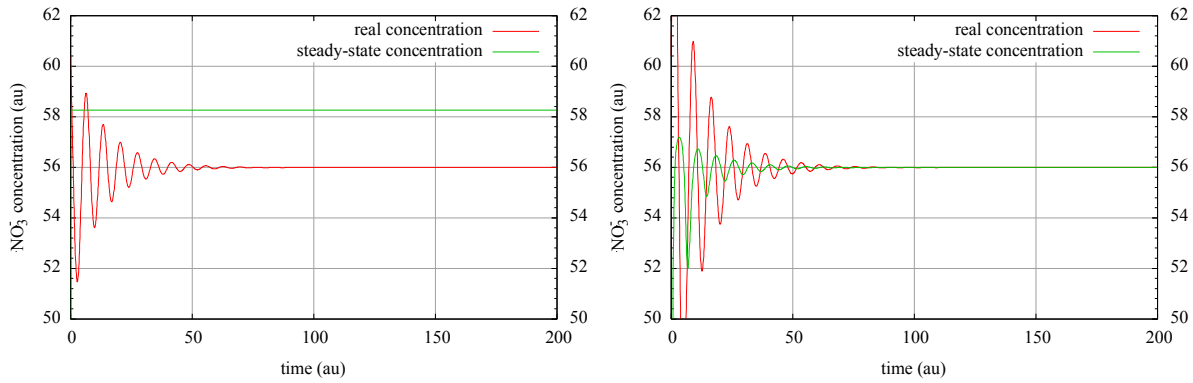

(a) (b)

Figure 4.6. (a) and (b) are calculated with the same parameters ($V_{max}^{E_{set}}$ =1.0 and $K_M^{E_{set}}$ =0.01) generated in Figure 4.1 and Figure 4.4, respectively. It is obvious that in (b) the curves of nitrate and its set point can go together at the end while in (a) real concentration is higher than steady-state concentration. In (a) $[NO_3^-]_{steady-state} = \frac{k_8 \cdot k_9}{k_1 \cdot k_2}$ which is a constant as long as k_1 is always the same (the variation of k_1 will be discussed in Section 4.3.2) while in (b) $[NO_3^-]_{steady-state} = \frac{k_8 \cdot k_{11} \cdot [NR \cdot E_{set}]}{k_1 \cdot k_2}$, and since $[NR{\cdot}E_{set}]$ is a variable, $[NO_3^-]_{steady-state}$ is changable.

4.1.2 The introduction of an inflow controller to regulate nitrate uptake

When external nitrate concentration is relatively low, the uptake mechanism of nitrate is similar to Michaelis-Menten kinetics both for fungi (49) and plants (4).(For fungi, this transport system is called HANT and it is associated with the high-affinity nitrate transporter) Under high nitrate conditions, nitrate transport shows linear kinetics as regard to external nitrate concentration. In this thesis, the coexistence of both these two transporter systems is not discussed. We assume that the nitrate uptake process is the high-affinity nitrate transport system of HANT for fungi or HATS for plants.

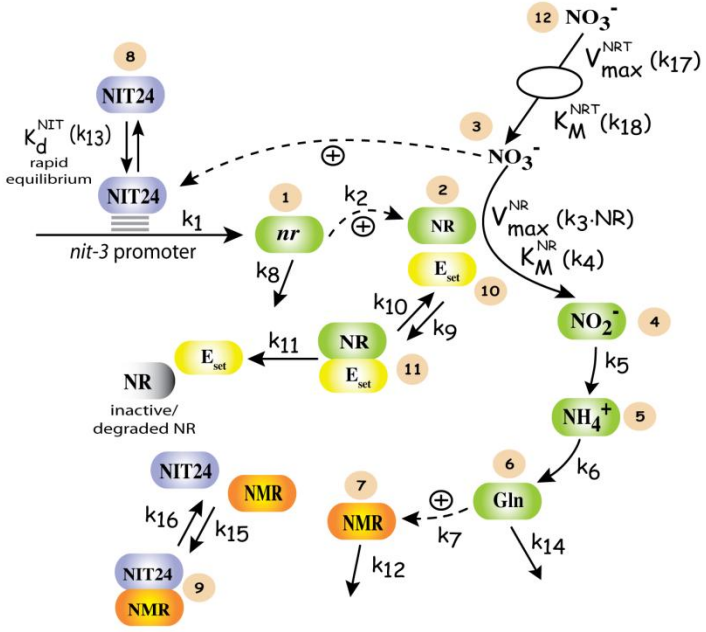

Figure 4.7: *Neurospora crassa*'s nitrate assimilation pathway. In this scheme environmental nitrate concentration is regarded as a reservoir that is expended through the uptake of *Neurospora crassa*. Michaelis-Menten kinetic expression is used for the transport rate of nitrate from the surroundings.

The expression of nitrate uptake rate in Figure 4.7 is $\frac{k_{17}\cdot[NO_3^-]_{env}}{k_{18}+[NO_3^-]_{env}}$ herein $[NO_3^-]_{env}$ refers to the concentration of environmental nitrate which falls gradually. Since $\frac{k_{17}\cdot[NO_3^-]_{env}}{k_{18}+[NO_3^-]_{env}}=\frac{k_{17}}{\frac{k_{18}}{[NO_3^-]_{env}}+1}$, the decrease of $[NO_3^-]_{env}$ leads to the increase of $\frac{k_{18}}{[NO_3^-]_{env}}+1$, thereby generating a lower uptake rate. Only through the regulation of *NR*, it is not sufficient to keep the homeostasis of cytosolic nitrate if environmental nitrate concentration is treated as a variable which is consumed gradually. As shown before, *NR* is only able to remove excess nitrate but not functional in making up for the loss.

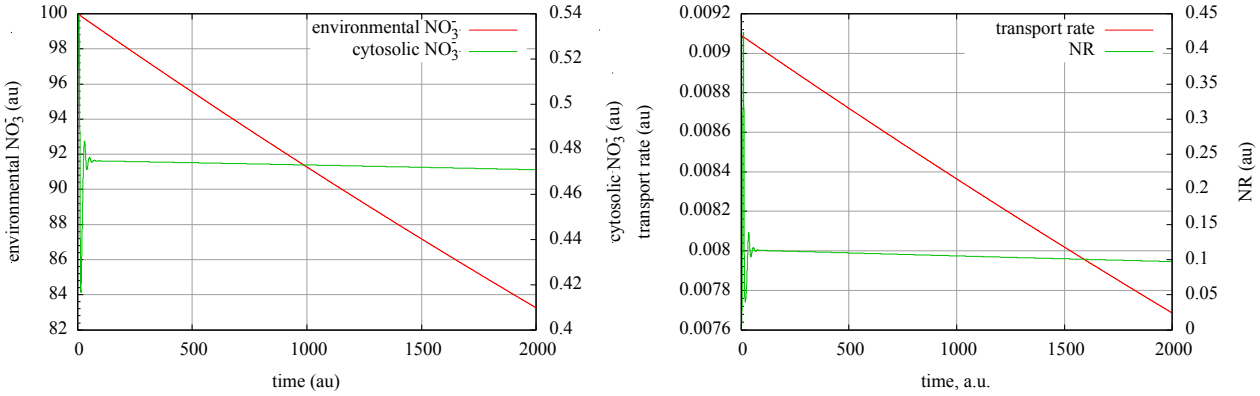

(a) (b)

Figure 4.8: The cytosolic nitrate decreases slightly as time goes by. A gradually decreasing transport rate is associated with a reducing *NR* level, which also generates a lower nitrite level (not shown here). [*NR*] is directly proportional to the inflow rate of nitrate transporting to it, which is the reason for its progressive decrease with a reducting absorption rate. Treatment of environmental nitrate as a variable poses this shortcoming of the outflow controller. The decrease of cytosolic nitrate dose not accord with the demand for homeostasis.

Introduction of an inflow controller to regulate the nitrate transport is helpful to solve this problem.

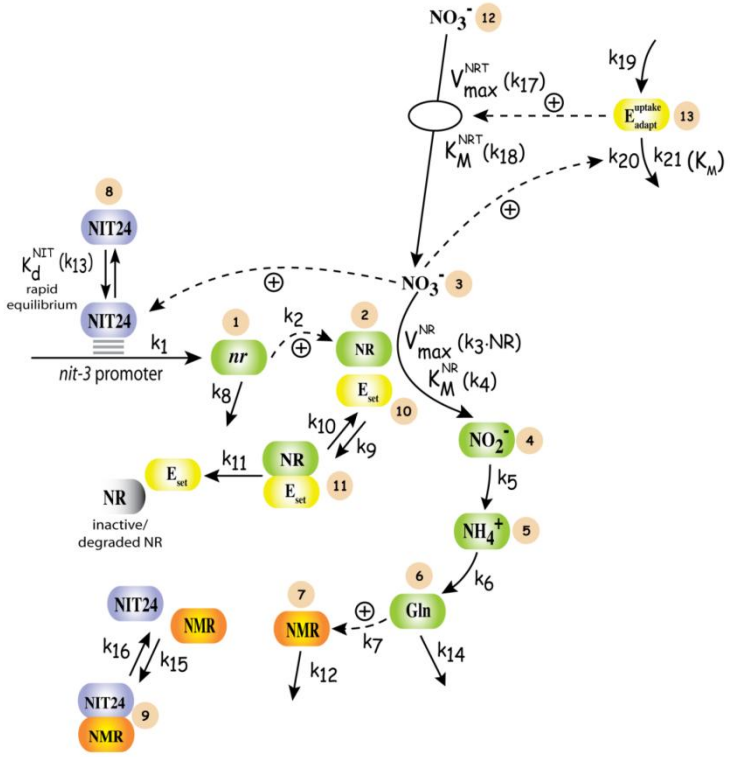

Figure 4.9: Scheme of nitrate transport and assimilation pathway for fungi (focusing on *Neurospora crassa*) in which inflow network V is introduced to express the nitrate absorption from the environment and E_{adapt}^{uptake} is the inflow controller. Taking the yeast *Pichia pastoris* as the research object, it was observed that cells of this lower eukaryote transformed with the nitrate transporter gene alone failed to display net nitrate transport despite having the ability to produce the protein. In addition, loss-of-function nitrate

reductase mutants appeared to be unable to accumulate nitrate. These researchers demonstrate that nitrate reductase activity is mandatory for nitrate accumulation in cells of the lower eukaryotes, the fungi (25). As I mentioned before, inflow feedback networks are suitable for the compensation of loss. If no usage happens, no need to compensate. This property coincides well with the experimental result above. Therefore, it is necessary to use an inflow controller to regulate the nitrate uptake.

The nitrate concentration of this inflow controller is determined by the differential equation of E_{adapt}^{uptake}:

$$\frac{d[E_{adapt}^{uptake}]}{dt} = k_{19} - \frac{k_{20}\cdot[NO_3^-]\cdot[E_{adapt}^{uptake}]}{k_{21}+[E_{adapt}^{uptake}]}$$

Putting $\frac{d[E_{adapt}^{uptake}]}{dt} = 0$ gives:

$$[NO_3^-] = \frac{k_{19}}{\frac{k_{20}\cdot[E_{adapt}^{uptake}]}{k_{21}+[E_{adapt}^{uptake}]}} = \frac{k_{19}}{k_{20}}\cdot\frac{k_{21}+[E_{adapt}^{uptake}]}{[E_{adapt}^{uptake}]} \tag{4.13}$$

If $k_{21}<<[E_{adapt}^{uptake}]$, we can treat $\frac{k_{21}+[E_{adapt}^{uptake}]}{[E_{adapt}^{uptake}]}$ as 1 approximately, which makes it possible to write:

$$[NO_3^-] = \frac{k_{19}}{k_{20}} \tag{4.14}$$

We call $[NO_3^-]$ determined by Equation 4.13 as steady-state concentration while Equation 4.14 defining concentration.

In order to meet the requirement that $k_{21}<<[E_{adapt}^{uptake}]$, it is necessary to assign a negligible value to k_{21}. However, when $[E_{adapt}^{uptake}]$ is small enough to be comparable to k_{21}, we can not use the expression $[NO_3^-] = \frac{k_{19}}{k_{20}}$ .to eastimate nitrate concentration.

In this case we have to derive nitrate concentration determining by inflow controller without approximation:

$$[NO_3^-] = \frac{k_{19}}{k_{20}}\cdot\frac{k_{21}+[E_{adapt}^{uptake}]}{[E_{adapt}^{uptake}]}$$

Since $\frac{k_{21}+[E_{adapt}^{uptake}]}{[E_{adapt}^{uptake}]} > 1$, $[NO_3^-] = \frac{k_{19}}{k_{20}}\cdot\frac{k_{21}+[E_{adapt}^{uptake}]}{[E_{adapt}^{uptake}]} > \frac{k_{19}}{k_{20}}$.

In our model (Figure 4.9), the increase of k_1 gives rise to a higher concnetration of *NR*. It is observed that the consumption rate of environmental nitrate is raised and the duration of homeostasis is decreased.

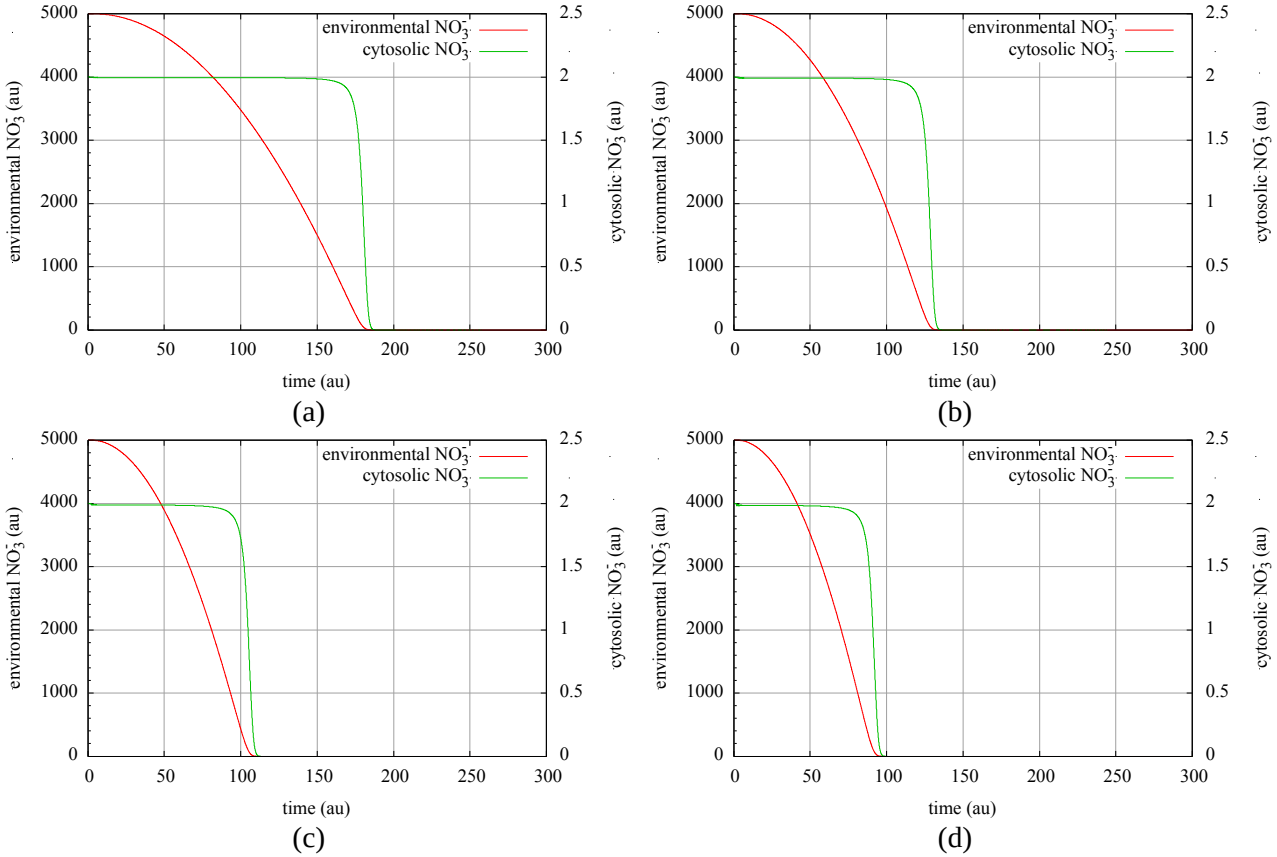

Figure 4.10: These graphs are generated from the model described in Figure 4.9 with different *NR* levels. (a) k_1 = 1.5 (b) k_1 = 2.0 (c) k_1 = 2.5 (d) k_1 = 3.0. Other rate constants are all the same. The shorter time when it takes to consume up the environmental nitrate means the faster uptake rate of nitrate into the cell.

In Figure 4.8, I show the example that only with one outflow controller, it is difficult to keep a constant nitrate level. With the introduction of an inflow controller, we can solve this problem.

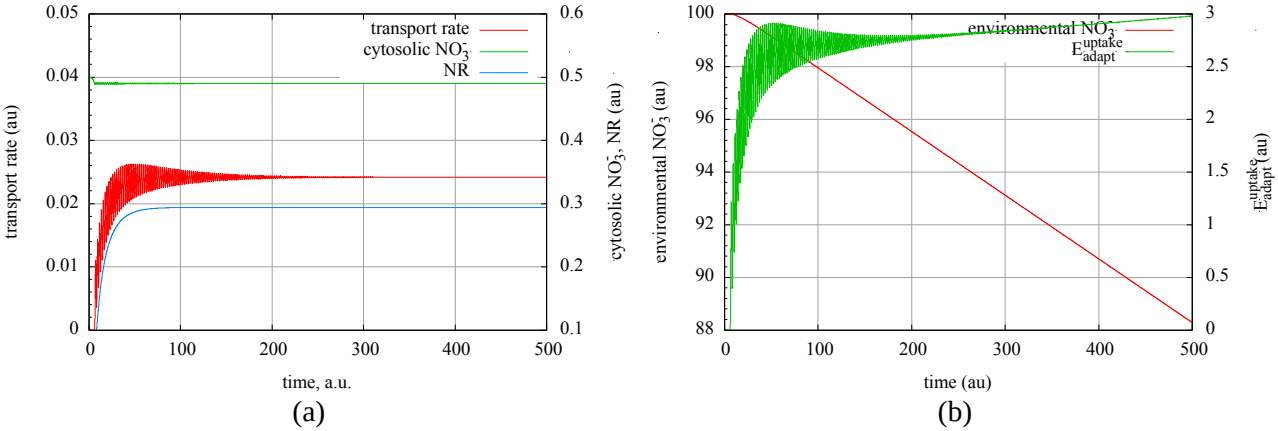

Figure 4.11: Except the presence of E_{adapt}^{uptake}, this calculation has all the same rate constants with Figure 4.8. The *NR* controlled defining concentration is 0.5 while E_{adapt}^{uptake} controlled one is 0.25. The contribution of E_{adapt}^{uptake} is to regulate the nitrate uptake rate which makes the cytosolic nitrate keep in a certain level without falling down. As I mention above, only with an outflow controller, transport rate slows down with the decrease of $[NO_3^-]_{env}$. In this new model which has an inflow controller, the expression of nitrate

absorption rate is $\frac{k_{17} \cdot [NO_3^-]_{env} \cdot [E_{adapt}^{uptake}]}{k_{18} + [NO_3^-]_{env}}$. In order to generate a constant transport rate, $[E_{adapt}^{uptake}]$ has to increase itself.

4.1.3 The problem caused by the combination of inflow and outflow controller

It is noteworthy that a phenomenon comes with the combination of the inflow and outflow controller in this case. When outflow controller's defining value is lower than or equivalent to inflow controller's, the concentration of outflow controller *NR* is always on the increase until the environmental nitrate is used up.

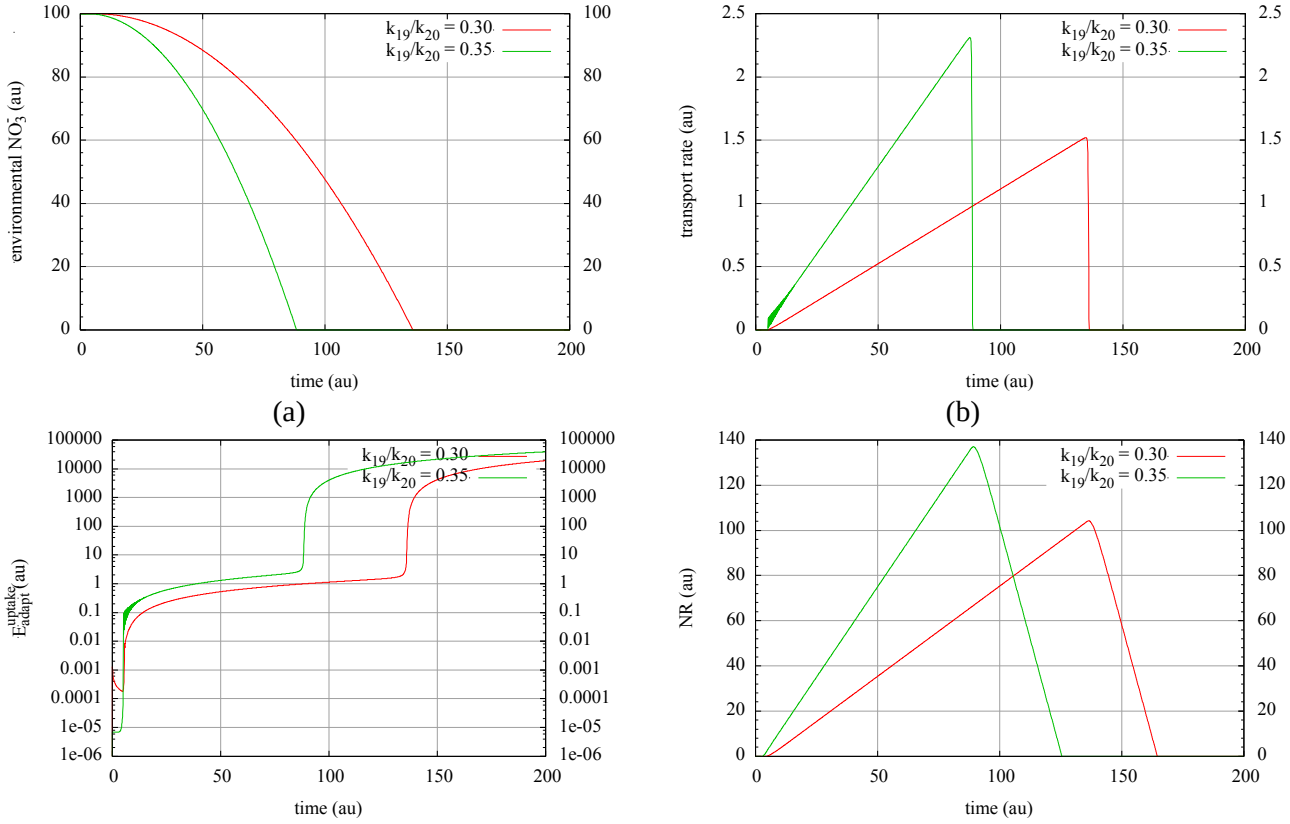

Figure 4.12: The results from two calculations in which defining inflow concentrations (k_{19}/k_{20}) are 0.30 and 0.35 individually are compared. In both calculations, *NR* controlled defining concentration is set to 0.25. The higher the inflow defining value, the faster nitrate uptake rate increases, which shortens the time for the depletion of environmental nitrate. The transport stops immediately the nitrate supply is depleted. The duration of a continuously rising transport rate is almost the same with the rise of transport rate.

According to the expression of nitrate absorption rate $\frac{k_{17} \cdot [NO_3^-]_{env} \cdot [E_{adapt}^{uptake}]}{k_{18} + [NO_3^-]_{env}}$, in order to generate a greater transport rate, $[E_{adapt}^{uptake}]$ has to increase itself. When $[NO_3^-]_{env} = 0$, $[E_{adapt}^{uptake}]$ increases in a faster speed, which is due to the fact that at this moment there is no nitrate to activiate its degradation. Although nitrate transport rate as well as [*NR*] rise, $[NO_3^-]$ can still keep in a certain level.

I have tried to find out the reason which causes the straight climb of [*NR*] from its differential equation:

$$\frac{d[NR]}{dt} = k_2 \cdot [nr] - k_9 \cdot [NR] \cdot [E_{set}] + k_{10} \cdot [NR \cdot E_{set}]$$

From $\frac{d[nr]}{dt} = 0$, we have:

$$k_1 \cdot [NO_3^-] - k_8 \cdot [nr] = 0$$

$$[nr] = \frac{k_1}{k_8} \cdot [NO_3^-] \quad (4.15)$$

From $\frac{d[NR \cdot E_{set}]}{dt} = 0$, we have:

$$k_9 \cdot [NR] \cdot [E_{set}] - (k_{10} + k_{11}) \cdot [NR \cdot E_{set}] = 0$$

$$-k_9 \cdot [NR] \cdot [E_{set}] + k_{10} \cdot [NR \cdot E_{set}] = -k_{11} \cdot [NR \cdot E_{set}] \quad (4.16)$$

Substituting Equation 4.15 and 4.16 to $\frac{d[NR]}{dt}$ gives:

$$\frac{d[NR]}{dt} = \frac{k_1 \cdot k_2}{k_8} \cdot [NO_3^-] - k_{11} \cdot [NR \cdot E_{set}]$$

The expression of $[NO_3^-]$ can be deduced from $\frac{d[NR]}{dt} = 0$:

$$[NO_3^-] = \frac{k_8 \cdot k_{11}}{k_1 \cdot k_2} \cdot [NR \cdot E_{set}] \quad (4.17)$$

If $[NO_3^-] = \frac{k_8 \cdot k_{11}}{k_1 \cdot k_2} \cdot [NR \cdot E_{set}]$, $\frac{d[NR]}{dt} = 0$.

If $[NO_3^-] > \frac{k_8 \cdot k_{11}}{k_1 \cdot k_2} \cdot [NR \cdot E_{set}]$, $\frac{d[NR]}{dt} > 0$ and [*NR*] increases.

If $[NO_3^-] < \frac{k_8 \cdot k_{11}}{k_1 \cdot k_2} \cdot [NR \cdot E_{set}]$, $\frac{d[NR]}{dt} < 0$ and [*NR*] decreases.

When outflow controller's defining value ($\frac{k_8 \cdot k_{11}}{k_1 \cdot k_2} \cdot [E_{set}]_{tot}$) is lower than or equivalent to inflow controller's ($\frac{k_{19}}{k_{20}}$), the nitrate is determined by the inflow controller, which means $[NO_3^-] = \frac{k_{19}}{k_{20}} \cdot \frac{k_{21} + [E_{adapt}^{uptake}]}{[E_{adapt}^{uptake}]}$.

So $[NO_3^-] = \frac{k_{19}}{k_{20}} \cdot \frac{k_{21} + [E_{adapt}^{uptake}]}{[E_{adapt}^{uptake}]} > \frac{k_{19}}{k_{20}} \geq \frac{k_8 \cdot k_{11}}{k_1 \cdot k_2} \cdot [E_{set}]_{tot} > \frac{k_8 \cdot k_{11}}{k_1 \cdot k_2} \cdot [NR \cdot E_{set}]$, $[NR]$ increases.

When $\frac{k_8 \cdot k_{11}}{k_1 \cdot k_2} \cdot [E_{set}]_{tot} > \frac{k_{19}}{k_{20}}$, we can not confirm the relationship between $\frac{k_{19}}{k_{20}} \cdot \frac{k_{21} + [E_{adapt}^{uptake}]}{[E_{adapt}^{uptake}]}$ and $\frac{k_8 \cdot k_{11}}{k_1 \cdot k_2} \cdot [NR \cdot E_{set}]$. Interestingly, in every calculation $[NO_3^-] = \frac{k_{19}}{k_{20}} \cdot \frac{k_{21} + [E_{adapt}^{uptake}]}{[E_{adapt}^{uptake}]}$ no matter $\frac{k_8 \cdot k_{11}}{k_1 \cdot k_2} \cdot [NR \cdot E_{set}]$ is higher or lower than $[NO_3^-]$. Under the condition that $\frac{k_8 \cdot k_{11}}{k_1 \cdot k_2} \cdot [NR \cdot E_{set}] > [NO_3^-]$, through a lower $[NR \cdot E_{set}]$, inflow set point $\frac{k_8 \cdot k_{11}}{k_1 \cdot k_2} \cdot [NR \cdot E_{set}]$ can be equal to $[NO_3^-] = \frac{k_{19}}{k_{20}} \cdot \frac{k_{21} + [E_{adapt}^{uptake}]}{[E_{adapt}^{uptake}]}$ so as to inhibit the situation $[NO_3^-] < \frac{k_8 \cdot k_{11}}{k_1 \cdot k_2} \cdot [NR \cdot E_{set}]$. However, if $[NO_3^-] = \frac{k_{19}}{k_{20}} \cdot \frac{k_{21} + [E_{adapt}^{uptake}]}{[E_{adapt}^{uptake}]} > \frac{k_{19}}{k_{20}} \geq \frac{k_8 \cdot k_{11}}{k_1 \cdot k_2} \cdot [E_{set}]_{tot} > \frac{k_8 \cdot k_{11}}{k_1 \cdot k_2} \cdot [NR \cdot E_{set}]$, it is impossible for $[NR \cdot E_{set}]$ to increase itself to meet the condition $[NO_3^-] = \frac{k_8 \cdot k_{11}}{k_1 \cdot k_2} \cdot [NR \cdot E_{set}]$ as $[NR \cdot E_{set}]$ can not exceed $[E_{set}]_{tot}$.

In order to avoid generating a continuously rising [*NR*], it is better to set nitrate defining outflow concentration higher than defining inflow one. Through it uptake rate becomes much lower. One way of explaining this is as follows: The aim of inflow controller is just to inhibit nitrate level falling below its required concentration through adding more nitrate while *NR* only needs to remove nitrate so that nitrate concentration will not exceed a certain limit. When inflow controller E_{adapt}^{uptake} transports nitrate according to its requirement, *NR* does not need to "work hard" since its requirement has been met. As will be shown in Figure 4.13, a lower *NR* level will result in a lower transport rate. Moreover, decreasing nitrate defining concentration for the inflow feedback network V increases the duration for homeostasis because nitrate transport rate is even slower.

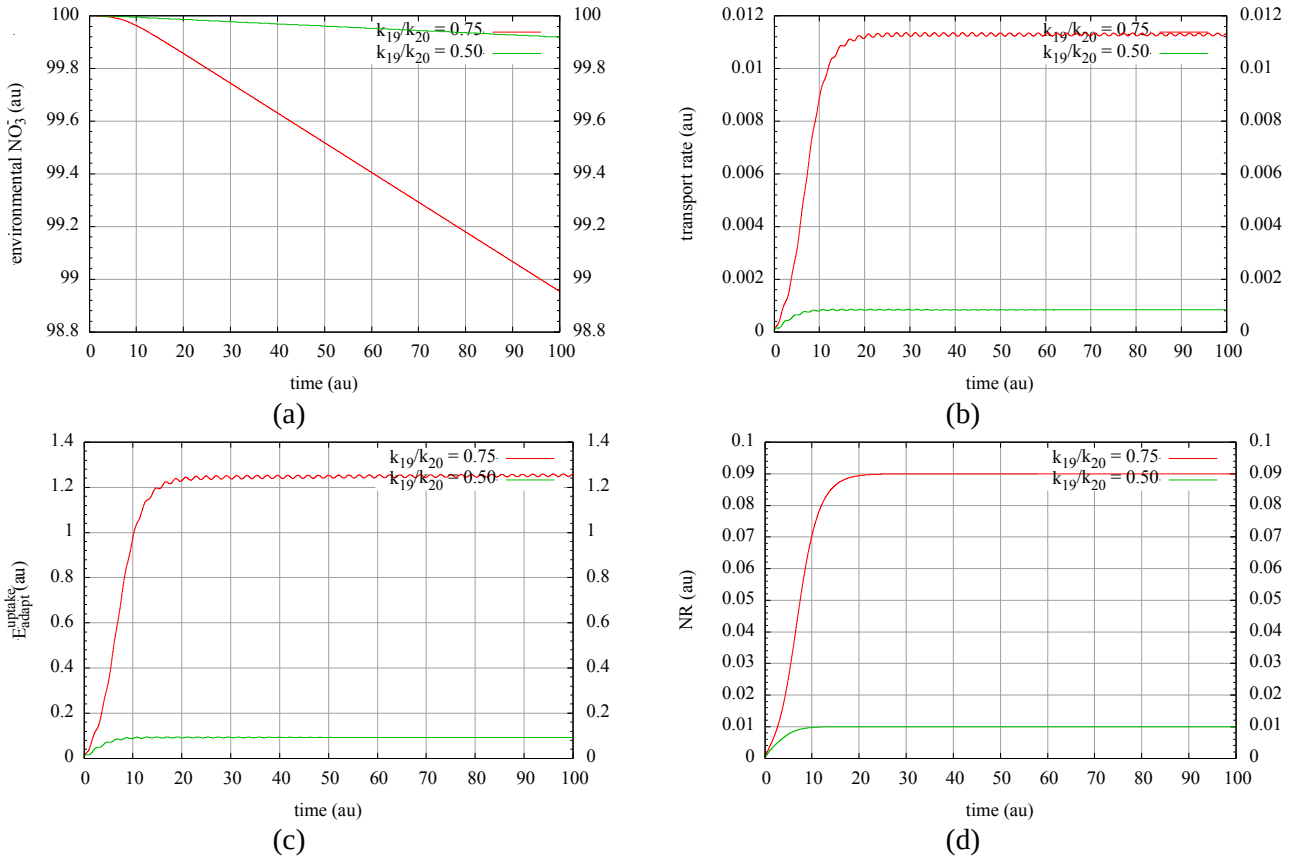

Figure 4.13: The results from the two calculations in which defining inflow values (k_{19}/k_{20}) are 0.75 and 0.50 individually are compared. In both calculations, *NR* controlled defining value is set to 0.8. The decrease of k_{19}/k_{20} causes a lower E_{adapt}^{uptake} level and also a lower uptake rate. E_{adapt}^{uptake} is responsible for activating the nitrate transport process, so there should be a positive relationship between its concentration and transport rate. The lower spending rate for nitrate resource, the more nitrate left after a certain period. According to the character of outflow controller, the *NR* level is directly proportional to the nitrate transport rate.

Starting from another perspective, we know nitrate inflow rate has to equal to its removal rate in order to meet the requirement $\frac{d[NO_3^-]}{dt} = 0$, which means:

$$\text{nitrate inflow rate} = \frac{k_3 \cdot [NR] \cdot [NO_3^-]}{k_4 + [NO_3^-]}$$

A higher defining inflow value causes higher concentrations of *NR* and NO_3^-, and nitrate inflow rate also rises.

According to what we have known about the property of *NR*, the outflow feedback network I is the most suitable for nitrate removal by *NR*. However, so far there is not enough evidence to determine which inflow feedback network should be used for the nitrate transport process. Interestingly, we found that when outflow feedback network I combines with inflow feedback

network II which has a higher or equivalent nitrate defining concentration compared with the former, sometimes the phenomenon of a continuously rising [*NR*] will not happen.

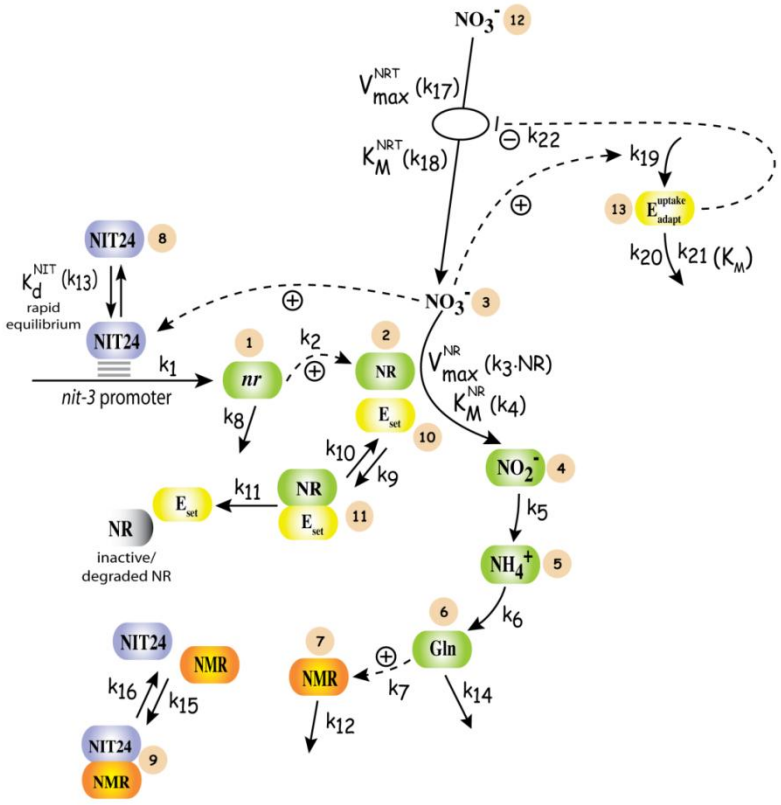

Figure 4.14: Scheme of nitrate transport and assimilation pathway for fungi (focusing on *Neurospora crassa*) which includes one outflow network I and one inflow network II.

The inflow nitrate defining concentration is decided by the differential equation of E_{adapt}^{uptake}:

$$\frac{d[E_{adapt}^{uptake}]}{dt} = k_{19} \cdot [NO_3^-] - \frac{k_{20} \cdot [E_{adapt}^{uptake}]}{k_{21} + [E_{adapt}^{uptake}]}$$

Putting $\frac{d[E_{adapt}^{uptake}]}{dt} = 0$ gives the expression of nitrate concentration:

$$[NO_3^-] = \frac{\frac{k_{20} \cdot [E_{adapt}^{uptake}]}{k_{21} + [E_{adapt}^{uptake}]}}{k_{19}} = \frac{k_{20}}{k_{19}} \cdot \frac{[E_{adapt}^{uptake}]}{k_{21} + [E_{adapt}^{uptake}]}$$

If $k_{21} << [E_{adapt}^{uptake}]$, we have the expression of nitrate defining value:

$$[NO_3^-] = \frac{k_{20}}{k_{19}}$$

In order to meet the requirement that $k_{21} << [E_{adapt}^{uptake}]$, it is necessary to assign a negligible value to k_{21}. However, when $[E_{adapt}^{uptake}]$ is small enough to be comparable to k_{21}, we can not use the expression $[NO_3^-] = \frac{k_{20}}{k_{19}}$.

In this case we have to derive the inflow defining value without approximation:

$$[NO_3^-] = \frac{k_{20}}{k_{19}} \cdot \frac{[E_{adapt}^{uptake}]}{k_{21} + [E_{adapt}^{uptake}]}$$

Since $\frac{[E_{adapt}^{uptake}]}{k_{21} + [E_{adapt}^{uptake}]} < 1$, $[NO_3^-] = \frac{k_{20}}{k_{19}} \cdot \frac{[E_{adapt}^{uptake}]}{k_{21} + [E_{adapt}^{uptake}]} < \frac{k_{20}}{k_{19}}$.

When inflow defining value $\frac{k_{20}}{k_{19}}$ is higher than or equivalent to outflow defining value $\frac{k_8 \cdot k_{11}}{k_1 \cdot k_2} \cdot [E_{set}]_{tot}$, we have $\frac{k_{20}}{k_{19}} \geq \frac{k_8 \cdot k_{11}}{k_1 \cdot k_2} \cdot [E_{set}]_{tot} > \frac{k_8 \cdot k_{11}}{k_1 \cdot k_2} \cdot [NR \cdot E_{set}]$. We can not confirm the relationship between $\frac{k_{20}}{k_{19}} \cdot \frac{[E_{adapt}^{uptake}]}{k_{21} + [E_{adapt}^{uptake}]}$ and $\frac{k_8 \cdot k_{11}}{k_1 \cdot k_2} \cdot [NR \cdot E_{set}]$ since both of them are lower than $\frac{k_{20}}{k_{19}}$. This makes it possible to meet the requirement that $\frac{k_{20}}{k_{19}} \cdot \frac{[E_{adapt}^{uptake}]}{k_{21} + [E_{adapt}^{uptake}]} = \frac{k_8 \cdot k_{11}}{k_1 \cdot k_2} \cdot [NR \cdot E_{set}] = [NO_3^-]$ and $\frac{d[NR]}{dt} = 0$ when $\frac{k_{20}}{k_{19}} \geq \frac{k_8 \cdot k_{11}}{k_1 \cdot k_2} \cdot [E_{set}]_{tot}$. In such a condition, we can say outflow and inflow controllers reach an agreement for the determination of nitrate concentration.

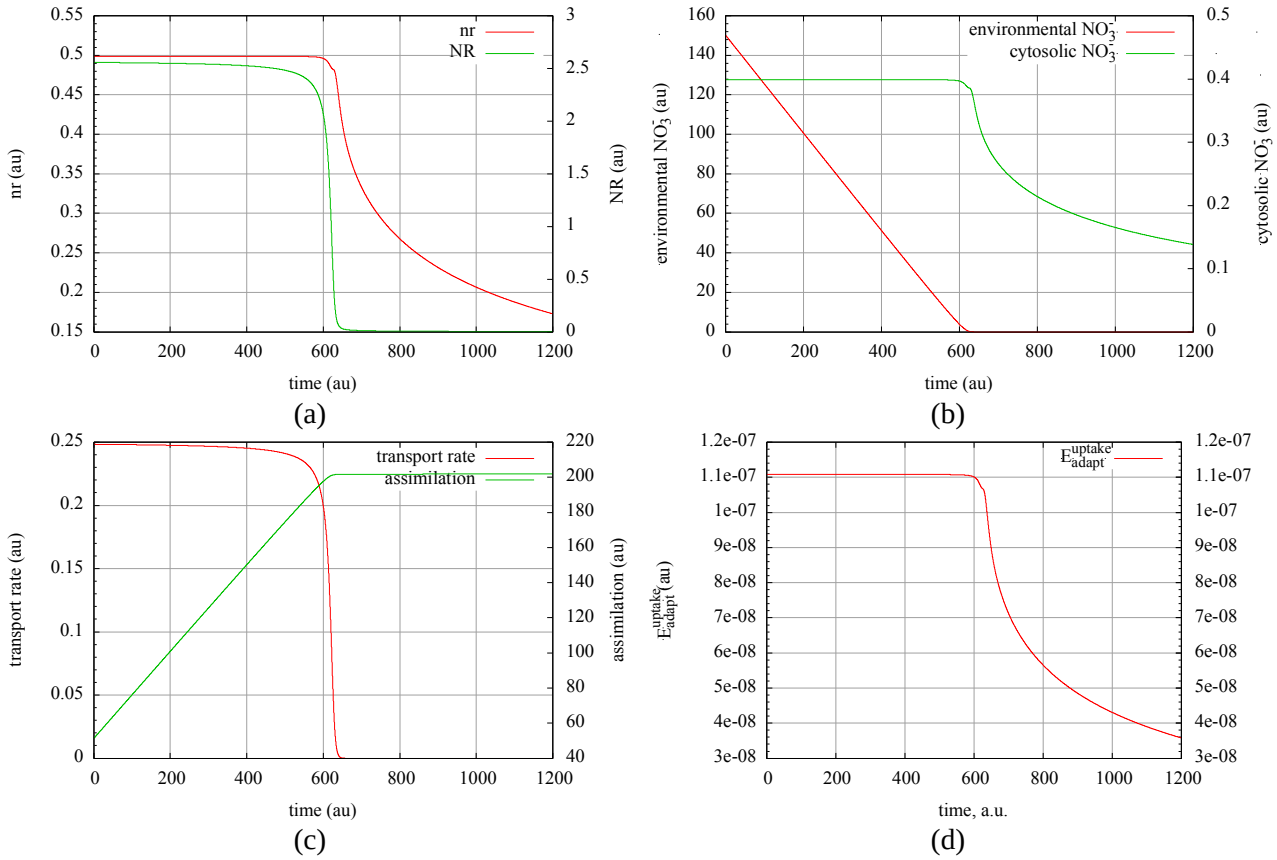

Figure 4.15: In this case, outflow defining set point (0.4) < inflow defining set point (4.0). After environmental nitrate is exhausted completely, the concentrations of *NR* and cytosolic nitrate start to decrease rapidly. Note that $[E_{adapt}^{uptake}]$ is lower than $k_{21} = 1\times10^{-6}$ and $\frac{k_{20}}{k_{19}} \cdot \frac{[E_{adapt}^{uptake}]}{k_{21}+[E_{adapt}^{uptake}]}$ is not little less than $\frac{k_{20}}{k_{19}}$.

But with such a combination, under the condition of a lower defining inflow value, sometimes $[NO_3^-] > \frac{k_8 \cdot k_{11}}{k_1 \cdot k_2} \cdot [NR \cdot E_{set}]$ still takes place, and it accompanies a rising [*NR*] and a probably much higher $[E_{adapt}^{uptake}]$ than k_{21}. I have not found out when outflow nitrate defining concentration is lower or equivalent to inflow defining one, what is the precondition for $[NO_3^-] > \frac{k_8 \cdot k_{11}}{k_1 \cdot k_2} \cdot [NR \cdot E_{set}]$ or $[NO_3^-] = \frac{k_8 \cdot k_{11}}{k_1 \cdot k_2} \cdot [NR \cdot E_{set}]$.

In addition to II, the combination of inflow controller IV and outflow controller I is also possible to avoid the existence of a continuously rising [*NR*] when the defining concentration of inflow controller is not less than that of *NR*. Moreover, the introduction of inflow controller VII is not helpful in avoding a rising [*NR*]. I will demonstrate its reason for these two combinations briefly.

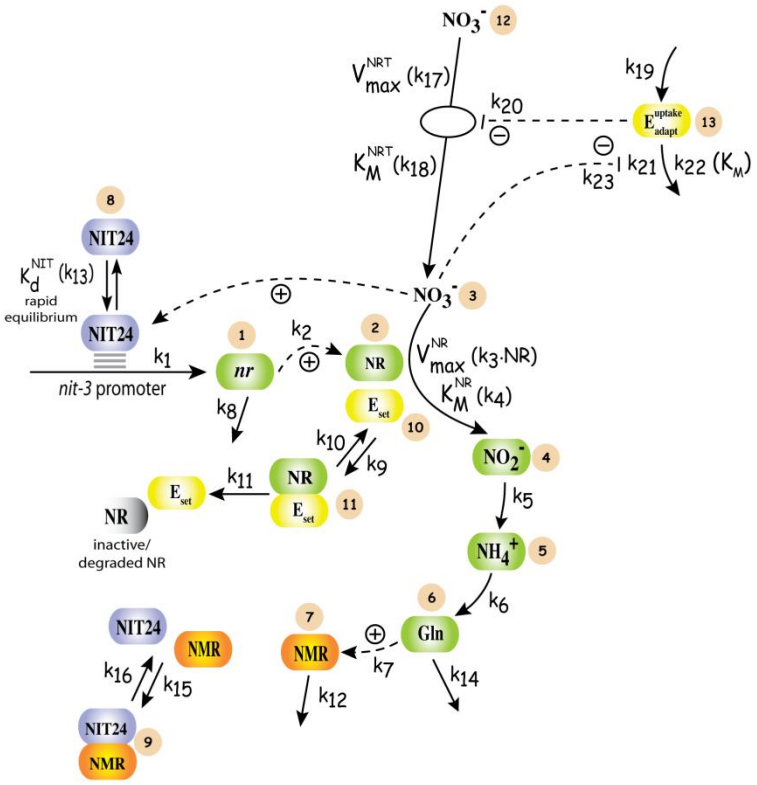

Figure 4.16: Scheme of nitrate transport and assimilation pathway for fungi (focusing on *Neurospora crassa*) which includes one outflow network I and one inflow network IV.

In Figure 4.16, nitrate concentration determined by inflow controller E_{adapt}^{uptake} is as follows:

steady-state concentration: $[NO_3^-] = \frac{k_{21}}{k_{19}} \cdot \frac{[E_{adapt}^{uptake}]}{k_{22} + [E_{adapt}^{uptake}]} - k_{23}$

defining concentration: $[NO_3^-] = \frac{k_{21}}{k_{19}} - k_{23}$

As $\frac{k_{21}}{k_{19}} - k_{23} > \frac{k_{21}}{k_{19}} \cdot \frac{[E_{adapt}^{uptake}]}{k_{22} + [E_{adapt}^{uptake}]} - k_{23}$, there still exists the possibility for the establishment of the relationship $\frac{k_{21}}{k_{19}} \cdot \frac{[E_{adapt}^{uptake}]}{k_{22} + [E_{adapt}^{uptake}]} - k_{23} = \frac{k_8 \cdot k_{11}}{k_1 \cdot k_2} \cdot [NR \cdot E_{set}]$ under the condition that $\frac{k_{21}}{k_{19}} - k_{23} \geq \frac{k_8 \cdot k_{11}}{k_1 \cdot k_2} \cdot [E_{set}]_{tot} > \frac{k_8 \cdot k_{11}}{k_1 \cdot k_2} \cdot [NR \cdot E_{set}]$

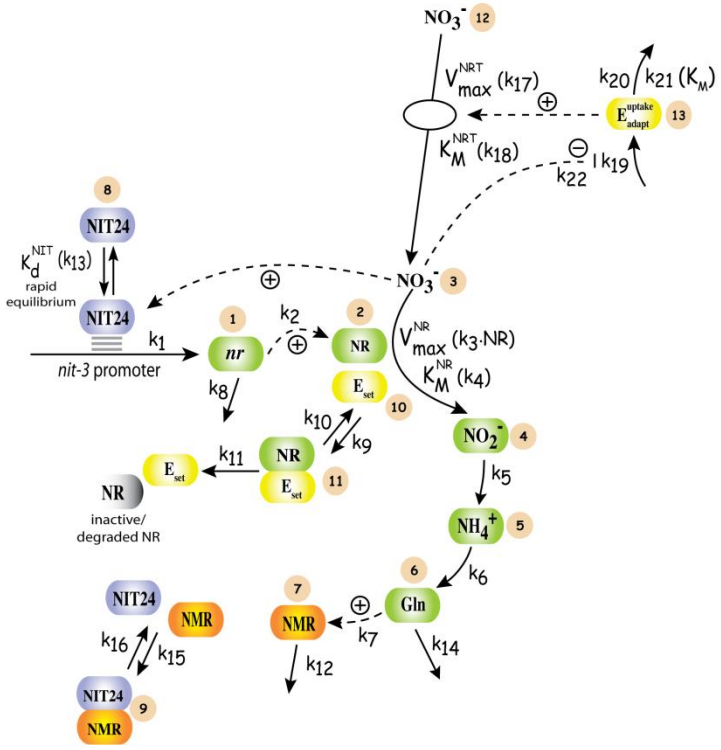

Figure 4.17: Scheme of nitrate transport and assimilation pathway for fungi (focusing on *Neurospora crassa*) which includes one outflow network I and one inflow network VII.

In Figure 4.17, nitrate concentration determined by inflow controller E_{adapt}^{uptake} is as follows:

steady-state concentration: $[NO_3^-] = \frac{k_{19}}{k_{20}} \cdot \frac{k_{21} + [E_{adapt}^{uptake}]}{[E_{adapt}^{uptake}]} - k_{22}$

defining concentration: $[NO_3^-] = \frac{k_{19}}{k_{20}} - k_{22}$

In such a combination, nitrate concentration is always determined by inflow controller.

Under the condition that $\frac{k_{19}}{k_{20}} - k_{22} \geq \frac{k_8 \cdot k_{11}}{k_1 \cdot k_2} \cdot [E_{set}]_{tot}$, we have

$\frac{k_{19}}{k_{20}} \cdot \frac{k_{21} + [E_{adapt}^{uptake}]}{[E_{adapt}^{uptake}]} - k_{22} > \frac{k_{19}}{k_{20}} - k_{22} \geq \frac{k_8 \cdot k_{11}}{k_1 \cdot k_2} \cdot [E_{set}]_{tot} > \frac{k_8 \cdot k_{11}}{k_1 \cdot k_2} \cdot [NR \cdot E_{set}]$, so $\frac{d[NR]}{dt} > 0$ and $[NR]$ rises.

4.2 The modeling of plant nitrate transport and assimilation

The nitrate transport in plant cell is a more complicated process than fungi and three additional pathways should be taken into consideration: nitrate efflux out of the cell, vacuolar nitrate uptake and release.

The model for plant nitrate transport and assimilation:

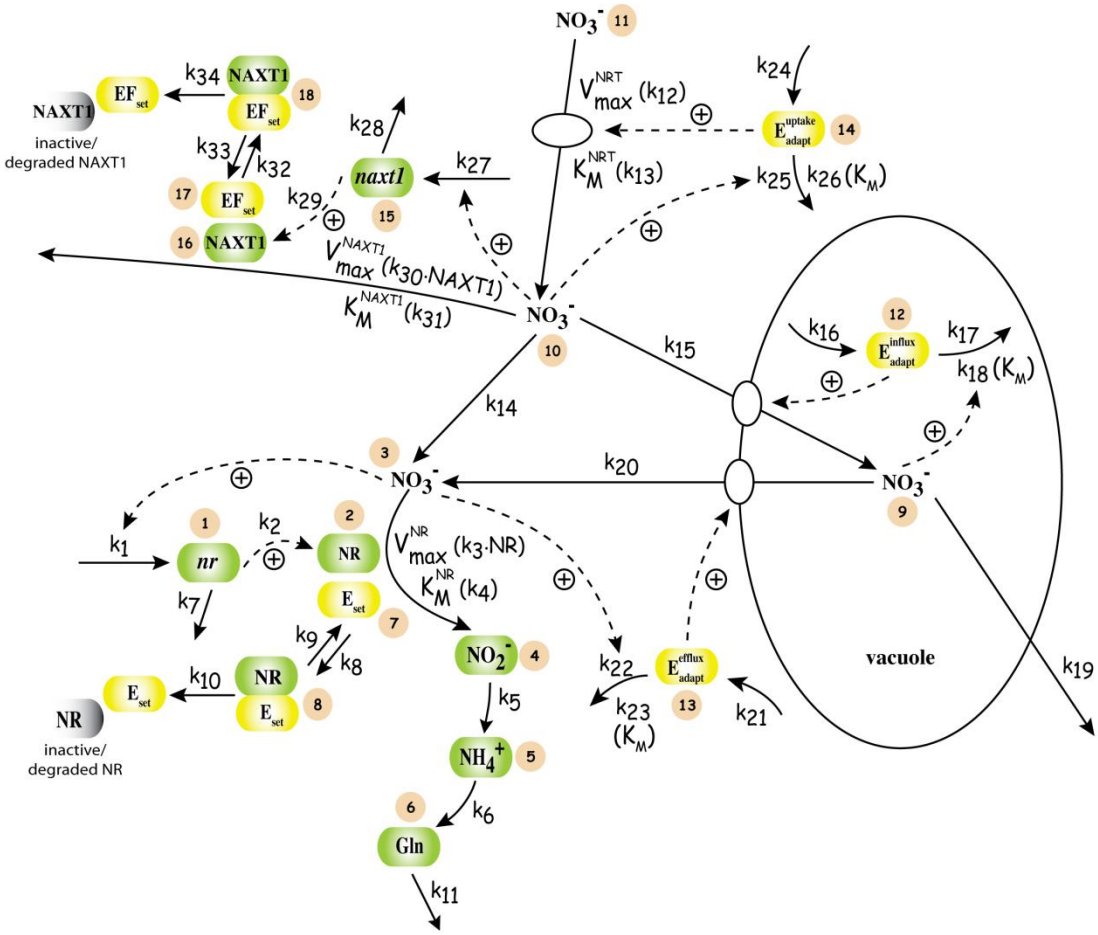

Figure 4.18: Scheme of nitrate transport and assimilation pathway for plants which includes two outflow networks I and three inflow networks V. The outflow controllers are *NR* and *NAXT1* while inflow controllers are E_{adapt}^{uptake}, E_{adapt}^{influx} and E_{adapt}^{efflux}. In plant cell, the vacuole takes up a majority of space. Here we introduce an arbitrary concentration turnover ratio between cytosolic and vacuolar nitrate when designing the calculation. The same amount of concentration transporting into and coming out of the vacuole is reduced to one nineteenth and nineteen times what it was, respectively. Taking into account nitrate distribution within the plant such as vacuolar storage and cytosolic nitrate activity we assume there is a branching point which is referred to Y(10) in this figure for nitrate distribution into theses two pathways. With double-barrelled nitrate-selective microelectrodes, it has been found that in barley root cells cytosolic nitrate activity is maintained in a steady-state during the first 24 hours of nitrate deprivation. But a net nitrate efflux from roots could be only detected for the first 5 hours after nitrate removal (10). According to such evidence, efflux system should be connected to the nitrate branching point instead of the one which is reduced by *NR*. It has been shown that in isolated tonoplast vesicles from storage tissue

of Beta vulgaris L. the initial rate of Ca^{2+}/H^{+} exchange, in the presence of K^{+} plus valinomycin (used to generate an acidic intravesicular space) displayed saturation kinetics with respect to extravesicular Ca^{2+} concentration. The pH gradient drove Ca^{2+} accumulation in the tonoplast vesicles (50). Similar results are observed with the respect to nitrate transport across the tonoplast of Cucumis sativus L. root cells (51). This is an indication for the existence of an inflow controller for vacuolar nitrate influx. The last controller network which is introduced in the model is for the efflux of vacuolar nitrate will be discussed in more detail in Section 4.2.1.

In Figure 4.18, cytosolic nitrate concentration determined by E_{adapt}^{efflux} is as follows:

steady-state concentration: $[NO_3^-]_{cyt} = \frac{k_{21}}{k_{22}} \cdot \frac{k_{23} + [E_{adapt}^{efflux}]}{[E_{adapt}^{efflux}]}$

defining concentration: $[NO_3^-]_{cyt} = \frac{k_{21}}{k_{22}}$

vacuolar nitrate concentration determined by E_{adapt}^{influx} is as follows:

steady-state concentration: $[NO_3^-]_{vac} = \frac{k_{16}}{k_{17}} \cdot \frac{k_{18} + [E_{adapt}^{influx}]}{[E_{adapt}^{influx}]}$

defining concentration: $[NO_3^-]_{vac} = \frac{k_{16}}{k_{17}}$

nitrate concentration of branching point determined by E_{adapt}^{uptake} is as follows:

steady-state concentration: $[NO_3^-]_{bra} = \frac{k_{24}}{k_{25}} \cdot \frac{k_{26} + [E_{adapt}^{uptake}]}{[E_{adapt}^{uptake}]}$

defining concentration: $[NO_3^-]_{bra} = \frac{k_{24}}{k_{25}}$

cytosolic nitrate determined by *NR* is as follows:

steady-state concentration: $[NO_3^-]_{cyt} = \frac{k_7 \cdot k_{10} \cdot ([E_{set}] + [NR \cdot E_{set}])}{k_1 \cdot k_2}$

defining concentration: $[NO_3^-]_{cyt} = \frac{k_7 \cdot k_{10} \cdot [NR \cdot E_{set}]}{k_1 \cdot k_2}$

cytosolic nitrate determined by *NR* is as follows:

steady-state concentration: $[NO_3^-]_{bra} = \frac{k_{28} \cdot k_{34} \cdot ([EF_{set}] + [NAXT1 \cdot EF_{set}])}{k_{27} \cdot k_{29}}$

defining concentration: $[NO_3^-]_{bra} = \frac{k_{28} \cdot k_{34} \cdot [NAXT1 \cdot EF_{set}]}{k_{27} \cdot k_{29}}$

4.2.1 The vacuolar efflux process regulating by an inflow controller

Actually, it has not been found the evidence for the existence of a controller regulating the efflux process of vacuolar nitrate. However, it is the fact that nitrate stored in the vacuole serves as a reservoir to sustain growth processes during subsequent periods when the external nitrogen

supply becomes limiting (10, 11, 12). So we try to fit this phenomenon on the basis of controller networks we have explored.

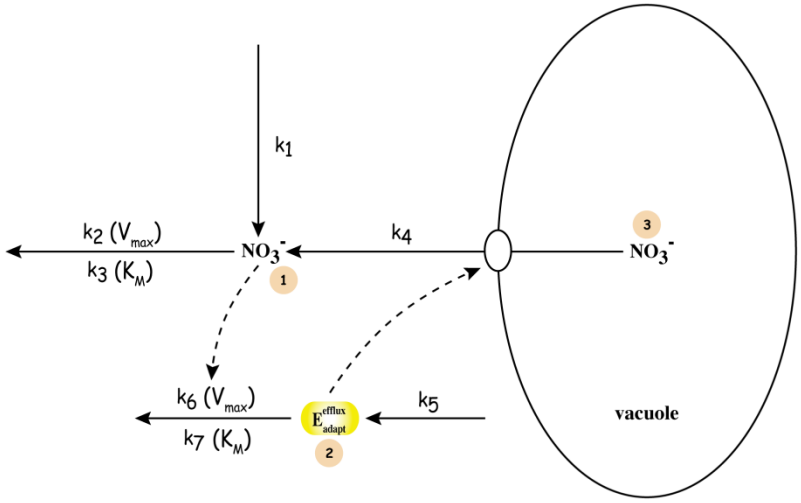

Figure 4.19. The inflow controller V is used to regulate the homeostasis of cytosolic nitrate which is maintained by the remobilization of vacuolar stored nitrate.

The cytosolic nitrate concentration of this inflow controller network is determined by the degradation step of the controller E_{adapt}^{efflux}.

$$\frac{d[E_{adapt}^{efflux}]}{dt} = k_5 - \frac{k_6 \cdot [NO_3^-]_{cyt} \cdot [E_{adapt}^{efflux}]}{k_7 + [E_{adapt}^{efflux}]}$$

wherein $[NO_3^-]_{cyt}$ refers to the first variable cytosolic nitrate which should be homeostatically controlled.

Putting $\frac{d[E_{adapt}^{efflux}]}{dt} = 0$ gives:

$$[NO_3^-]_{cyt} = \frac{k_5}{k_6} \cdot \frac{k_7 + [E_{adapt}^{efflux}]}{[E_{adapt}^{efflux}]}$$

Under the condition that $k_7 << [E_{adapt}^{efflux}]$,

$$[NO_3^-]_{cyt} = \frac{k_5}{k_6}$$

The vacuolar nitrate efflux rate is defined as $k_4 \cdot [NO_3^-]_{vac} \cdot [E_{adapt}^{efflux}]$. The variation trend of the controller can reflect the period for which homeostasis of cytosolic nitrate is observed.

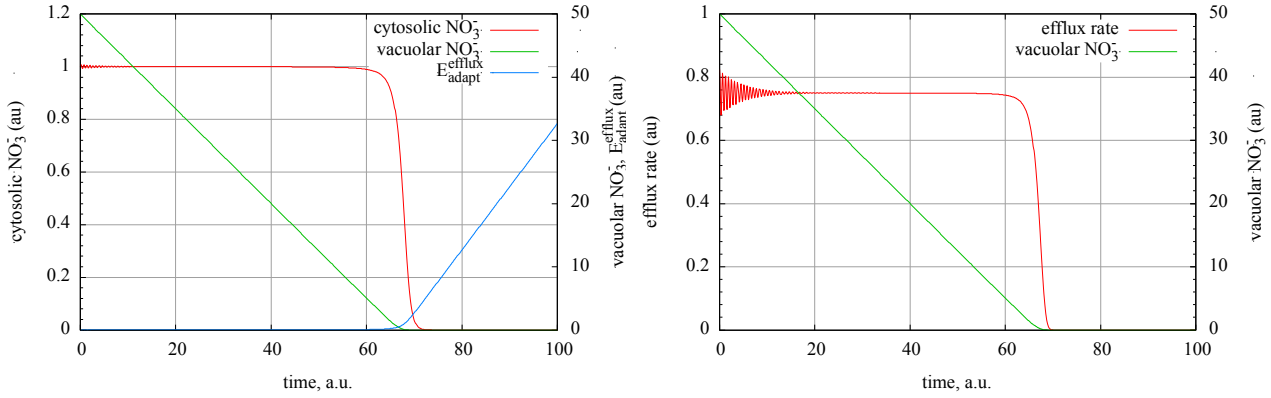

(a) (b)

Figure 4.20: The remobilization of vacuolar stored nitrate sustaining the homeostasis of cytosolic nitrate. The nitrate outflow from the vacuole gives rise to a steady decline of vacuolar nitrate until it is used up. The amount of inflow controller goes up steadily as soon as the vacuole is empty, and before that it is close to zero. The cytosolic nitrate drops quickly and runs out in a short moment immediately after no remobilization can occur. This can be an automatic switch to show how long the homeostasis can be maintained by this inflow controller.

In Figure 4.20, when cytosolic nitrate decreases to 0, $\frac{d[E_{adapt}^{efflux}]}{dt} = k_5$ and $[E_{adapt}^{efflux}]$ increases with zero-order kinetics. Actually, as long as its synethsis rate k_5 is higher than its degradation rate $\frac{k_6 \cdot [NO_3^-] \cdot [E_{adapt}^{efflux}]}{k_7 + [E_{adapt}^{efflux}]}$, $[E_{adapt}^{efflux}]$ will increase.

It is not only vacuolar nitrate but also environmental nitrate can be treated as a nitrate reservoir. Therefore, similar to $[E_{adapt}^{efflux}]$ in Figure 4.19(a), in Graph c of Figure 4.12, the concentration of inflow controller E_{adapt}^{uptake} climbs quickly when nitrate supply is used up.

If removal of cytosolic NO_3^- increases, a smaller period during which its homeostasis can be maintained is observed.

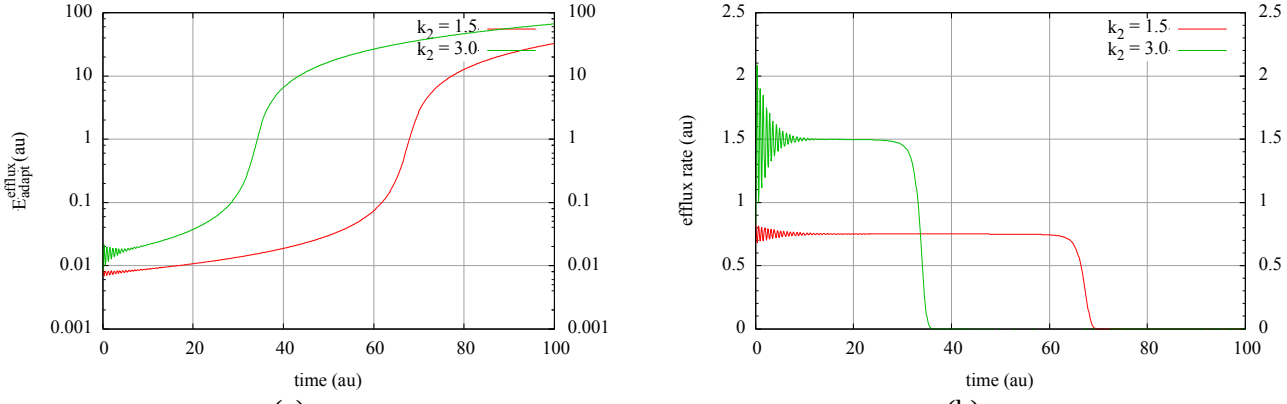

(a) (b)

Figure 4.21: (a) Corresponding to a higher removal rate of cytosolic NO_3^-, $[E_{adapt}^{efflux}]$ increases in order to transport more to compensate for the loss. (b) A higher removal rate yields a higher efflux rate from the vacuole and therefore a shorter period of homeostasis.

However, increasing k_4 will not shorten the duration of homeostasis as the concentration of controller will change in the opposite direction with k_4.

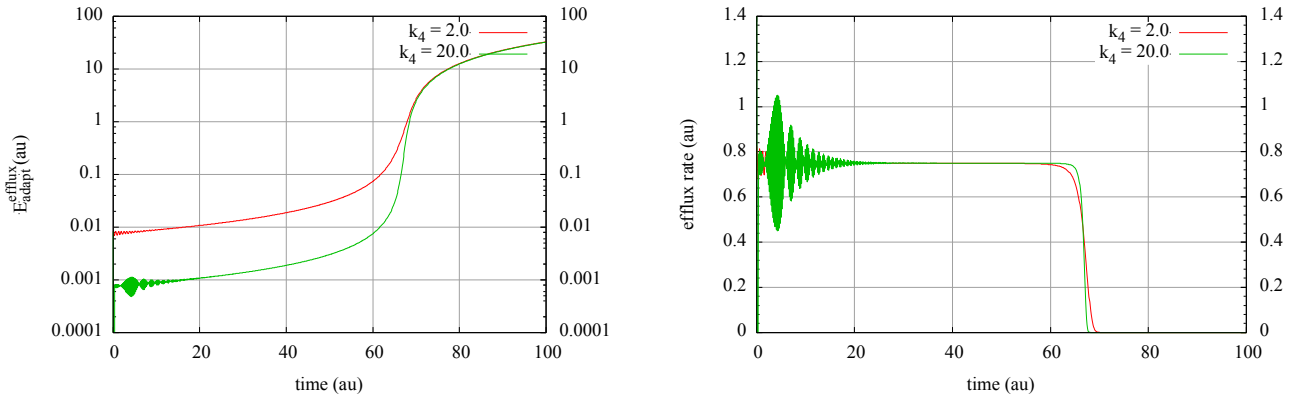

(a) (b)

Figure 4.22: (a) A higher k_4 is related to a lower $[E_{adapt}^{efflux}]$ (E_{adapt}^{efflux} is responshible for transporting nitrate out of the vacuole) (b) Due to the regulation of E_{adapt}^{efflux}, efflux rate does not change much even k_4 is rised by one order of magnitude.

We have four inflow controller networks to choose for the vacuolar nitrate efflux. In the last case, inflow controller V is applied. Under this condition, after nitrate is removed from the vacuole, the controller increases by zero-order kinetics due to its synthesis rate.

The other three inflow controllers function similarly. But after this compensation process, the different controllers will show different variation tendencies. Distinct from inflow controller V, we have found inflow controller II decreases when the reservoir is run out.

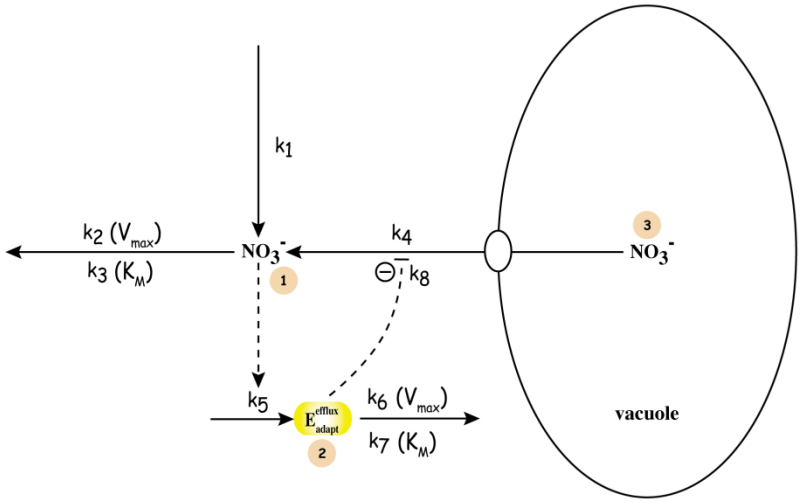

Figure 4.23: The inflow controller II is used to regulate the homeostasis of cytosolic nitrate which is maintained by the remobilization of vacuolar stored nitrate.

According to the differential equation of $[E_{adapt}^{efflux}]$:

$$\frac{d[E_{adapt}^{efflux}]}{dt} = k_5 \cdot [NO_3^-]_{cyt} - \frac{k_6 \cdot [E_{adapt}^{efflux}]}{k_7 + [E_{adapt}^{efflux}]}$$

Putting $\frac{d[E_{adapt}^{efflux}]}{dt} = 0$ gives:

$$[NO_3^-]_{cyt} = \frac{k_6}{k_5} \cdot \frac{[E_{adapt}^{efflux}]}{k_7 + [E_{adapt}^{efflux}]}$$

Under the condition that $k_7 << [E_{adapt}^{efflux}]$,

$$[NO_3^-]_{cyt} = \frac{k_6}{k_5}$$

The concentration of this controller decreases when nitrate homeostasis breaks.

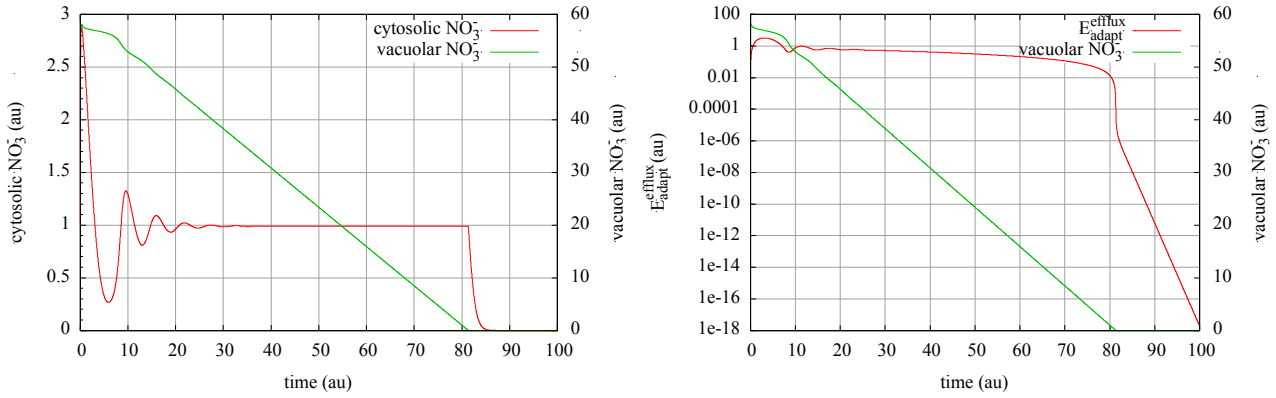

(a) (b)

Figure 4.24: (a) The homeostasis of cytosolic NO_3^- can be maintained as long as vacuolar NO_3^- is not depleted. (b) From the beginning, $[E_{adapt}^{efflux}]$ shows downtrend. After vacuolar NO_3^- is swallowed up, there will be no cytosolic NO_3^- to activate the production of E_{adapt}^{efflux} whose degration is still under way , so its decrease rate increases markedly.

When k_2 increases, $[E_{adapt}^{efflux}]$ will decrease more quickly to generate a higher efflux to make up for the loss of consumed nitrate.

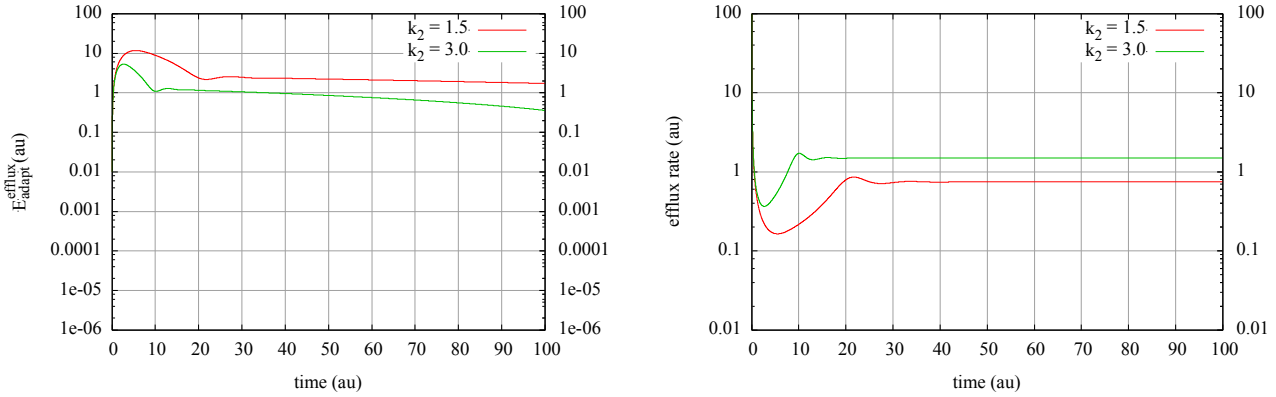

(a) (b)

Figure 4.25: Increasing k_2 makes the concentration of E_{adapt}^{efflux} decreases more quickly, and generates a higher efflux rate.

When k_4 increases, $[E_{adapt}^{efflux}]$ will also rise to counteract the effect of k_4 to the growth of efflux rate (efflux rate = $\frac{k_4 \cdot [NO_3^-]_{vac}}{k_8 + [E_{adapt}^{efflux}]}$) so that there will be no obvious change for efflux rate.

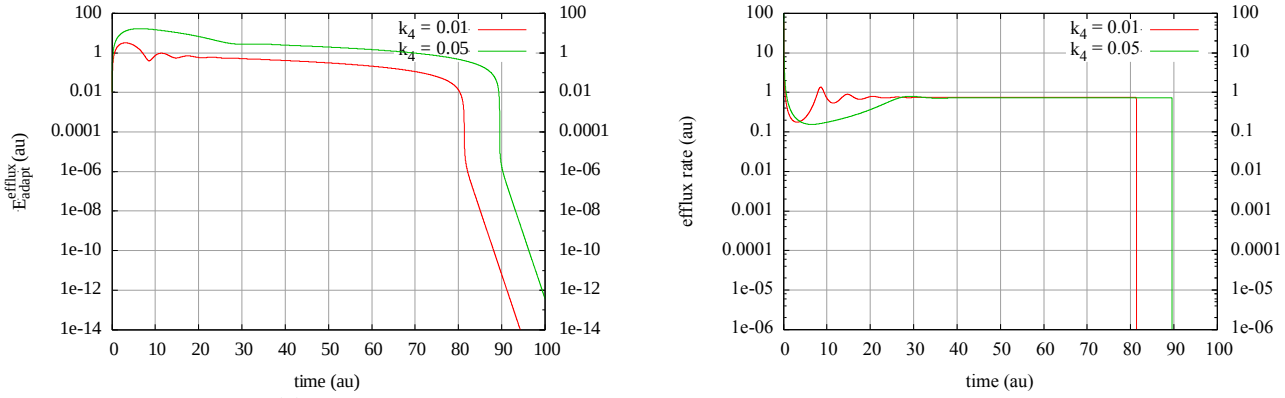

Figure 4.26: The concentration of $[E_{adapt}^{efflux}]$ arises with the increase of k_4, but efflux rate does not change.

4.2.2 The phenomena which can be succeeded to model

In this section I will show some phenomena which can be succeeded to model with Figure 4.18.

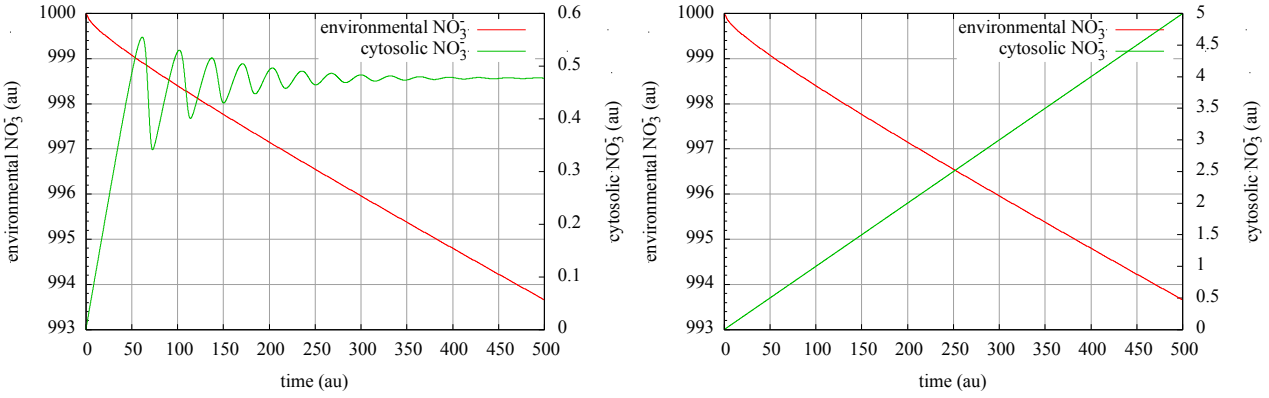

Figure 4.27: Loss-of-function nitrate reductase *Arabidopsis thaliana* strains retained the ability to transport nitrate. Furthermore, because of the lack of nitrate reductase activity, nitrate accumulated to a significantly higher level in such mutant compared with the wild-type level (25). This figure is for the comparison of plant nitrate uptake and nitrate accumulation between (a) wild type strain (b) nitrate reductase loss-of-function strain. Even without nitrate reducatase activity, nitrate transport can also happen since plants have more than one pathway for removing nitrate coming into the cell. For example, nitrate efflux can also happen in nitrate reductase loss-of-function strain (not shown here), and this removal step causes the uptake inflow controller E_{adapt}^{uptake} to transport nitrate into the cell to compensate for the loss.

When environmental nitrate is used up, the homeostasis of cytosolic nitrate is still maintained due to the remobilization of vacuolar storage.

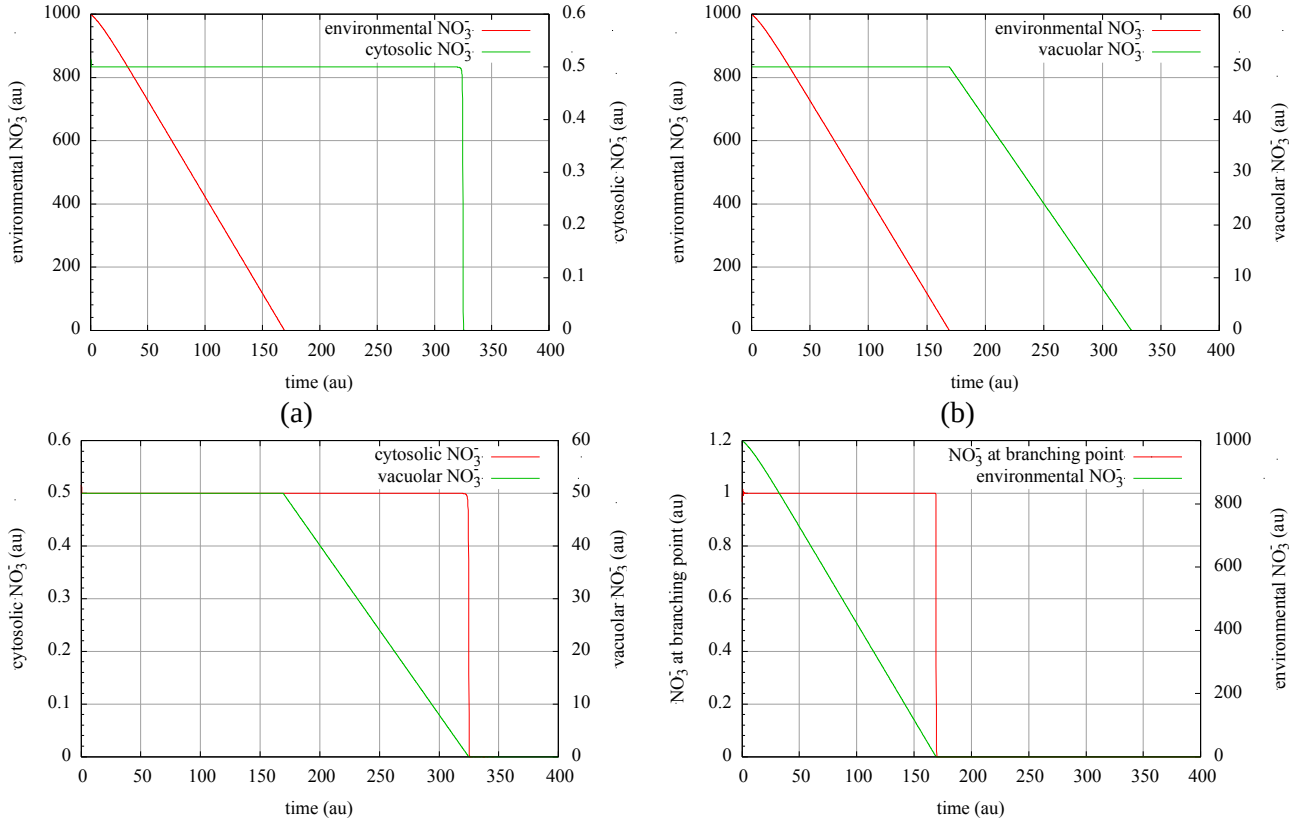

Figure 4.28: The relationship between $[NO_3^-]_{env}$, $[NO_3^-]_{bra}$, $[NO_3^-]_{cyt}$ and $[NO_3^-]_{vac}$. This calculation is based on the condition that the nitrate defining concentrations determined by *NR* and *NAXT1* are 0.5 and 2.0 while those by E_{adapt}^{uptake}, E_{adapt}^{efflux} and E_{adapt}^{influx} are 1.0, 0.5 and 50. (a) the homeostasis of cytosolic nitrate can still maintain after consuming up external nitrate supply (b) vacular nitrate began to decrease the moment nitrate supply is finished (c) the remobilization of vacuolar nitrate is responsible for maintaining the homeostasis of cytosolic nitrate when no external supply. (d) as long as environmental nitrate is not depleted, the homeostasis of nitrate at branching point is held.

We assume as long as $[NO_3^-]_{bra} \neq 0$, there is nitrate flowing out to the environment. As shown in Figure 4.28, the nitrate at branching point can only stay in a shorter duration of homeostasis than the cytosolic nitrate, which means nitrate efflux stops before the homeostasis of cytosolic nitrate breaks down.

Last but not least, it is often observed that the decrease of vacuolar nitrate with time out of external nitrate is a curve. Focalizing on two Chinese rice cultivars, Nong Ken (NK) and Yang Dao (YD), remobilization of nitrate in vacuoles is studied. These researchers suggest an exponential relationship $y=ae^{-bx}$ for the reduction of vacuolar nitrate (12).

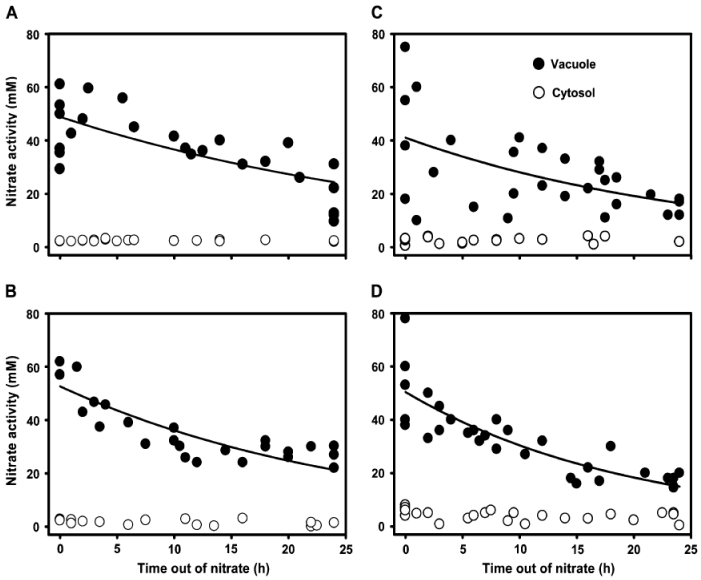

Figure 4.29: The nitrate activities in epidermal cells of rice roots and leaves measured with ion-selective microelectrodes during the first 24 h after removal of the external nitrate supply: (A) NK roots; (B) YD roots; (C) NK leaves; (D)YD leaves. The YD rice plants were cultivated in 10 mM nitrate and then nitrate was removed (no nitrogen source) from the cultivation solution. The nutrient solution for all these double-barrelled nitrate-selective microelectrode measurements contained no N (12).

In our model, the nitrate release from the vacuole gives rise to a linear decrease of vacuolar stored nitrate (see Figure 4.20 and 4.24). We found that in addition to the nitrate outflux from the vacuole, introducing a first order removal step for the vacuolar stored nitrate which is referred to k_{19} in Figure 4.18 can solve this problem.

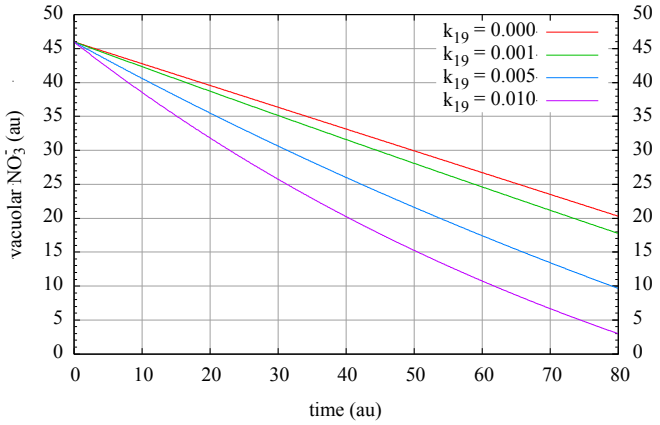

Figure 4.30: With a gradually increaseing leakage rate, the drop of vacuolar nitrate is closer to a curve. (This graph is generated with Figure 4.18 after external nitrate supply is used up)

Now the introduction of this leakage comes with a question: in plant physiology does this leakage really exist? As I mentioned before, nitrate can be transported from the vacuole into the symplasm and further transport to the xylem (see Figure 1.1). This makes it possible to add a simple first-order removal step to vacuolar nitrate. Actually, we can also give a first-order removal to cytosolic nitrate to stand for its transport into symplasm. However, this step is not included in the model, and adding it will not give dramatic influence to our modeling result.

4.2.3 The synergy of different controllers

When it comes to set nitrate defining values for nitrate branching point, it is reasonable to put the efflux outflow defining value higher than the uptake inflow defining one. From the experimental result, we know that in most cases there is little nitrate efflux detectable. In addition, when designing the calculation, we do not add nitrate efflux back to the environmental nitrate supply. If there is a significant efflux, this treatment will cause non-ignorable inaccuracy.

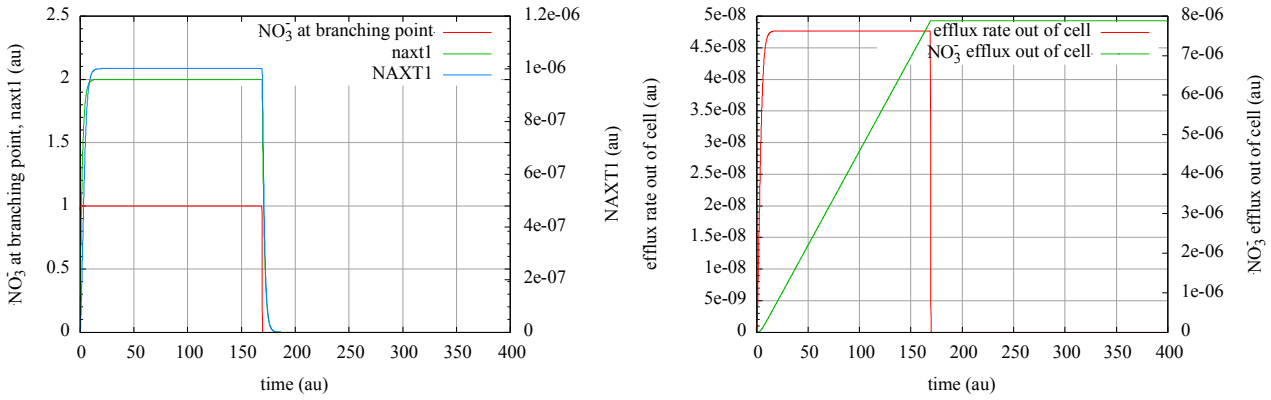

(a) (b)

Figure 4.31: When the nitrate defining point of *NAXT1* (2.0) is higher than that of E_{adapt}^{uptake} (1.0), (a) [*NAXT1*] is negligible while [*naxt1*] is not negligible. From the differential equation of [*naxt1*]: $\frac{d[naxt1]}{dt} = k_{27} \cdot [NO_3^-]_{bra} - k_{28} \cdot [naxt1]$, putting it to 0 gives the relationship $[naxt1] = \frac{k_{27}}{k_{28}} \cdot [NO_3^-]_{bra}$. In the calculation which corresponds to these two graphs, $\frac{k_{27}}{k_{28}} = 2$ and $[NO_3^-]_{bra}$ almost equals to 1, so [*naxt1*] is around 2. (b) Due to an extremely low [*NAXT1*], nitrate efflux rate as well as efflux amount out of cell are minimal. But efflux rate ($\frac{k_{30} \cdot [NO_3^-]_{bra} \cdot [NAXT1]}{k_{31} + [NO_3^-]_{bra}}$) whose variation is deppendt on [*NAXT1*] is constant before it collapses. When $[NO_3^-]_{bra}$ goes to 0, efflux stops immediately. Here efflux rate is constant before it stops. But in reality a progressively decreasing efflux is more likely than a stable one. In our model, $[NO_3^-]_{bra}$ can always keep in a certain level so long as exernal nitrate reservoir is not expended up, which makes it impossible to create a decreasing efflux.

Similar to the model described in Figure 4.9, the increase of inflow defining concentration by E_{adapt}^{uptake} generates a higher nitrate absorption rate and therefore shortens the duration it takes to deplete the environmental nitate. When nitrate defining concentration of *NAXT1* is not higher than that of E_{adapt}^{uptake}, [*NAXT1*] increases continuously until $[NO_3^-]_{bra}$ goes to 0. Before dropping $[NO_3^-]_{bra}$ can still keep in a certain level.

In Figure 4.28, we set the cytosolic nitrate defining concentrations by inflow controller (E_{adapt}^{efflux}) and outflow controller (*NR*) the same. If the former is higher than the latter, the similar result is observed: after the depletion of external nitrate, the homeostasis of cytosolic nitrate is held by the remobilization of vacuolar nitrate. The homeostasis of nitrate at branching point can be maintained until the depletion of external nitrate source. The cytosolic nitrate keeps in the same

level before and after the remobilization of vacuolar stored nitrate. However, if the inflow nitrate defining concentration is lower, a different level of cytosolic nitrate is observed after vacuolar nitrate starts to decrease. Next I will use three examples to demonstrate their principles.

In Figure 4.18, "vacuolar efflux rate" is defined as $19 \cdot k_{20} \cdot [NO_3^-]_{vac} \cdot [E_{adapt}^{efflux}]$. As long as k_{20} is not 0, the vacuolar nitrate efflux happens from the beginning in every case.

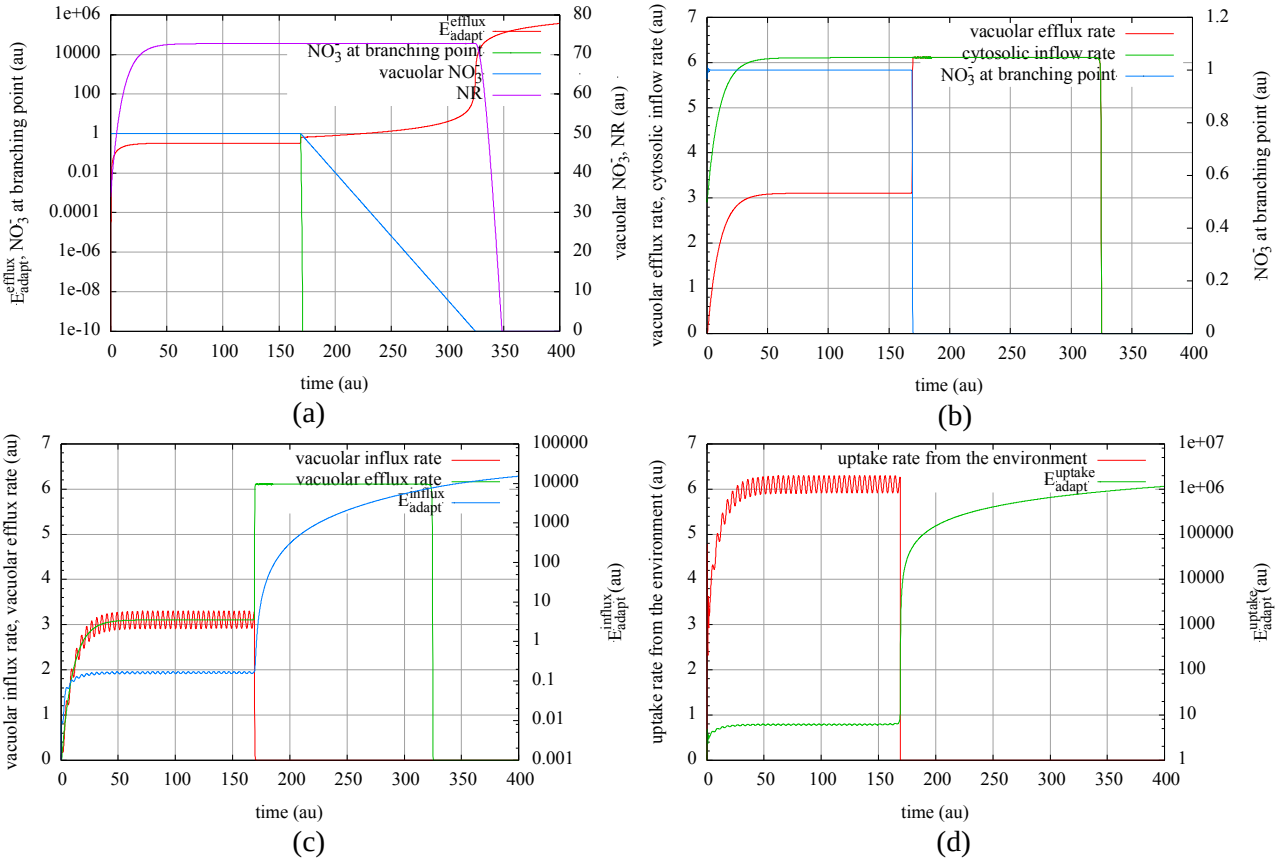

Figure 4.32: These four graphs are generated under the same condition that defining $[NO_3^-]$ by *NR* = defining $[NO_3^-]$ by E_{adapt}^{efflux} = 0.5, defining $[NO_3^-]$ by *NAXT1* = 2.0 > defining $[NO_3^-]$ by E_{adapt}^{uptake} = 1.0. (a) [*NR*] decreases quickly immediately the vacuole is empty. $[E_{adapt}^{efflux}]$ starts to increase the instant that $[NO_3^-]_{bra}$ goes to 0., which illustrates $[E_{adapt}^{efflux}]$ tries to transport more nitrate into the cytosol when the vacuole becomes the only nitrate source. According to the expression of vacuolar efflux rate ($19 \cdot k_{20} \cdot [NO_3^-]_{vac} \cdot [E_{adapt}^{efflux}]$), as long as $[NO_3^-]_{vac}$ can keep in the same level, $[E_{adapt}^{efflux}]$ can also be constant so as to generate a stable outflow transport. But when it comes to a decreasing $[NO_3^-]_{vac}$, it is impossible to get a constant efflux rate without a rising $[E_{adapt}^{efflux}]$. (b) Here cytosolic inflow rate is defined as the sum of vacuolar efflux rate ($19 \cdot k_{20} \cdot [NO_3^-]_{vac} \cdot [E_{adapt}^{efflux}]$) and nitrate flux from branching point ($k_{14} \cdot [NO_3^-]_{bra}$). When $[NO_3^-]_{bra}$ decreases to 0, vacuolar nitrate remobilization becomes the only source for cytosolic inflow and its rate increases to a higher level in order to keep the same level of cytosolic inflow rate. (Dealing with the same nitrate inflow speed, the outflow controller *NR* does not need to change its concentration. This is in agreement with the variation of [*NR*] in Graph a) (c) Until $[NO_3^-]_{bra} = 0$, vacuolar influx rate ($19 \cdot k_{15} \cdot [NO_3^-]_{bra} \cdot [E_{adapt}^{influx}]$) is vibrating around the same level with vacuolar efflux rate, which is the reason why $[NO_3^-]_{vac}$ can keep in a certain amount during this period. It is acheived by the regulation

of inflow controller E_{adapt}^{influx} whose concentration increases quickly when $[NO_3^-]_{vac}$ starts to decreas. In Figure 4.18, inflow controller network V is used for regulating the vacuolar nitrate efflux. The other three inflow networks will function similarly. (d) Uptake rate from the environment shows the similar variation tendency with vacuolar influx rate in Graph c. In order to makes up for the loss of $[NO_3^-]_{bra}$ which is sucked by the vacuole, the uptake rate should amount to the vacuolar influx.

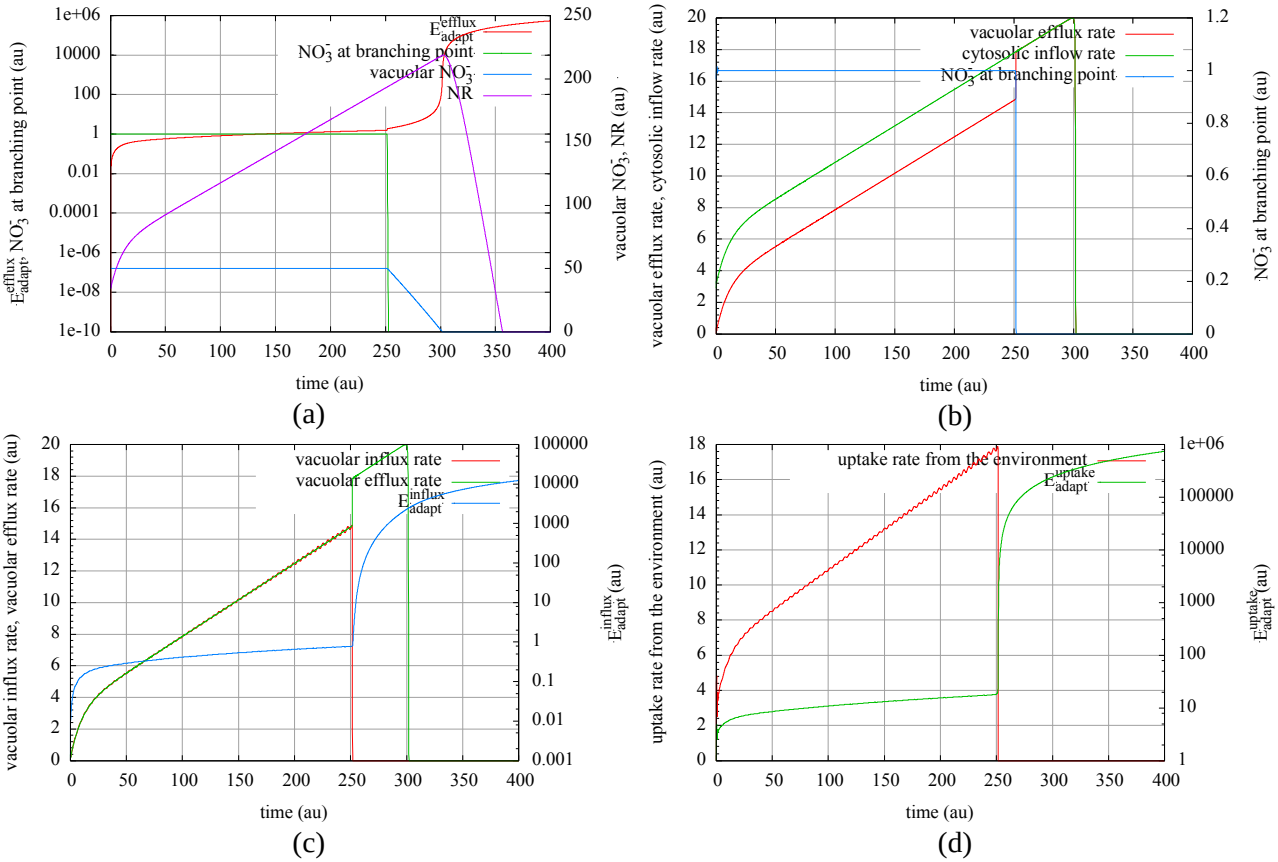

Figure 4.33. These four graphs are generated under the same condition that defining $[NO_3^-]$ by *NR* (0.5) is lower than defining $[NO_3^-]$ by E_{adapt}^{efflux} (0.55), defining $[NO_3^-]$ by *NAXT1* (2.0) is higher than defining $[NO_3^-]$ by E_{adapt}^{uptake} (1.0). (a) $[E_{adapt}^{efflux}]$ increases more quickly the moment $[NO_3^-]_{bra}$ goes to 0. [*NR*] is ever-increasing until the vacuole is empty. (b) When $[NO_3^-]_{bra} = 0$, vacuolar efflux rate equals to cytosolic inflow rate. The variation of the latter coincides with [*NR*]. (c) In order to compensate for the nitrate release caused by a continuously rising efflux, $[E_{adapt}^{influx}]$ also needs to increase itself to transport more nitrate into the vacuole. (d) Due to the growth of vacuolar efflux rate, uptake rate from the environment also needs to increase, which is achieved by the rise of $[E_{adapt}^{uptake}]$.

The $[NO_3^-]_{cyt}$ in both examples of Figure 4.32 and Figure 4.33 is always in the same level until the nitrate stored in the vacuole is used up.(not shown). The precondition that defining $[NO_3^-]$ by *NR* is not higher than that by E_{adapt}^{efflux} causes the unreasonable phenomenon that [*NR*] remains a continuously rising status (Note that although in Graph a of Figure 4.32, the increase of [*NR*] was almost invisible, but it did exist. Moreover, sometimes an obvious ever-increasing [*NR*] can also happen when defining $[NO_3^-]$s by *NR* and E_{adapt}^{efflux} are the same). In order to avoid it, we can try to assign a higher NO_3^- defining concentration of *NR*.

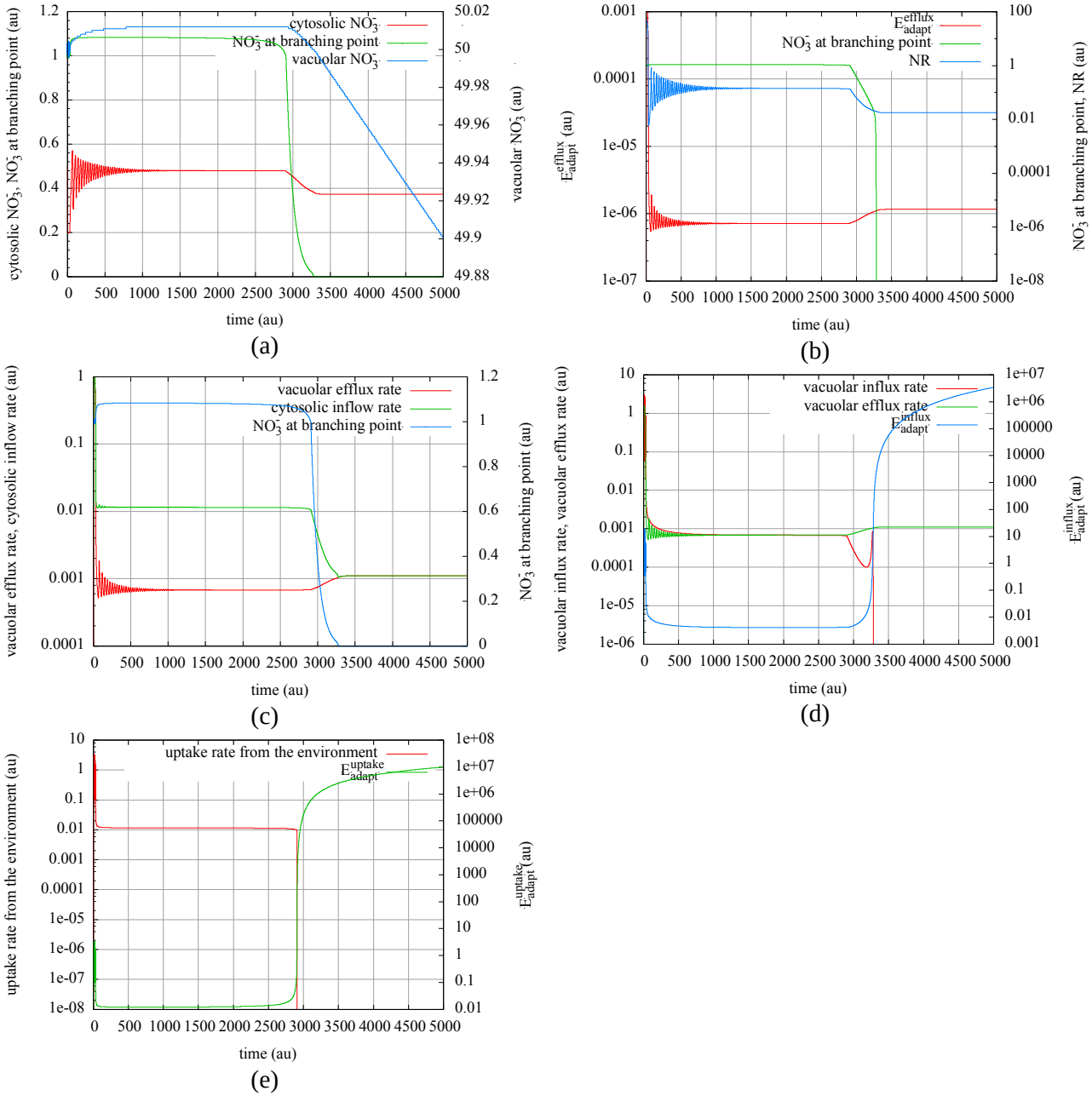

Figure 4.34. These five graphs are generated based on the condition that the defining concentrations determined by *NR*, E_{adapt}^{efflux}, *NAXT1*, E_{adapt}^{uptake} are 0.5, 0.2, 2.0, 1.0, respectively. (a) Distinct from the situation that defining concentration by *NR* is not higher than that by E_{adapt}^{efflux} ($[NO_3^-]_{cyt}$ can keep in the same level before the depletion of vauolar nitrate), here $[NO_3^-]_{cyt}$ undergoes a transition process which happens when $[NO_3^-]_{vac}$ starts to decrease. The depletion rate of $[NO_3^-]_{vac}$ is extraordinary low. (b) Similar to $[NO_3^-]_{cyt}$, $[NR]$ also shifts to a lower level when $[NO_3^-]_{bra}$ falls down. But at the meanwhile, $[E_{adapt}^{efflux}]$ rises to a higher level. (c) Differing from Figure 4.32 (b) and Figure 4.33 (b), the increase of vacuolar efflux rate is not enough to hold the same level of cytosolic inflow rate so that it falls to a lower level (d) Through the regulation of E_{adapt}^{influx}, vacuolar influx rate maintains in the same level until $[NO_3^-]_{vac}$ starts to drop and $[E_{adapt}^{influx}]$ climbs quickly. (e) Under the control of E_{adapt}^{uptake}, uptake rate from the environment keeps in a similar level and it does not need to increase since vacuolar influx rate is not increasing. In the three examples (Figure 4.32, 4.33 and 4.34), the amount of nitrate efflux to the environment is marginal.

In plant physiology, the remobilization of vacuolar stored nitrate allows the cytosolic nitrate concentration to keep in a similar level during subsequent periods when the external nitrogen supply becomes limiting. (10, 11, 12) This is not in agreement with our modeling result in Figure 4.30. Giving the same nitrate defining concentration both for *NR* and E_{adapt}^{efflux} helps us to fit this phenomenon. But this approach may lead to the problem of creating a continuously rising *NR* level, which is not realistic in plant physiology. The combination of inflow controller E_{adapt}^{efflux} and outflow controller *NR* is responsible for such an unreasonable phenomenon. In the model of fungal nitrate transport and assimilation, we tried to use inflow type II instead of V to avoid creating a continuously rising [*NR*] as defining concentrations of inflow (E_{adapt}^{uptake}) and outflow (*NR*) controller are the same.Here the combination of inflow controller II and outflow controller I is also helpful when modeling a transition for an automatic switch to regulate the remobilization of vacuolar nitrate with little change of NO_3^- level.

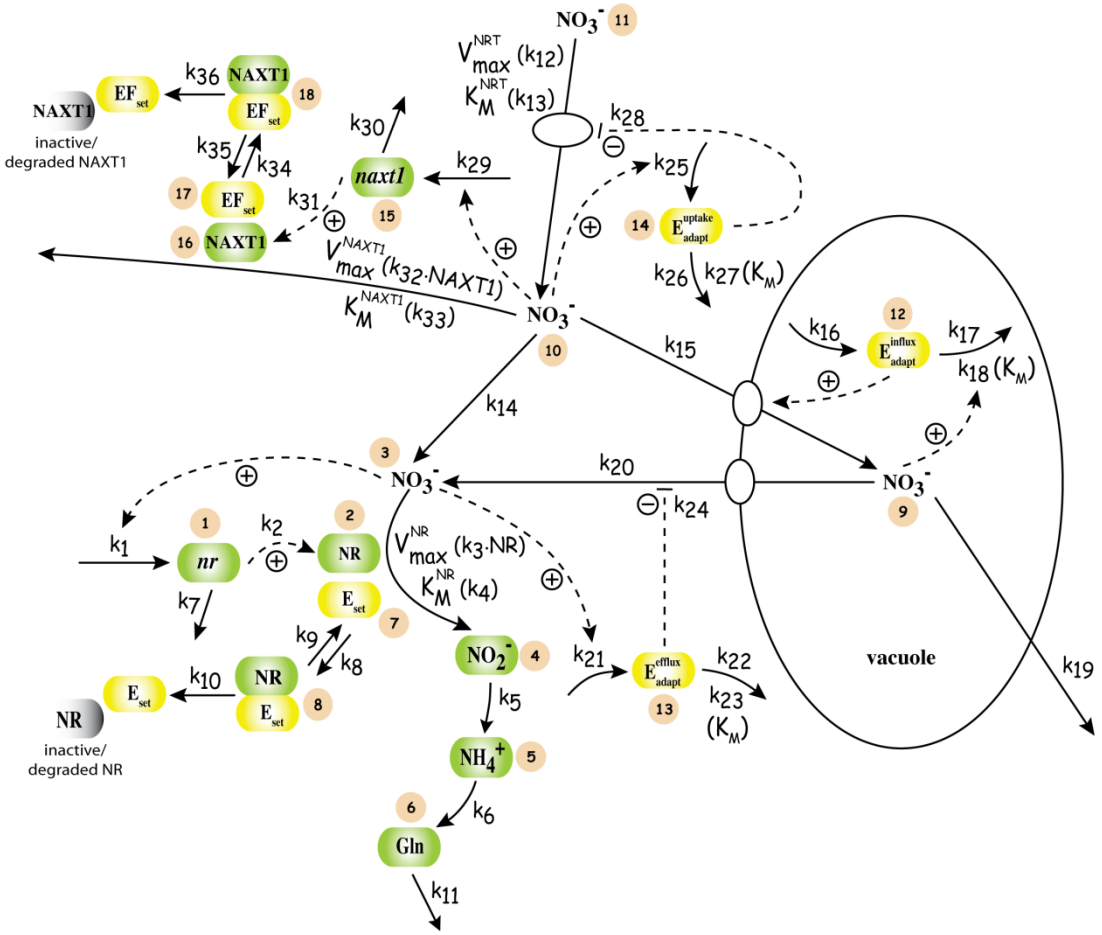

Figure 4.35: Scheme of nitrate transport and assimilation pathway for plants in which the inflow controller motif II is used for the nitrate flow out of the vacuole and the nitrate uptake from the environment. The inflow controller motif V is still used for the nitrate inflow into the vacuole.

In Figure 4.35, cytosolic nitrate concentration determined by E_{adapt}^{efflux} is as follows:

steady-state concentration: $[NO_3^-]_{cyt} = \frac{k_{22}}{k_{21}} \cdot \frac{[E_{adapt}^{efflux}]}{k_{23} + [E_{adapt}^{efflux}]}$

defining concentration: $[NO_3^-]_{cyt} = \frac{k_{22}}{k_{21}}$

vacuolar nitrate concentration determined by E_{adapt}^{influx} is as follows:

steady-state concentration: $[NO_3^-]_{vac} = \frac{k_{16}}{k_{17}} \cdot \frac{k_{18} + [E_{adapt}^{influx}]}{[E_{adapt}^{influx}]}$

defining concentration: $[NO_3^-]_{vac} = \frac{k_{16}}{k_{17}}$

nitrate concentration of branching point determined by E_{adapt}^{uptake} is as follows:

steady-state concentration: $[NO_3^-]_{bra} = \frac{k_{26}}{k_{25}} \cdot \frac{[E_{adapt}^{uptake}]}{k_{27} + [E_{adapt}^{uptake}]}$

defining concentration: $[NO_3^-]_{bra} = \frac{k_{26}}{k_{25}}$

cytosolic nitrate concentration determined by *NR* is as follows:

steady-state concentration: $[NO_3^-]_{cyt} = \frac{k_7 \cdot k_{10} \cdot ([E_{set}] + [NR \cdot E_{set}])}{k_1 \cdot k_2}$

defining concentration: $[NO_3^-]_{cyt} = \frac{k_7 \cdot k_{10} \cdot [NR \cdot E_{set}]}{k_1 \cdot k_2}$

cytosolic nitrate concentration determined by *NAXT1* is as follows:

steady-state concentration: $[NO_3^-]_{bra} = \frac{k_{30} \cdot k_{36} \cdot ([EF_{set}] + [NAXT1 \cdot EF_{set}])}{k_{29} \cdot k_{31}}$

defining concentration: $[NO_3^-]_{bra} = \frac{k_{30} \cdot k_{36} \cdot [NAXT1 \cdot EF_{set}]}{k_{29} \cdot k_{31}}$

With the introduction of inflow controller II, it is possible to avoid a continuously rising *NR* when nitrate defining concentrations determined by *NR* and E_{adapt}^{efflux} controllers are the same. In Figure 4.35, we still keep a higher efflux defining nitrate concentration than that of E_{adapt}^{efflux}.

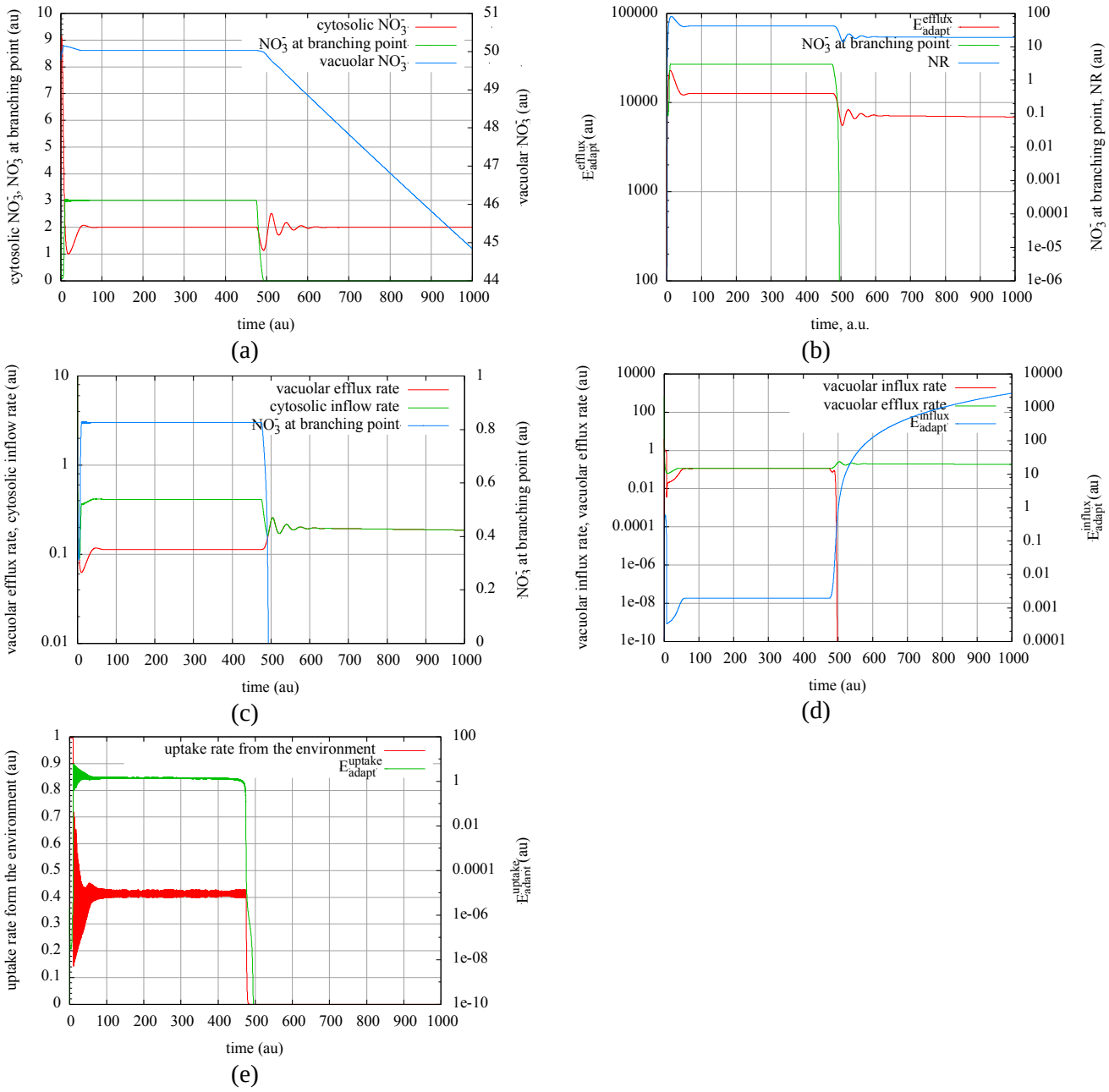

Figure 4.36: Both the nitrate defining concentrations controlled by *NR* and E_{adapt}^{efflux} are set to 2.0, and *NAXT1* controlled one is 4.0 which is higher than that of E_{adapt}^{uptake} (3.0). (a)When the homeostasis of cytosolic nitrate is held by the discharge of vacuole, the similar level of $[NO_3^-]_{cyt}$ is kept. (b) When $[NO_3^-]_{bra}$ drops, both $[E_{adapt}^{efflux}]$ and $[NR]$ go to a lower level. (c) the reason for the decrese of $[NR]$ is that cytosolic inflow rate moves to a lower level although vacuolar efflux rate rises. In order to generate a faster vacuolar efflux, in Graph b $[E_{adapt}^{efflux}]$ has to decrease itself . Note that the definition of vacuolar efflux rate is $\frac{k_{20} \cdot [NO_3^-]_{vac}}{k_{24} + [E_{adapt}^{efflux}]}$ and it increases with the decrease of $[E_{adapt}^{efflux}]$. (d) Due to the existence of E_{adapt}^{influx}, vacuolar influx almost equals to vacuolar efflux (e) uptake rate can keep in a certain level before it falls down.

So far we are unable to design a remobilization process which can meet both these two requirements of maintaining the same *NR* and nitrate level. Even if the cytoslic nitrate is always controlled by *NR* before and after the exhaustion of external nitrate supply, which can make the cytosolic nitrate keep in the same level, it is still difficult to ensure a nitrate flow with a consistent rate to be reduced by *NR*. Dealing with different nitrate fluxes, [*NR*] will not be uniform.

4.3 Circadian oscillations in nitrate assimilation

4.3.1 The character of the oscillation of *NR* feedback loop (no *NMR* production)

4.3.1.1 The trait of limit cycle oscillations

Next I want to model some oscillation phenomena for *Neurospora crassa*. Due to limited time, I have not explored the oscillation caused by inflow controller feedback loop. For the sake of simplicity, Figure 4.1 is taken as research subject here. In an attempt to determine a nitrate concentration, it is necessary to assign a negligible value to $K_M^{E_{set}}$, which will be discussed in more detail in Section 4.3.1.2.

With our outflow model for *Neurospora crassa*, a limit cycle oscillation is observed, which means after a sudden rise or decrease in nitrate concentration, the oscillation of *nr*, *NR* and NO_3^- will go back to its original situation. From such limit cycle oscillation it is easy to see the variation of amplitude after the introduction of phase plane between variables.

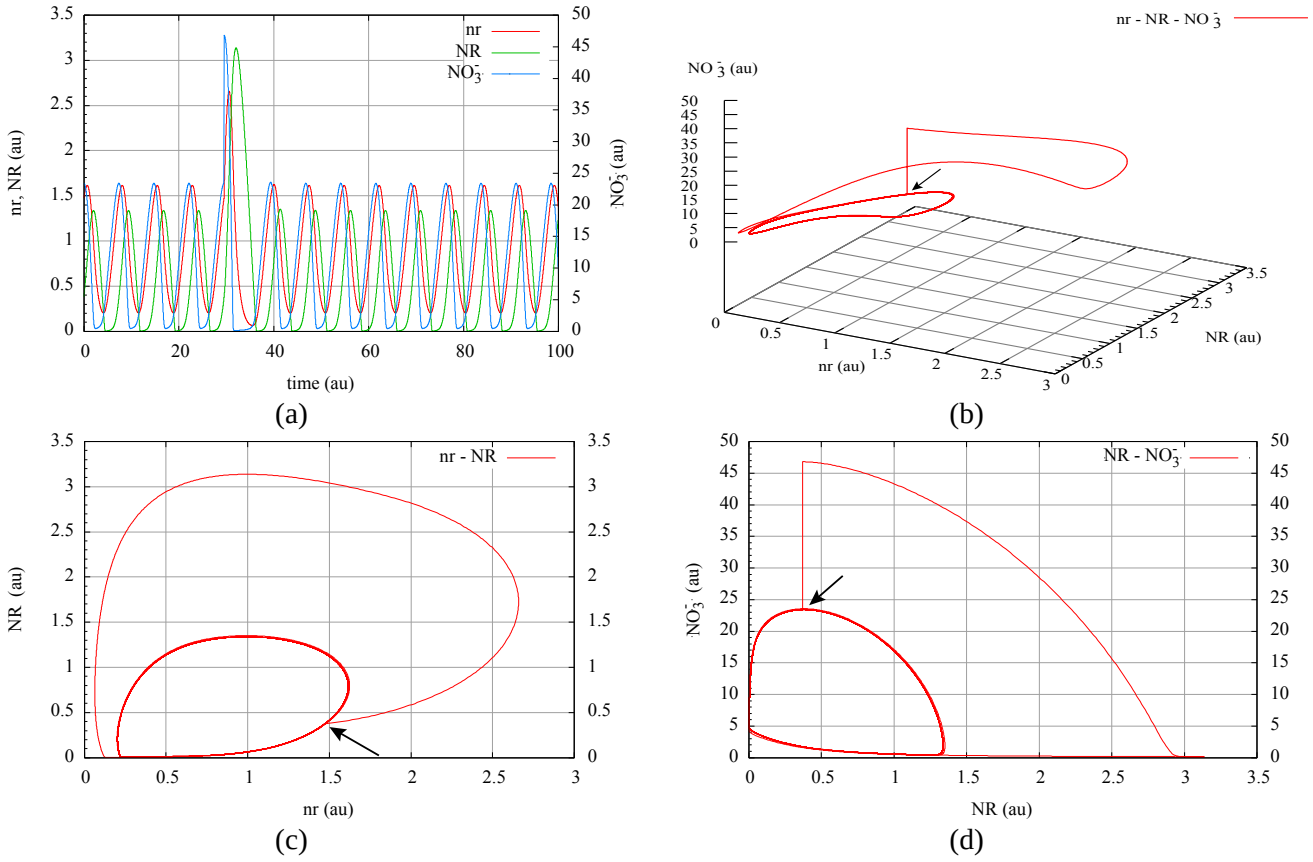

Figure 4.37. The concentration of nitrate is doubled when it happens to be a maximum (indicated by the arrow in Graph b, c and d). Responding to this perturbation, *NR* increases its concentration in order to keep the homeostasis. Shortly, the oscillation of each variable goes back to the original state. This is the feature of limit cycle oscillation. Actually, not noly NO_3^-, those changes happened to the concentrations of *nr*, *NR*, NO_2^-, NH_4^+ and *Gln* will not affect the result, either.

Distinct from a sudden increase in the nitrate concentration, the change of inflow rate constant will give us a divergent oscillation which can not go back to its initial condition. This also happens when other rate constants change. As regard to what kind of influence can be given by each rate constant, we will disscuss it in Section 4.3.1.3.

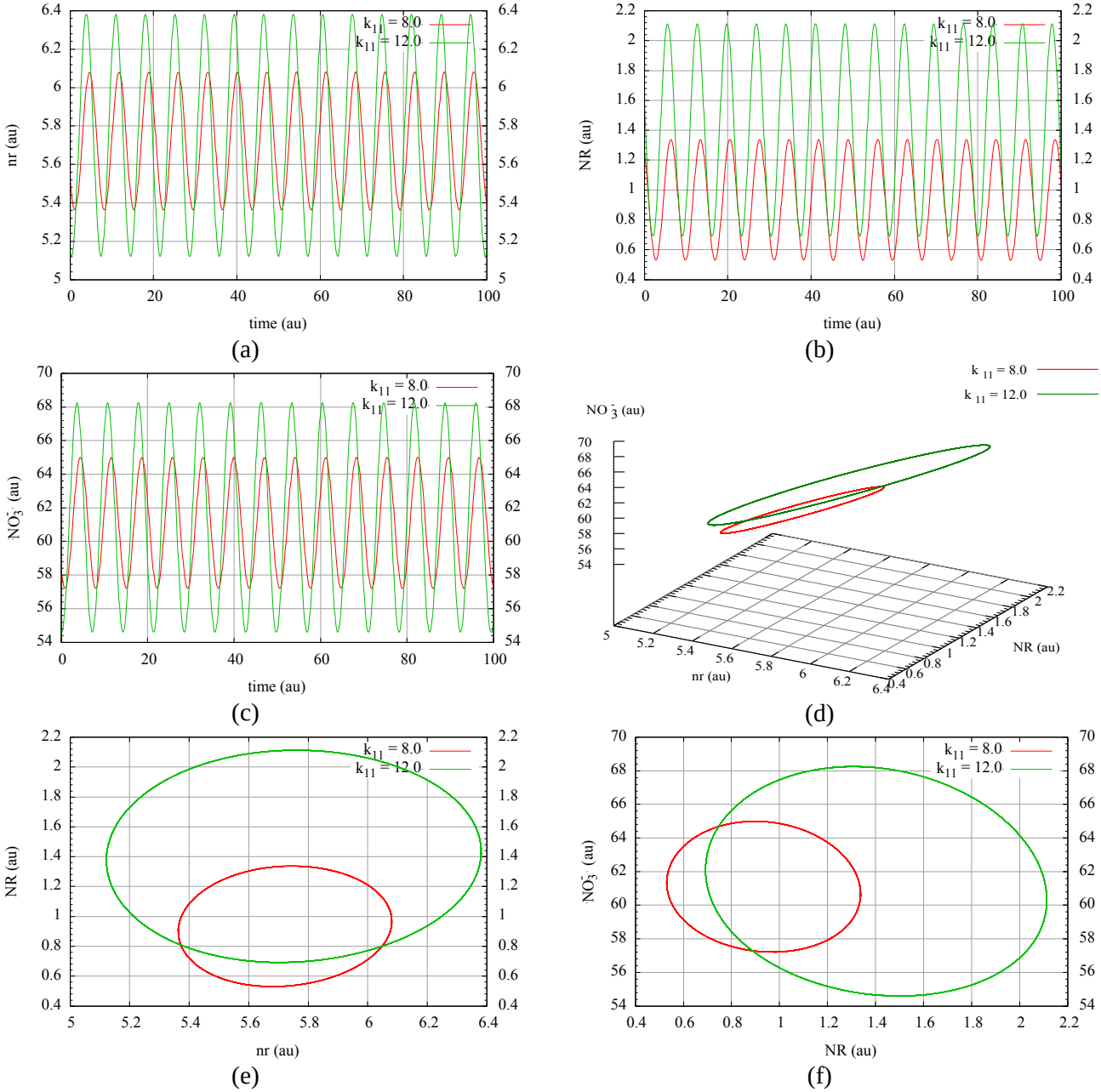

Figure 4.38. Distinct from Figure 4.37, when transport rate reaches a new level, the system will approach a new limit cycle. In this example, a larger cycle is observed when transport rate rises by 50%. It is clear that the amplitude of all these three variables increases.

Generally, in our model described in Figure 4.1, the oscillation state is regulated by rate constants but independent of the concentrations.

4.3.1.2 The necessity for zero-order removal of *NR*

Next I will demonstrate the necessity for the existence of a zero-order removal step. From the view of determining a definite period length, a negligible $K_M^{E_{set}}$ is essential. Decreasing $K_M^{E_{set}}$ will not destroy the existing oscillation and causes little change to set point, but give rise to a longer period. When $K_M^{E_{set}}$ is decreased to a certain extent, the period length becomes stable.

As I mentioned before, a too low $K_M^{E_{set}}$ value will cause some negative values of *NR* and other intermediates. So I will use Figure 4.4 as the model to demonstrate this question. Through rising $k_f^{E_{set}}$ (k_9), the drop of $K_M^{E_{set}}$ is accomplished.

Table 4.1: Period lengths on different $K_M^{E_{set}}$ values

$k_f^{E_{set}}$	$k_r^{E_{set}}$	$k_{cat}^{E_{set}}$	$K_M^{E_{set}}$	Period length
1×10^{1}	0.5	0.5	1×10^{-1}	12.9243
1×10^{2}	0.5	0.5	1×10^{-2}	31.4533
1×10^{3}	0.5	0.5	1×10^{-3}	33.7769
1×10^{4}	0.5	0.5	1×10^{-4}	34.0846
1×10^{5}	0.5	0.5	1×10^{-5}	34.1286
1×10^{6}	0.5	0.5	1×10^{-6}	34.1345
1×10^{7}	0.5	0.5	1×10^{-7}	34.1321
1×10^{8}	0.5	0.5	1×10^{-8}	34.1286

(In Table 4.1, $K_M^{E_{set}}$ is defined as $\frac{k_r^{E_{set}} + k_{cat}^{E_{set}}}{k_f^{E_{set}}}$. The variation of $K_M^{E_{set}}$ is accomplished by increasing or decreasing $k_f^{E_{set}}$.)

A low $K_M^{E_{set}}$ is also mandatory for the existence of oscillation. I have not found out a reasonable explanation to it. Here we treat it as a known condition.

Thinking this necessity in term of steady-state concentration, uniform result is obtained.

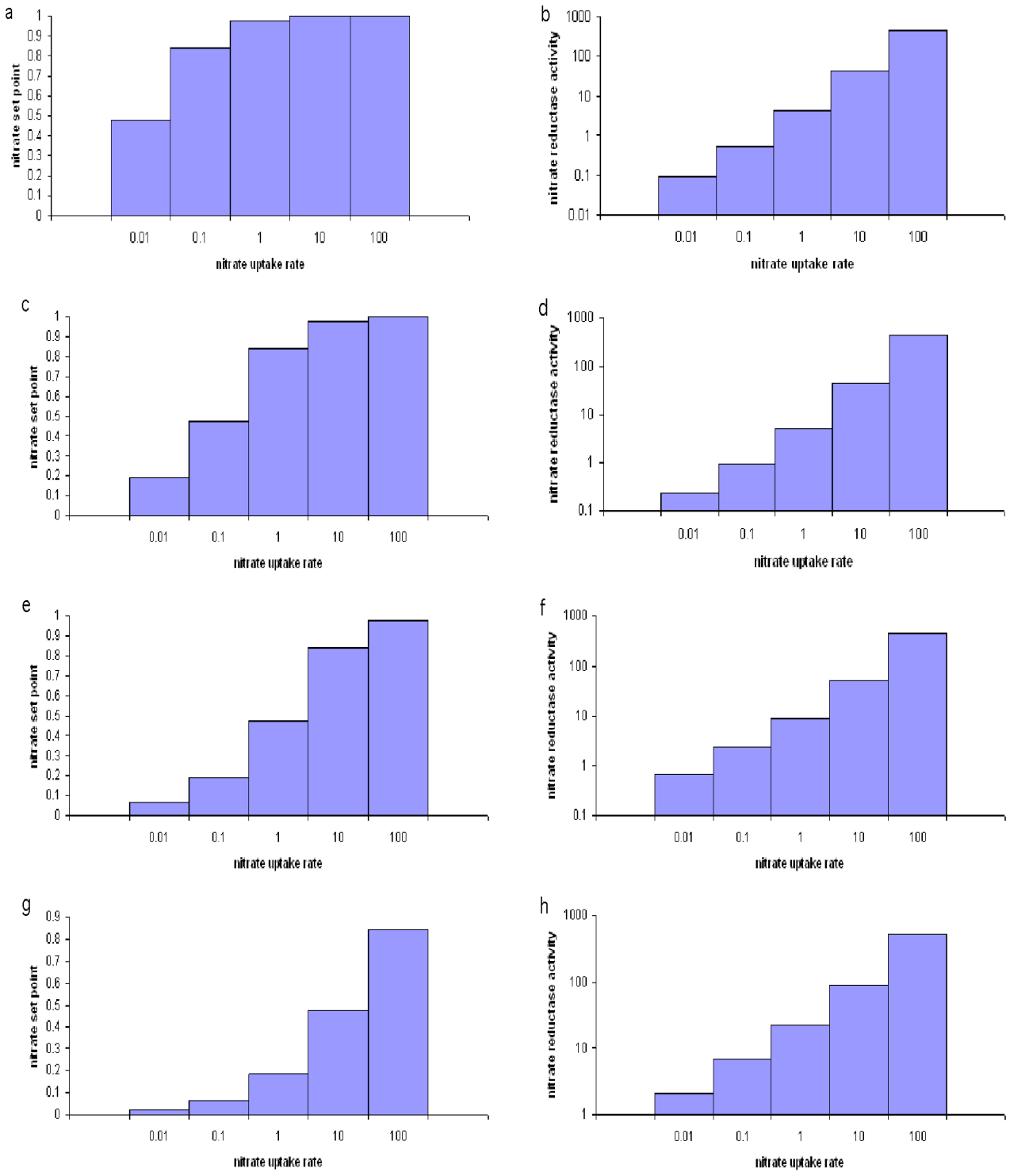

Figure 4.39. Data are generated in Figure 4.4. Nitrate transport rate is assumed to be constant. In different $K_M^{E_{set}}$ values (in a and b, $K_M^{E_{set}}$ = 0.1; in c and d, $K_M^{E_{set}}$ =1.0; in e and f, $K_M^{E_{set}}$ =10.0; in g and h, $K_M^{E_{set}}$ =100.0) nitrate set point (or steady state concentration) and nitrate reductase activity are plotted against nitrate uptake rates which are varied by over five orders of magnitude. In each calculation nitrate defining point is 1.0. The increase of $K_M^{E_{set}}$ is achieved by rising k_9, through which nitrate defining concentration is still the same. Note that the coordinate of nitrate reductase activity is established in logarithmic scale.

For each case the higher the inflow is, the closer the nitrate is to its defining concentration. A higher $K_M^{E_{set}}$ causes a higher *NR* level and a lower nitrate level. Furthermore, it gives rise to a relatively strong sensitivity of nitrate set point to environmental variation, which is not in conformity with the requirement of homeostasis. From it we can see the necessity for the existence of a zero-order removal step for *NR* degradation. But no matter the degree of such sensitivity is high or low, the amount of *NR* is always significantly related to the growth of inflow.

4.3.1.3 The influence of rate constants

In our model, there are many ways to create or destroy the oscillation. Through those rate constants inside the *NR* feedback loop, we can easily generate oscillatory or non-oscillatory behavior. For example, the rise of K_M^{NR} causes the loss of oscillation. Through changing the amount of [*nr*] and [*NR*] by their synthesis or degradation rates, it is feasible to create a new oscillatory state with the divergent amplitude and period length.

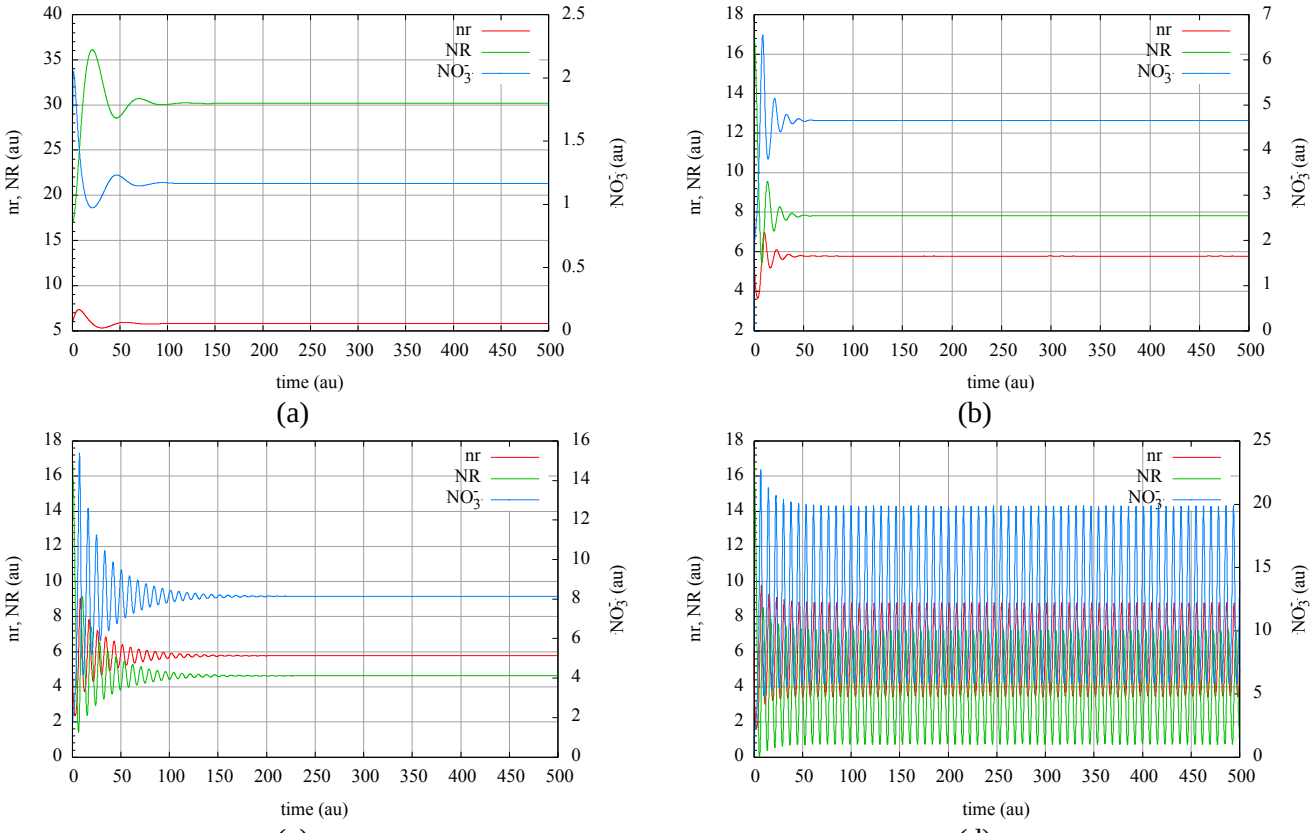

Figure 4.40. A large k_4 causes the loss of oscillation. Via increasing k_8, a new oscillation is generated. (a) k_8 = 0.1 (b) k_8 = 0.4 (c) k_8 = 0.7 (d) k_8 = 1.0.

No matter any way we use to generate a new oscillation, it will change nitrate set point. In this case the increase of k_8 results in a lower *NR* level. This will lead to the growth of nitrate set point.

Table 4.2: Period length when changing rate constants to adjust the oscillation (no *NMR* production)

k_4	k_0	k_2	k_8	k_9	k_{11}	k_{13}	Period length
1.10	0.50	1.00	0.05	5.7875	8.00	0.0001	23.83
95.50	0.05	1.00	0.05	5.7875	8.00	0.0001	38.71
95.50	0.50	0.10	0.05	5.7875	8.00	0.0001	38.71
95.50	0.50	1.00	5.00	5.7875	8.00	0.0001	7.02
95.50	0.50	1.00	0.05	57.875	8.00	0.0001	15.45
95.50	0.50	1.00	0.05	5.7875	0.80	0.0001	36.55
95.50	0.50	1.00	0.05	5.7875	8.00	2.00	34.52

The first set of data in Table 4.2 states the reference condition. If k_4 is increased to 95.5 (a high enough value which is able to destroy the oscillation), the rate constants through whose change the oscillation can be rescued are listed. Each time the only one rate constant (which is marked by red color) is changed while others are still the same. Those rate constants that are useless to get the oscillation back are not included in this table.

We also need to point out that with those rate constants which are able to readjust the oscillation, destroying the oscillation that already exists can be also easily achieved.

Table 4.3: Period length and set point varying with different rate constants (no *NMR* production)

k_0	k_2	k_3	k_4	k_8	k_9	k_{10}	k_{11}	k_{13}	Period length	Set point
0.50	1.00	22.0	1.10	0.05	5.7875	0.01	8.00	0.20	19.9333	1.1575
0.75	1.00	22.0	1.10	0.05	5.7875	0.01	8.00	0.20	22.0955	0.7717
0.25	1.00	22.0	1.10	0.05	5.7875	0.01	8.00	0.20	17.1571	2.3150
0.50	1.50	22.0	1.10	0.05	5.7875	0.01	8.00	0.20	22.0955	0.7717
0.50	0.50	22.0	1.10	0.05	5.7875	0.01	8.00	0.20	17.1536	2.3150
0.50	1.00	33.0	1.10	0.05	5.7875	0.01	8.00	0.20	13.9114	1.1575
0.50	1.00	11.0	1.10	0.05	5.7875	0.01	8.00	0.20	30.8933	1.1575
0.50	1.00	22.0	1.65	0.05	5.7875	0.01	8.00	0.20	20.8087	1.1575
0.50	1.00	22.0	0.55	0.05	5.7875	0.01	8.00	0.20	19.0320	1.1575
0.50	1.00	22.0	1.10	0.075	5.7875	0.01	8.00	0.20	14.3794	1.7362
0.50	1.00	22.0	1.10	0.025	5.7875	0.01	8.00	0.20	36.7500	0.5787
0.50	1.00	22.0	1.10	0.05	8.68125	0.01	8.00	0.20	14.3145	1.7363
0.50	1.00	22.0	1.10	0.05	2.89375	0.01	8.00	0.20	33.8241	0.5787
0.50	1.00	22.0	1.10	0.05	5.7875	0.015	8.00	0.20	18.0944	1.1575
0.50	1.00	22.0	1.10	0.05	5.7875	0.005	8.00	0.20	22.0023	1.1575
0.50	1.00	22.0	1.10	0.05	5.7875	0.01	12.0	0.20	27.9714	1.1575
0.50	1.00	22.0	1.10	0.05	5.7875	0.01	4.00	0.20	9.1954	1.1575
0.50	1.00	22.0	1.10	0.05	5.7875	0.01	8.00	0.30	18.9038	1.4469
0.50	1.00	22.0	1.10	0.05	5.7875	0.01	8.00	0.10	21.4273	0.8681

The first set of data in Table 4.3 states the reference condition. Based on it, each rate constant is increased or decreased by 50% (the changed constant is in red color), individually. From this table, the constants k_3, k_4, k_{10} and k_{11} can only influence the period. Because the derivation of nitrate set point involves approximation, it is not sufficient to justify the independency between set point and k_3, k_4, k_{10} and k_{11} in this table.

The variation of period length depending on rate constants is very variable and it is not possible to pool results in different reference conditions. We have not found out the law of period increase or decrease tendency yet.

A higher $K_M^{E_{set}}$ can make the oscillation dwindle away, in which condition it is easy to determine a definite [*NR*] or $[NO_3^-]$. In Table 4.4 below, k_{10} is increased to 1.0 in which condition no oscillation can happen. Each rate constant is increased to decreased by 50% (in red color), [*nr*], [*NR*], $[NO_3^-]$, $[NO_2^-]$, $[NH_4^+]$ and [*Gln*] are noted down.

Table 4.4: $[NR]$, $[NO_3^-]$, $[NO_2^-]$, $[NH_4^+]$and $[Gln]$ varying with different rate constants (no *NMR* production)

k_0	k_2	k_3	k_4	k_5	k_6	k_8	k_9	k_{10}	k_{11}	k_{13}	k_{14}	$[nr]$	$[NR]$	$[NO_3^-]$	$[NO_2^-]$	$[NH_4^+]$	$[Gln]$
1.0	1.0	20.0	50.0	1.0	1.0	5.0	5.0	1.0	8.0	0.2	1.0	2.6726	1.1483	26.7261	8.0000	8.0000	8.0000
1.5	1.0	20.0	50.0	1.0	1.0	5.0	5.0	1.0	8.0	0.2	1.0	2.9356	1.4220	19.5703	8.0000	8.0000	8.0000
0.5	1.0	20.0	50.0	1.0	1.0	5.0	5.0	1.0	8.0	0.2	1.0	2.2804	0.8385	45.6083	8.0000	8.0000	8.0000
1.0	1.5	20.0	50.0	1.0	1.0	5.0	5.0	1.0	8.0	0.2	1.0	1.9570	1.4220	19.5703	8.0000	8.0000	8.0000
1.0	0.5	20.0	50.0	1.0	1.0	5.0	5.0	1.0	8.0	0.2	1.0	4.5608	0.8385	45.6083	8.0000	8.0000	8.0000
1.0	1.0	30.0	50.0	1.0	1.0	5.0	5.0	1.0	8.0	0.2	1.0	2.2942	0.8479	22.9416	8.0000	8.0000	8.0000
1.0	1.0	10.0	50.0	1.0	1.0	5.0	5.0	1.0	8.0	0.2	1.0	3.3333	2.0000	33.3333	8.0000	8.0000	8.0000
1.0	1.0	20.0	75.0	1.0	1.0	5.0	5.0	1.0	8.0	0.2	1.0	2.9356	1.4220	29.3555	8.0000	8.0000	8.0000
1.0	1.0	20.0	25.0	1.0	1.0	5.0	5.0	1.0	8.0	0.2	1.0	2.2804	0.8385	22.8042	8.0000	8.0000	8.0000
1.0	1.0	20.0	50.0	1.5	1.0	5.0	5.0	1.0	8.0	0.2	1.0	2.6726	1.1483	26.7261	5.3333	8.0000	8.0000
1.0	1.0	20.0	50.0	0.5	1.0	5.0	5.0	1.0	8.0	0.2	1.0	2.6726	1.1483	26.7261	16.0000	8.0000	8.0000
1.0	1.0	20.0	50.0	1.0	1.5	5.0	5.0	1.0	8.0	0.2	1.0	2.6726	1.1483	26.7261	8.0000	5.3333	8.0000
1.0	1.0	20.0	50.0	1.0	0.5	5.0	5.0	1.0	8.0	0.2	1.0	2.6726	1.1483	26.7261	8.0000	16.0000	8.0000
1.0	1.0	20.0	50.0	1.0	1.0	7.5	5.0	1.0	8.0	0.2	1.0	2.4332	0.9480	36.4984	8.0000	8.0000	8.0000
1.0	1.0	20.0	50.0	1.0	1.0	2.5	5.0	1.0	8.0	0.2	1.0	3.1323	1.6770	15.6613	8.0000	8.0000	8.0000
1.0	1.0	20.0	50.0	1.0	1.0	5.0	7.5	1.0	8.0	0.2	1.0	3.6498	0.9480	36.4984	8.0000	8.0000	8.0000
1.0	1.0	20.0	50.0	1.0	1.0	5.0	2.5	1.0	8.0	0.2	1.0	1.5661	1.6770	15.6613	8.0000	8.0000	8.0000
1.0	1.0	20.0	50.0	1.0	1.0	5.0	5.0	1.5	8.0	0.2	1.0	2.2942	1.2718	22.9416	8.0000	8.0000	8.0000
1.0	1.0	20.0	50.0	1.0	1.0	5.0	5.0	0.5	8.0	0.2	1.0	3.3333	1.0000	33.3333	8.0000	8.0000	8.0000
1.0	1.0	20.0	50.0	1.0	1.0	5.0	5.0	1.0	12.0	0.2	1.0	3.0619	1.5798	30.6186	12.0000	12.0000	12.0000
1.0	1.0	20.0	50.0	1.0	1.0	5.0	5.0	1.0	4.0	0.2	1.0	2.0412	0.6899	20.4124	4.0000	4.0000	4.0000
1.0	1.0	20.0	50.0	1.0	1.0	5.0	5.0	1.0	8.0	0.3	1.0	2.5376	1.0305	31.7197	8.0000	8.0000	8.0000
1.0	1.0	20.0	50.0	1.0	1.0	5.0	5.0	1.0	8.0	0.1	1.0	2.8571	1.3333	21.4286	8.0000	8.0000	8.0000
1.0	1.0	20.0	50.0	1.0	1.0	5.0	5.0	1.0	8.0	0.2	1.5	2.6726	1.1483	26.7261	8.0000	8.0000	5.3333
1.0	1.0	20.0	50.0	1.0	1.0	5.0	5.0	1.0	8.0	0.2	0.5	2.6726	1.1483	26.7261	8.0000	8.0000	16.0000

Except the case when changing k_3, k_4 and k_{11}, every time the increase of [*NR*] causes the decrease of $[NO_3^-]$. Increasing or decreasing k_{11} is the only way to increase or decrease every variable at the same time. In Table 4.4 since k_{10} is not negligible, nitrate can not keep in the same level with a varied k_{11} value. In addition to k_{11}, the removal step of NO_2^-, NH_4^+ and *Gln* (k_5, k_6 and k_{14}) can also affect their concentration but in the opposite direction. Distinct from k_3, k_4 and k_{11}, k_1, k_2, k_8, k_9 and k_{10} achieves the control of nitrate by adjusting the amount of [*nr*] or [*NR*].

In oscillation mode, almost all the above conclusion from Table 4.4 still stands.

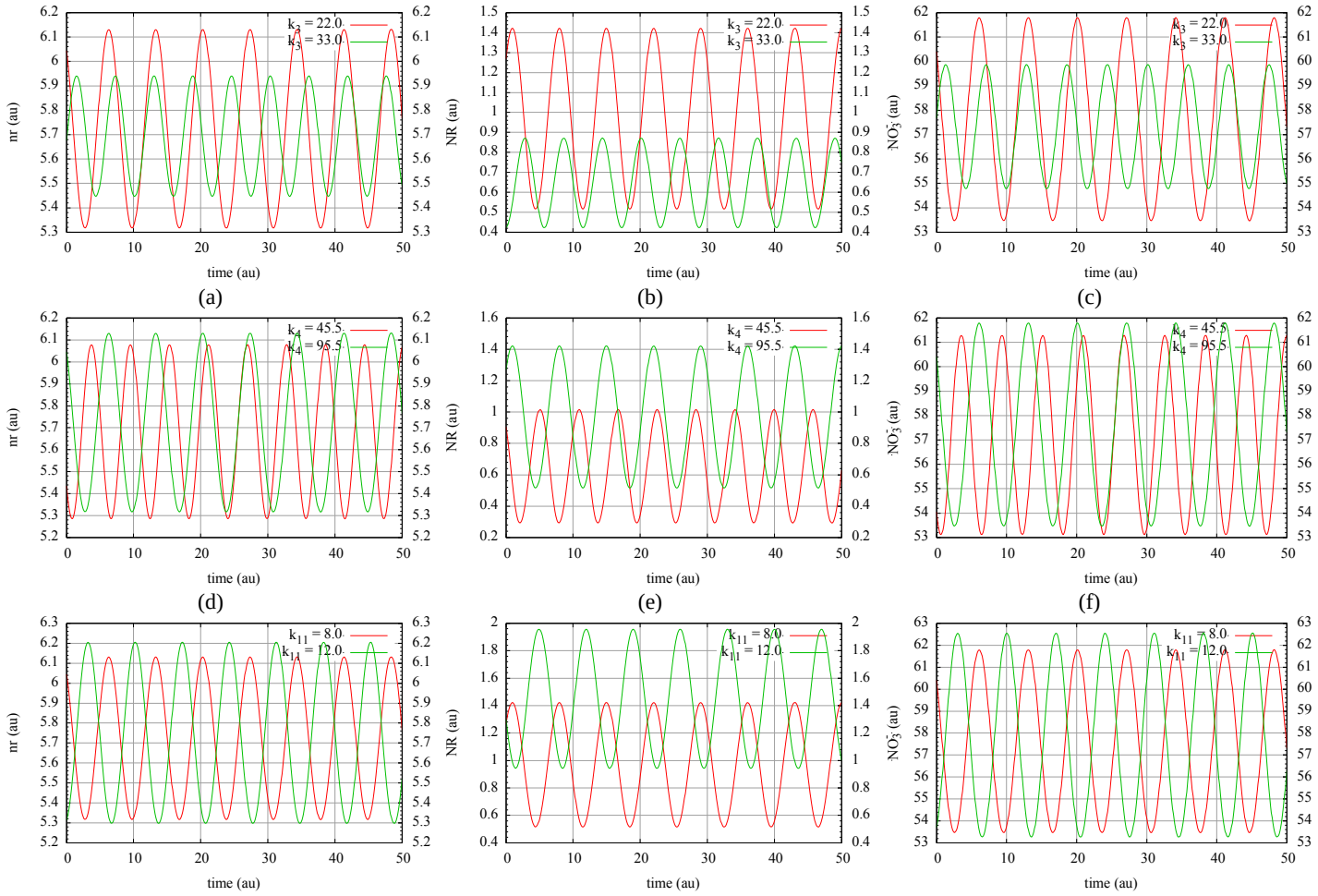

Figure 4.41: It is obvious that k_3, k_4 or k_{11} can give a stronger influence to [*NR*] than [*nr*] and $[NO_3^-]$. The increase of k_3 causes the decrease of [*NR*] and $[NO_3^-]$ while the increase of k_4 and k_{11} causes the rise of [*NR*] and $[NO_3^-]$. In every case the curves of [*nr*] and $[NO_3^-]$ are quite similar, and $[NO_3^-]$ changes in the same direction with [*NR*].

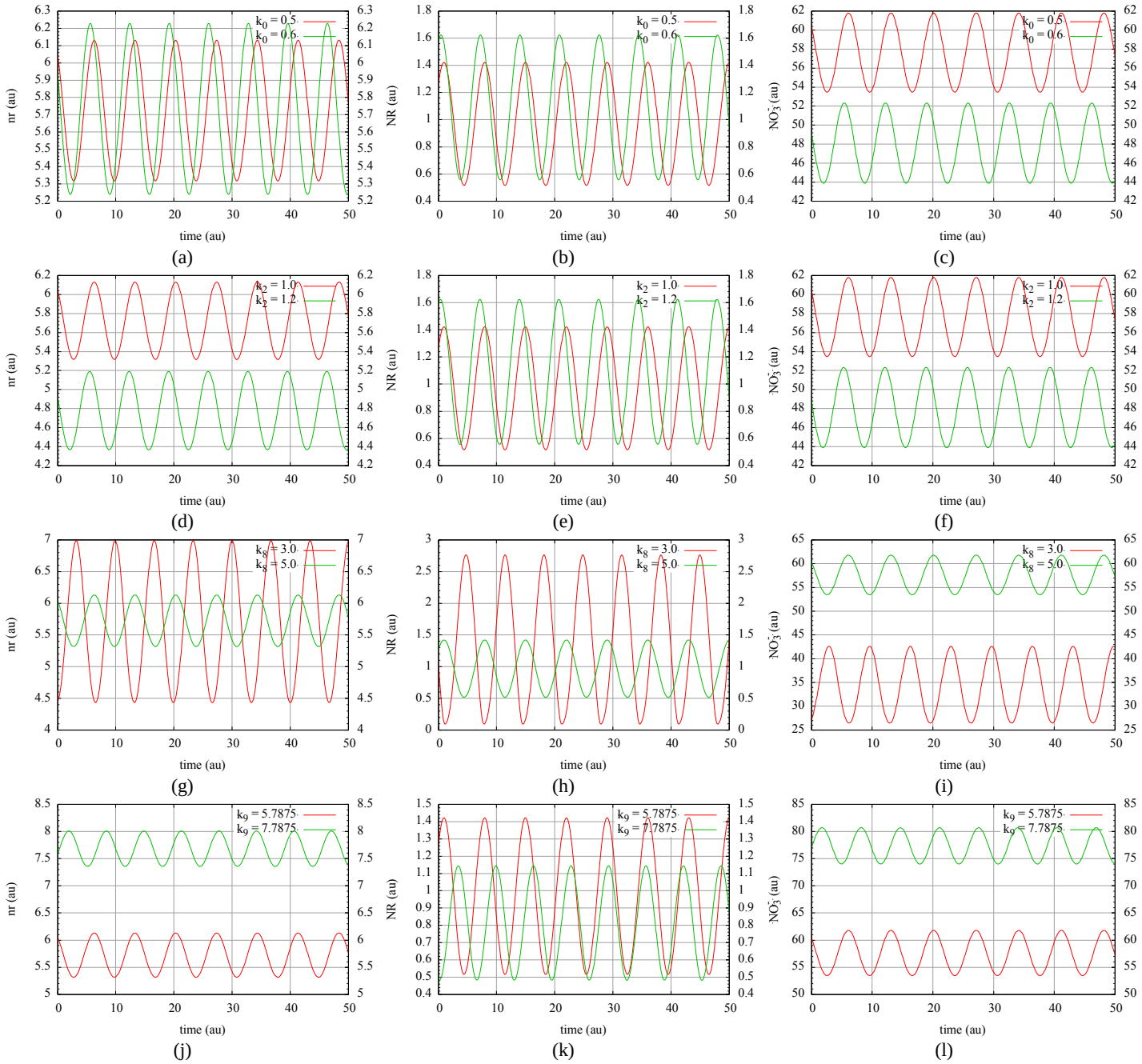

Figure 4.42: Even in the oscillation mode, the increase of nitrate with the decrease of k_0 and k_2 or with the rise of k_8 and k_9 is still obvious. When k_0 or k_8 is changed, [nr] shows little difference, which is different with the situation when k_2 or k_9 is changed. Distinct from k_0 and k_8, [nr] and [NO_3^-] show a quite similar tendency with different k_2 and k_9 values. The reason for terming these four rate constants together is they share the characteristic of a less obvious change in [NR] compared with [NO_3^-] and [NR] always changes in the opposite direction with [NO_3^-].

The variation of [*nr*], [*NR*] and $[NO_3^-]$ with k_{10} is variable and I have not summed up its discipline.

A low k_{10} is necessary for the existence of oscillation, and increasing k_{10} makes it easy to destroy the oscillation. Under oscillatory state, it is difficult to observe the variation of [*nr*], [*NR*] and $[NO_3^-]$ with a tiny change of k_{10}. The principle for k_{13} to affect the oscillation is to create a new value of k_1 (which will be discussed in more detail in Section 4.3.2), so it is possible to follow from the phenomenon observed along with the increase of k_0 to work out the influence caused by k_{13}.

Before the occurrence of damping, the variation of nitrate with k_3, k_4 and k_{11} is barely perceptible. However, even under the oscillatory state, the variation of nitrate with k_1, k_2, k_8 and k_9 can be easily observed.

From the perspective of the dynamics of *NR* and NO_3^-, these rate constants which affect the oscillation can be separated into two groups: one causing the increase or decrease of [*NR*] and $[NO_3^-]$ at the meanwhile (k_3, k_4 and k_{11}), the other leading the opposite variation tendency for these two variable (k_1, k_2, k_8 and k_9).

The attempt of expanding the process of the nitrate reduction by *NR* and *NR* reduction by E_{set} with Michaelis-Menten kinetics is helpful to demonstrate something.

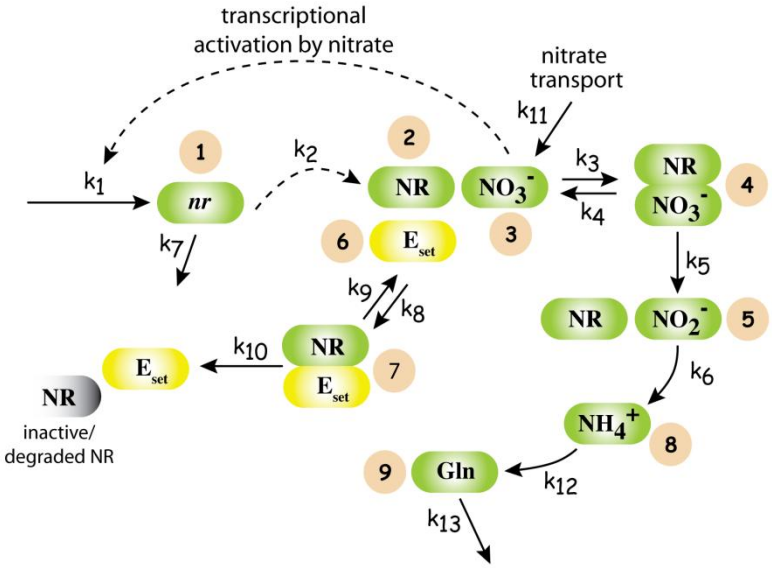

Figure 4.43: Scheme of nitrate reduction by *NR* and *NR* removal step by E_{set} where Michaelis-Menten kinetics is fully expanded.

In Figure 4.43,

$$V_{\max}^{NR} = k_5 \cdot ([NR] + [NR \cdot NO_3^-])$$
$$K_M^{NR} = \frac{k_4 + k_5}{k_3}$$
$$V_{\max}^{E_{set}} = k_{10} \cdot ([E_{set}] + [NR \cdot E_{set}])$$
$$K_M^{E_{set}} = \frac{k_9 + k_{10}}{k_8}$$

The differential equations for Figure 4.43 are as below:

$$\frac{d[nr]}{dt} = k_1 \cdot [NO_3^-] - k_7 \cdot [nr]$$
$$\frac{d[NR]}{dt} = k_2 \cdot [nr] - k_3 \cdot [NR] \cdot [NO_3^-] + (k_4 + k_5) \cdot [NR \cdot NO_3^-] - k_8 \cdot [NR] \cdot [E_{set}] + k_9 \cdot [NR \cdot E_{set}]$$
$$\frac{d[NO_3^-]}{dt} = k_{11} - k_3 \cdot [NR] \cdot [NO_3^-] + k_4 \cdot [NR \cdot NO_3^-]$$
$$\frac{d[NR \cdot NO_3^-]}{dt} = k_3 \cdot [NR] \cdot [NO_3^-] - (k_4 + k_5) \cdot [NR \cdot NO_3^-]$$
$$\frac{d[NO_2^-]}{dt} = k_5 \cdot [NR \cdot NO_3^-] - k_6 \cdot [NO_2^-]$$
$$\frac{d[E_{set}]}{dt} = -k_8 \cdot [NR] \cdot [E_{set}] + (k_9 + k_{10}) \cdot [NR \cdot E_{set}]$$
$$\frac{d[NR \cdot E_{set}]}{dt} = k_8 \cdot [NR] \cdot [E_{set}] - (k_9 + k_{10}) \cdot [NR \cdot E_{set}]$$
$$\frac{d[NH_4^+]}{dt} = k_6 \cdot [NO_2^-] - k_{12} \cdot [NH_4^+]$$
$$\frac{d[G\ln]}{dt} = k_{12} \cdot [NH_4^+] - k_{13} \cdot [G\ln]$$

From $\frac{d[NR \cdot NO_3^-]}{dt} = 0$ and $\frac{d[NR \cdot E_{set}]}{dt} = 0$, we have

$$-k_3 \cdot [NR] \cdot [NO_3^-] + (k_4 + k_5) \cdot [NR \cdot NO_3^-] = 0 \quad (4.18)$$
$$-k_8 \cdot [NR] \cdot [E_{set}] + k_9 \cdot [NR \cdot E_{set}] = -k_{10} \cdot [NR \cdot E_{set}] \quad (4.19)$$

Substituting Equation 4.18 and 4.19 to $\frac{d[NR]}{dt} = 0$ gives:

$$k_2 \cdot [nr] - k_{10} \cdot [NR \cdot E_{set}] = 0 \quad (4.20)$$

From $\frac{d[nr]}{dt} = 0$, we can deduce:

$$[nr] = \frac{k_1}{k_7} \cdot [NO_3^-] \tag{4.21}$$

Substituting Equation 4.21 to Equation 4.20:

$$\frac{k_1 \cdot k_2}{k_7} \cdot [NO_3^-] - k_{10} \cdot [NR \cdot E_{set}] = 0 \tag{4.22}$$

Therefore,

$$[NO_3^-] = \frac{k_7 \cdot k_{10}}{k_1 \cdot k_2} \cdot [NR \cdot E_{set}] \tag{4.23}$$

Equation 4.23 is the definition of nitrate set value in Figure 4.43.

Substituting Equation 4.23 to Equation 4.21 gives:

$$[nr] = \frac{k_{10}}{k_2} \cdot [NR \cdot E_{set}] \tag{4.24}$$

From $\frac{d[NR \cdot NO_3^-]}{dt} = 0$, we have:

$$-k_3 \cdot [NR] \cdot [NO_3^-] + k_4 \cdot [NR \cdot NO_3^-] = -k_5 \cdot [NR \cdot NO_3^-] \tag{4.25}$$

Substituting Equation 4.25 to $\frac{d[NO_3^-]}{dt} = 0$ gives us:

$$k_{11} - k_5 \cdot [NR \cdot NO_3^-] = 0$$

So

$$[NR \cdot NO_3^-] = \frac{k_{11}}{k_5} \tag{4.26}$$

Substituting Equation 4.26 to $\frac{d[NO_2^-]}{dt} = 0$ gives:

$$k_5 \cdot \frac{k_{11}}{k_5} - k_6 \cdot [NO_2^-] = 0$$

So

$$[NO_2^-] = \frac{k_{11}}{k_6} \tag{4.27}$$

Substituting Equation 4.27 to $\frac{d[NH_4^+]}{dt} = 0$ gives:

$$k_6 \cdot \frac{k_{11}}{k_6} - k_{12} \cdot [NH_4^+] = 0$$

So

$$[NH_4^+] = \frac{k_{11}}{k_{12}} \tag{4.28}$$

Substituting Equation 4.28 to $\frac{d[Gln]}{dt} = 0$ gives:

$$k_{12} \cdot \frac{k_{11}}{k_{12}} - k_{13} \cdot [G\ln] = 0$$

So
$$[Gln] = \frac{k_{11}}{k_{13}} \tag{4.29}$$

The concentration of NO_2^-, NH_4^+ and *Gln* can be calculated as the ratio of nitrate transport rate with their individual degradation rate, which corresponds well with Table 4.4 (In Table 4.4, $[NO_2^-] = \frac{k_{11}}{k_5}, [NH_4^+] = \frac{k_{11}}{k_6}, [Gln] = \frac{k_{11}}{k_{14}}$).

Substituting Equation 4.26 to $\frac{d[NO_3^-]}{dt} = 0$ gives:

$$k_{11} - k_3 \cdot [NR] \cdot [NO_3^-] + k_4 \cdot \frac{k_{11}}{k_5} = 0$$

So
$$[NR] \cdot [NO_3^-] = \frac{k_{11} \cdot (1 + \frac{k_4}{k_5})}{k_3} = \frac{k_{11} \cdot (k_5 + k_4)}{k_3 \cdot k_5} = \frac{k_{11} \cdot K_M^{NR}}{k_5} \tag{4.30}$$

It seems that increase of transport rate or K_M^{NR} will cause the increase of $[NR]$ and $[NO_3^-]$ at the same time, while increase of k_{cat}^{NR} (k_5) will cause the decrease of $[NR]$ and $[NO_3^-]$ simultaneously. Actually, here we can not confirm this conclusion as it may happen $[NR]$ and $[NO_3^-]$ vary in the opposite direction.

Assume $[E_{set}] + [NR \cdot E_{set}] = [E_{set}]_{tot}$, which is constant, then we have

$$[E_{set}] = [E_{set}]_{tot} - [NR \cdot E_{set}] \tag{4.31}$$

From $\frac{d[NR \cdot E_{set}]}{dt} = 0$, we have:

$$k_8 \cdot [NR] \cdot [E_{set}] = (k_9 + k_{10}) \cdot [NR \cdot E_{set}] \tag{4.32}$$

Substituting Equation 4.31 to Equation 4.32,

$$k_8 \cdot [NR] \cdot ([E_{set}]_{tot} - [NR \cdot E_{set}]) = (k_9 + k_{10}) \cdot [NR \cdot E_{set}]$$

We can reform it as:

$$k_8 \cdot [NR] \cdot [E_{set}]_{tot} - k_8 \cdot [NR] \cdot [NR \cdot E_{set}] = (k_9 + k_{10}) \cdot [NR \cdot E_{set}]$$

$$k_8 \cdot [NR] \cdot [E_{set}]_{tot} = (k_9 + k_{10} + k_8 \cdot [NR]) \cdot [NR \cdot E_{set}]$$

$$[NR] \cdot [E_{set}]_{tot} = (\frac{k_9 + k_{10}}{k_8} + [NR]) \cdot [NR \cdot E_{set}]$$

$$= (K_M^{E_{set}} + [NR]) \cdot [NR \cdot E_{set}]$$

$$[E_{set}]_{tot} = (\frac{K_M^{E_{set}}}{[NR]} + 1) \cdot [NR \cdot E_{set}] \quad (4.33)$$

Since $[E_{set}]_{tot}$ is constant, the increase of [*NR*] will inevitably cause the decrease of $(\frac{K_M^{E_{set}}}{[NR]} + 1)$ and the rise of $[NR \cdot E_{set}]$, vice versa, which means [*NR*] and $[NR \cdot E_{set}]$ always change in the same direction.

Now we can confirm the conclusion that increase of transport rate or K_M^{NR} will cause the increase of $[NR]$ and $[NO_3^-]$, while increase of k_{cat}^{NR} (k_5) will cause the decrease of [*NR*] and $[NO_3^-]$.

From Equation 4.33, we can deduce:

$$[NR \cdot E_{set}] = \frac{[E_{set}]_{tot}}{1 + \frac{K_M^{E_{set}}}{[NR]}}$$

Under oscillation mode, $K_M^{E_{set}}$ is quite small, which makes it possible to assume $1 + \frac{K_M^{E_{set}}}{[NR]} \approx 1$, and therefore, $[NR \cdot E_{set}] \approx [E_{set}]_{tot}$.

Substituting $[NR \cdot E_{set}] \approx [E_{set}]_{tot}$ to Equation 4.24 $[nr] = \frac{k_{10}}{k_2} \cdot [NR \cdot E_{set}]$ gives

$[nr] \approx \frac{k_{10}}{k_2} \cdot [E_{set}]_{tot} = \frac{V_{\max}^{E_{set}}}{k_2}$, which is independent of k_1 and k_7. This is why in Graph a and g of Figure 4.42 we can not observe the obvious shift of equilibrium position for the vibration of [*nr*].

From the expression of set point $\frac{k_7 \cdot k_{10}}{k_1 \cdot k_2} \cdot [NR \cdot E_{set}]$ which seems to be independent of k_{11}, k_3 and k_4, creating a different $[NR \cdot E_{set}]$ is the only way for these three rate constants to affect nitrate set point.

As shown above, either the rise of k_{11} or K_M^{NR} or the drop of k_5 increases [*NR*], which makes $1+\frac{K_M^{E_{set}}}{[NR]}$ close to 1 and $[NO_3^-]$ close to $\frac{k_7 \cdot k_{10}}{k_1 \cdot k_2} \cdot [E_{set}]_{tot}$.

In oscillation mode, $[NR \cdot E_{set}]$ is close to $[E_{set}]_{tot}$, so $[NO_3^-] = \frac{k_7 \cdot k_{10}}{k_1 \cdot k_2} \cdot [NR \cdot E_{set}]$ has little to climb. This is the reason why in Figure 4.41 the rise or fall of [*NR*] is much more obvious than $[NO_3^-]$.

Except rate constants, $[E_{set}]_{tot}$ can also affect the oscillation because its variation causes a different $[NR \cdot E_{set}]$. In addition to $[NR \cdot E_{set}]$, [*NR*] will also change with $[E_{set}]_{tot}$.

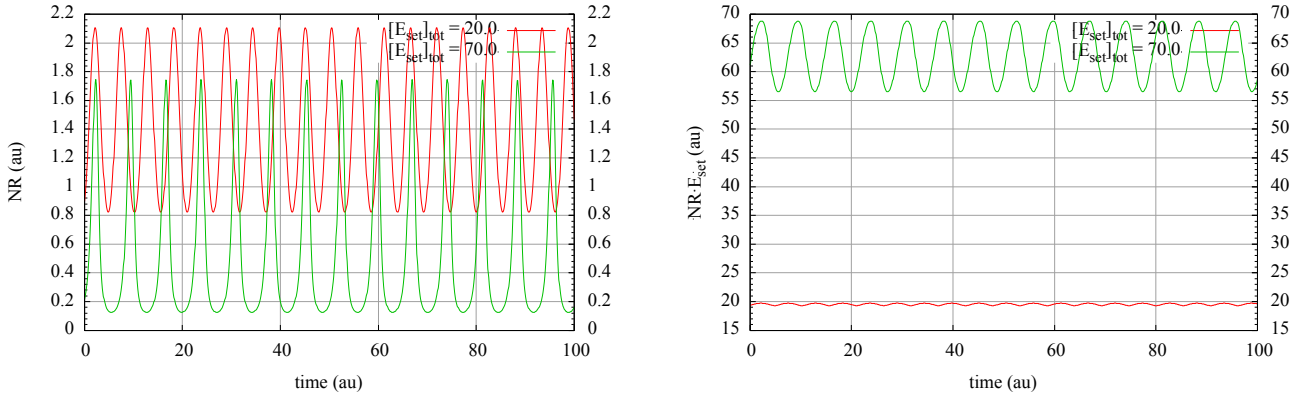

(a) (b)

Figure 4.44: When $[E_{set}]_{tot}$ increases, $[NR]$ decreases and $[NR \cdot E_{set}]$ rises.

It is worthy of mentioning that distinct from other variables, the oscillation is dependent of $[E_{set}]_{tot}$. The increase of decrease of $[E_{set}]_{tot}$ causes the increase or decrease of $V_{max}^{E_{set}}$ which is defined as $k_{10} \cdot ([E_{set}] + [NR \cdot E_{set}])$, and $V_{max}^{E_{set}}$ can affect period length, set point and also the existence of oscillation, which has been confirmed before with the model decribed in Figure 4.1. When desining the program, we did not assume the direct synthesis or degradation step to E_{set} or $NR{\cdot}E_{set}$. From the beginning to the end, $[E_{set}]_{tot}$ which is the sum of $[E_{set}]$ and $[NR{\cdot}E_{set}]$ will always be constant.

Substituting Equation 4.23 $[NO_3^-] = \frac{k_7 \cdot k_{10}}{k_1 \cdot k_2} \cdot [NR \cdot E_{set}]$ to Equation 4.30 $[NR] \cdot [NO_3^-] = \frac{k_{11} \cdot K_M^{NR}}{k_5}$ gives:

$$[NR] \cdot \frac{k_7 \cdot k_{10}}{k_1 \cdot k_2} \cdot [NR \cdot E_{set}] = \frac{k_{11} \cdot K_M^{NR}}{k_5}$$

$$[NR] \cdot [NR \cdot E_{set}] = \frac{k_1 \cdot k_2 \cdot k_{11} \cdot K_M^{NR}}{k_5 \cdot k_7 \cdot k_{10}} \qquad (4.34)$$

In order to satisfy both Equation 4.34 and Equation 4.33 $[E_{set}]_{tot} = (\frac{K_M^{E_{set}}}{[NR]} + 1) \cdot [NR \cdot E_{set}]$, with the climb of $[E_{set}]_{tot}$, there is only one possibility that [*NR*] decreases and $[NR \cdot E_{set}]$ increases.

According to Equation 4.24 $[nr] = \frac{k_{10}}{k_2} \cdot [NR \cdot E_{set}]$ and Equation 4.23 $[NO_3^-] = \frac{k_7 \cdot k_{10}}{k_1 \cdot k_2} \cdot [NR \cdot E_{set}]$, both [*nr*] and $[NO_3^-]$ are directly proportional to $[NR \cdot E_{set}]$. So the rise of $[E_{set}]_{tot}$ leads to the growth of [*nr*] as well as $[NO_3^-]$.

4.3.2 The effect caused by *NMR* and *NIT24*

4.3.2.1 The interaction among *NMR*, *NIT24* and *Pr*

In the model, there are two oscillatory pace makers. One is the *NR* outflow controller loop in which the homeostatic controlled variable nitrate activates the production of *NR* to remove itself. The other can be characterized as a transcriptional-translational negative feedback oscillation. Even without varying those rate constants in *NR* feedback loop, it is still possible to generate a new oscillation or destroy the existing oscillation. Before discussing this topic, it is necessary to talk about the interaction of *NMR* and *NIT24* in more detail.

The content below is still referred to the model described in Figure 4.1. When designing the calculation, we assume that total promoter site is Pr_0 and that occupied promoter is *Pr*·*NIT24*, while unoccupied is *Pr*. Then we have

$$[Pr]_0 = [Pr] + [Pr \cdot NIT24] \tag{4.35}$$

The complex of *Pr* and *NIT24* is treated as a rapid equilibrium process:

$$Pr{\cdot}NIT24 \overset{K_d^{NIT}}{\rightleftharpoons} Pr + NIT24$$

K_d^{NIT} is the dissociation constant of *Pr*·*NIT24*

$$K_d^{NIT} = \frac{[Pr] \cdot [NIT24]}{[Pr \cdot NIT24]} \tag{4.36}$$

From Equation 4.36, we can deduce

$$[Pr] = \frac{K_d^{NIT} \cdot [Pr \cdot NIT24]}{[NIT24]} \tag{4.37}$$

Substituting Equation 4.37 to 4.35 gives:

$$\begin{aligned} [Pr]_0 &= \frac{K_d^{NIT} \cdot [Pr \cdot NIT24]}{[NIT24]} + [Pr \cdot NIT24] \\ &= [Pr \cdot NIT24] \cdot (1 + \frac{K_d^{NIT}}{[NIT24]}) \end{aligned} \tag{4.38}$$

From Equation 4.38, we can get:

$$[Pr \cdot NIT24] = \frac{[Pr]_0}{1 + \frac{K_d^{NIT}}{[NIT24]}} \tag{4.39}$$

We assume the transcription rate of the *nit-3* promoter, which is the formation rate of *nit-3* mRNA as below:

$$\begin{aligned} \frac{d[nr]}{dt} &= k \cdot \frac{[Pr]_0}{1 + \frac{K_d^{NIT}}{[NIT24]}} \\ &= \frac{k \cdot [Pr]_0 \cdot [NIT24]}{K_d^{NIT} + [NIT24]} \end{aligned} \tag{4.40}$$

Taking degradation step of *nr* into account, we can express *nr* transcript rate:

$$\frac{d[nr]}{dt} = \frac{k \cdot [Pr]_0 \cdot [NIT24]}{K_d^{NIT} + [NIT24]} - k_8 \cdot [nr] \tag{4.41}$$

where k_8 is the degradation rate constant for *nr*.

Since nitrate activates the transcription, Equation 4.41 can be written as:

$$\begin{aligned} \frac{d[nr]}{dt} &= \frac{k \cdot [Pr]_0 \cdot [NIT24] \cdot [NO_3^-]}{K_d^{NIT} + [NIT24]} - k_8 \cdot [nr] \\ &= \frac{k_0 \cdot [NIT24] \cdot [NO_3^-]}{K_d^{NIT} + [NIT24]} - k_8 \cdot [nr] \end{aligned} \tag{4.42}$$

where $k_0 = k \cdot [Pr]_0$.

In our program, we write this equation as follows:

$$\frac{d[nr]}{dt} = k_1 \cdot [NO_3^-] - k_8 \cdot [nr] \tag{4.43}$$

where $k_1 = \frac{k_0 \cdot [NIT24]}{K_d^{NIT} + [NIT24]}$.

4.3.2.2 The influence on oscillations caused by this interaction

Through *NMR* we are able to affect the oscillation since *NMR* can occupy one portion of *NIT24* whose amount is limited so that the *NIT24* prepared for the combination with *nit-3* promoter decreases.

According to the expression of k_1:

$$k_1 = \frac{k_0 \cdot [NIT24]}{K_d^{NIT} + [NIT24]}$$

We can reform it as:

$$k_1 = \frac{k_0}{1 + \frac{K_d^{NIT}}{[NIT24]}}$$

So the increase of [*NIT24*] gives rise to a higher k_1.

There are two ways to achieve the decrease of *NIT24* which needs to combine with *nit-3* promoter for its transcription. Through the rise of k_7, the concentration of *NMR* is increased, which means it will combine more *NIT24*. The other way is to reduce the binding coefficient of *NMR* and *NIT24* which is defined as $K_d^{NMR} = \frac{[NIT24]\cdot[NMR]}{[NIT24 \cdot NMR]}$ in order to enhance the ability for *NMR* to rob *NIT24*. I will show the case of rising k_7.

When $k_7 = 0$, our model is referred to *nmr* mutant. The absence of *NMR* leads to a higher [*NIT24*] compared with the situation when *NMR* exists (wild type) so that *nmr* mutant has a higher nitrate reductase expression compared with wild type (52).

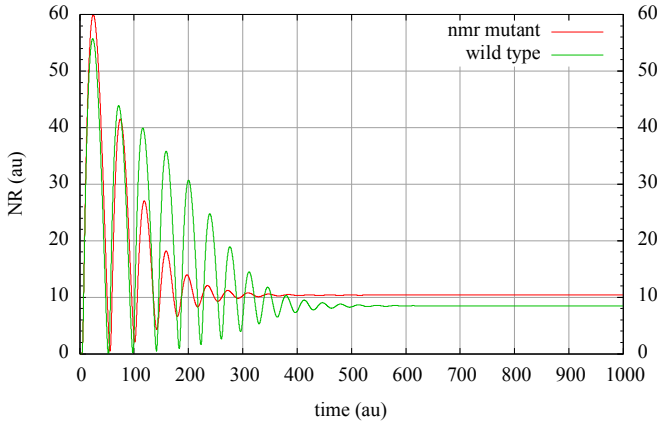

Figure 4.45: The *NR* level of *nmr* mutant (k_7=0) is higher than wild type (k_7=1).

As I mentioned before, the change of k_1 is able to destroy an existing oscillation and also rescue a destroyed oscillation. Through varing [*NMR*], k_1 can be changed, which can also destroy or rescue the oscillation. Below is an example that the growth of k_7 can counteract the influence of k_4.

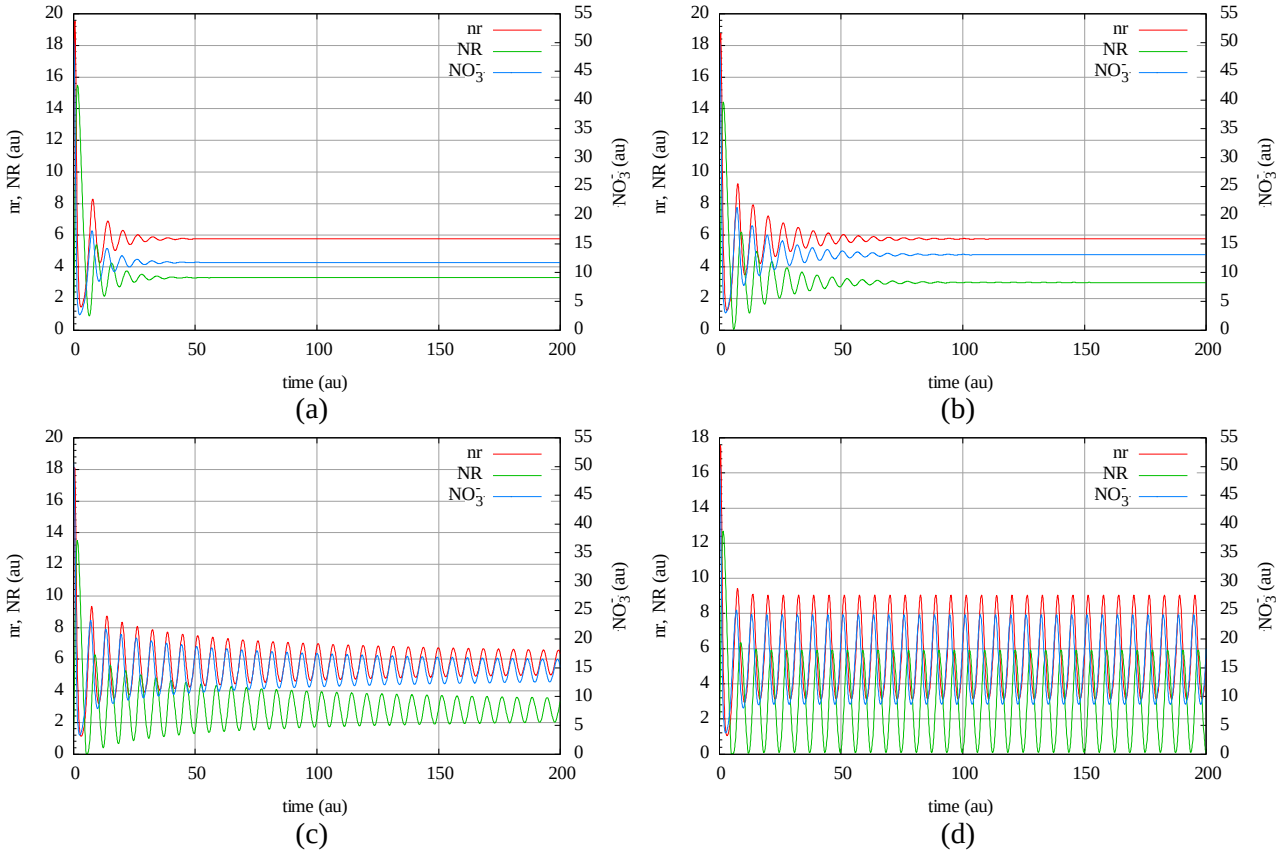

Figure 4.46: In Graph a, k_7 = 0.0. We assume [*NMR*] = [*NMR·NIT24*] =0 when k_7 = 0.0. Through increasing k_7 gradually, a new oscillation can be generated. In b, c and d, k_7 are 1.0, 2.0 and 3.0, respectively. When k_7 rises to a certain degree, the oscillation is back.

In order to make the principle clear, it is necessary to show the the variation trend of [*NMR*] and [*NIT24*].

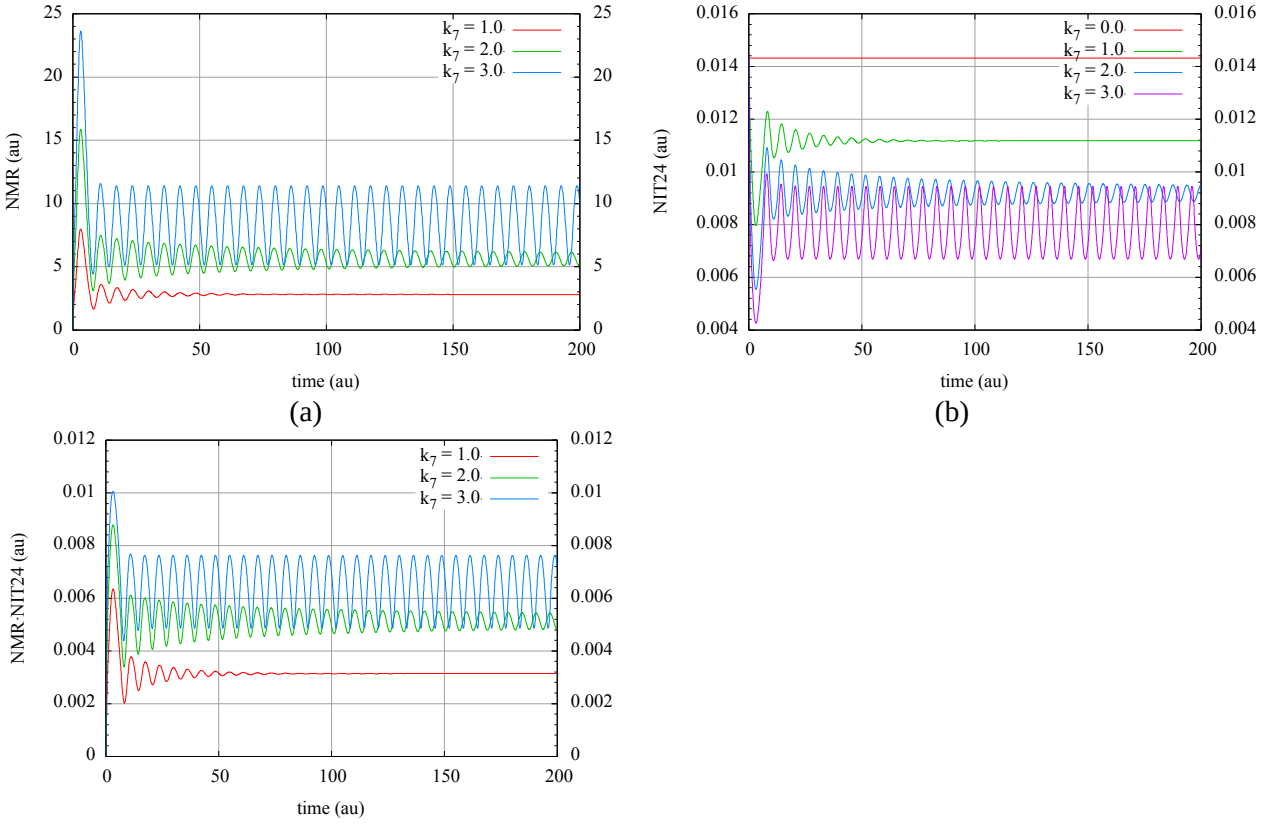

Figure 4.47: When k_7 = 0.0, [*NMR*] = [*NMR·NIT24*] =0. With the rise of k_7, [*NMR*] increases, which also creates a higher [*NMR·NIT24*]. The rise of [*NMR·NIT24*] would definitely lead to the decrease of [*NIT24*] so that k_1 falls down. This is the way *NMR* affects the oscillation.

Table 4.5: Period length and set point varying with k_7, k_{12}, k_{15} and k_{16}

k_7	k_{12}	k_{15}	k_{16}	Period	Set point
5.00	1.50	1.00	10.0	6.3800	19.6958
7.50	1.50	1.00	10.0	6.5828	21.6628
2.50	1.50	1.00	10.0	6.2367	14.7412
5.00	2.25	1.00	10.0	6.1900	14.8918
5.00	0.75	1.00	10.0	7.0704	30.7777
5.00	1.50	1.50	10.0	6.5828	25.4319
5.00	1.50	0.50	10.0	6.2367	14.6036
5.00	1.50	1.00	15.0	6.2645	14.5283
5.00	1.50	1.00	5.00	6.8000	29.3582

Through combining *NIT24*, *NMR* can influence period length and set point. The effect of increasing k_7 or k_{15} is just to reduce available *NIT24* for *nit-3* promoter. The decrease of k_{12} or k_{16} plays the similar role with rising k_7 or k_{15}, respectively.

From Table 4.5, the rise of k_7 or k_{15} gives rise to a longer period. This is not in agreement with the phenomenon that the period decreases with the drop of k_0 which also decreases k_1 we observe in Table 4.3. It also illustrates the uncertainty of period length depending on rate constants.

As regard to set point, no matter by which way the decrease of k_1 is achieved, it will decrease set value.

4.3.2.3 Further discussion about the design of nitrogen metabolism repression

In our assumption for designing the model, *NIT24* only contains two parts: *NIT24* and *NMR·NIT24*. Based on this hypothesis, we define the expression of differential equation of *NIT24* concentration as below:

$$\frac{d[NIT24]}{dt} = k_{15} \cdot [NMR] \cdot [NIT24] - k_{16} \cdot [NMR \cdot NIT24] \tag{4.44}$$

The total concentration of *NIT24* can be expressed as:

$$[NIT24]_0 = [NIT24] + [NMR{\cdot}NIT24] \tag{4.45}$$

From the concept of K_d^{NIT}, which is defined in Equation 4.36:

$$K_d^{NIT} = \frac{[Pr] \cdot [NIT24]}{[Pr \cdot NIT24]}$$

together with the assumption (Equation 4.35):

$$[Pr]_0 = [Pr] + [Pr{\cdot}NIT24]$$

the expression of $k_1 = k_0 \cdot \frac{[NIT24]}{K_d^{NIT} + [NIT24]}$ is deduced. In this process the *NIT24* via its *Pr*-form is neglected.

When $k_7 = 0$,

$$[NMR] = [NMR{\cdot}NIT24] = 0 \tag{4.46}$$

then we have

$$\frac{d[NIT24]}{dt} = 0$$

Substituting Equation 4.46 to Equation 4.45 gives:

$$[NIT24]_0 = [NIT24]$$

However, even in such a case, we still use the expression $k_1 = k_0 \cdot \frac{[NIT24]}{K_d^{NIT} + [NIT24]}$, and the definition of $K_d^{NIT} = \frac{[Pr] \cdot [NIT24]}{[Pr \cdot NIT24]}$ is still valid. Otherwise, $k_1 = k_0 \cdot \frac{[NIT24]}{K_d^{NIT} + [NIT24]}$ fails to be established. This indicates the existence of both [*NIT24*] and [*Pr·NIT24*] at the same time, which is in contradiction with the relationship $[NIT24]_0 = [NIT24]$.

It is wrong to assume there is an equilibrium process between *Pr* and *Pr·NIT24*. Without *NMR* production, it does not matter whether *Pr·NIT24* is introduced or not since calculating k_1 with the

expression $k_1 = k_0 \cdot \frac{[NIT24]}{K_d^{NIT} + [NIT24]}$ can be considered as a process of formula transformation, which will not affect the modeling result expect the value of k_1.

In order to solve this problem, we have to treat *Pr·NIT24* and *Pr* as two new variables, or assume after being occupied by *NMR* for one portion, all the *NIT24* will combine with *nit-3* promoter. In the first choice, *NMR* and *nit-3* promoter will compete with each other to combine with the limited amount of *NIT24*.

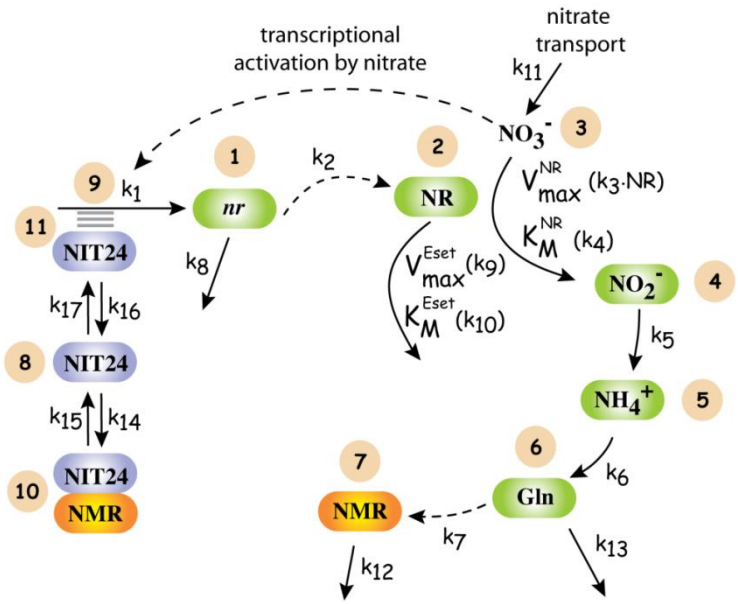

Figure 4.48: Scheme of nitrate assimilation pathway for *Neurospora crassa* in which *nit-3* promoter is treated as a separated variable (Y(9)) and Y(11) is referred to the complex *Pr·NIT24*.

Therefore, Equation 4.45 should be expressed as:

$$[NIT24]_0 = [NIT24] + [NMR{\cdot}NIT24] + [Pr{\cdot}NIT24]$$

The differential equation of [*Pr*], [*NIT24*], [*Pr·NIT24*] and [*NMR·NIT24*] can be defined as:

$$\frac{d[Pr]}{dt} = k_{16} \cdot [Pr \cdot NIT24] - k_{17} \cdot [Pr] \cdot [NIT24]$$

$$\frac{d[NIT24]}{dt} = k_{16} \cdot [Pr \cdot NIT24] + k_{15} \cdot [NMR \cdot NIT24] - k_{17} \cdot [Pr] \cdot [NIT24] - k_{14} \cdot [NMR] \cdot [NIT24]$$

$$\frac{d[Pr \cdot NIT24]}{dt} = k_{17} \cdot [Pr] \cdot [NIT24] - k_{16} \cdot [Pr \cdot NIT24]$$

$$\frac{d[NMR \cdot NIT24]}{dt} = k_{14} \cdot [NMR] \cdot [NIT24] - k_{15} \cdot [NMR \cdot NIT24]$$

The question that does this competition process really exist follows with this solution. As we know, *nit-3* promoter is a piece of gene, while *NMR* is a protein. I do not think it is realistic for this competition relationship between them. So I prefer the second solution in which *nit-3* promoter has to wait for its transcription until the complex of [*NIT24*] and [*NMR*] has completed.

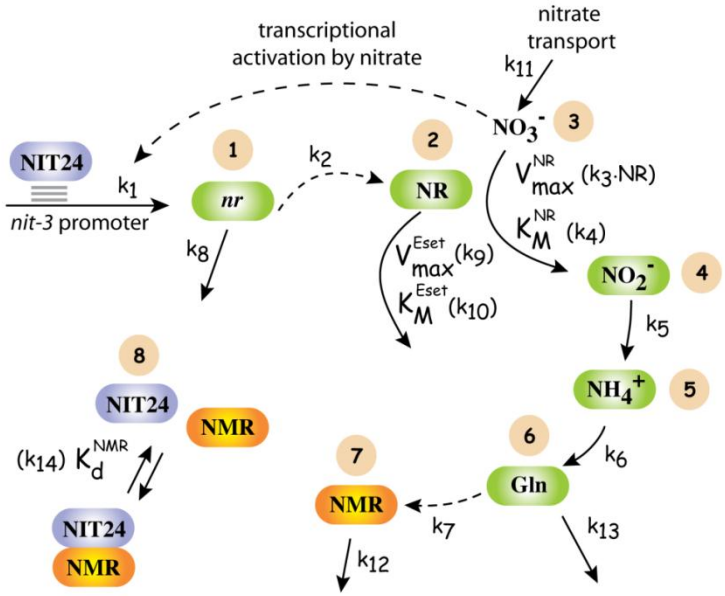

Figure 4.49: Scheme of nitrate assimilation pathway for *Neurospora crassa* in which the equilibrium between *nit-3* promoter and *NIT24* does not exist, and $[NIT24]_{tot}$ is still only composed of [*NIT24*] and [*NMR·NIT24*].

In such a model, we only need one equilibrium constant K_d^{NMR} for the complex of *NIT24* and *NMR* instead of two rate constants for the synthesis and decomposition step of *NMR·NIT24* separately.

$$NMR{\cdot}NIT24 \overset{K_d^{NMR}}{\rightleftharpoons} NMR+NIT24$$

K_d^{NMR} is defined as:

$$K_d^{NMR} = \frac{[NMR]\cdot[NIT24]}{[NMR\cdot NIT24]}$$

From it, we can get:

$$[NMR\cdot NIT24] = \frac{[NMR]\cdot[NIT24]}{K_d^{NMR}} \tag{4.47}$$

Substituting Equation 4.47 to Equation 4.45 $[NIT24]_0 = [NIT24] + [NMR \cdot NIT24]$ gives:

$$[NIT24]_0 = [NIT24] + \frac{[NMR] \cdot [NIT24]}{K_d^{NMR}}$$
$$= [NIT24] \cdot (1 + \frac{[NMR]}{K_d^{NMR}})$$

Then we can express [*NIT24*] as:

$$[NIT24] = \frac{[NIT24]_0}{1 + \frac{[NMR]}{K_d^{NMR}}}$$

So the rate of *nit-3* mRNA (*nr*) formation:

$$\frac{d[nr]}{dt} = k_1 \cdot [NIT24] \cdot [NO_3^-]$$

More experimental result on the interaction between *nit-3* promoter and transcription factor *NIT24* as well as the principle how *NMR* affects the nitrate reductase induction is needed for designing the process of nitrogen metabolite repression in the model.

5. Conclusion:

In our model for fungal nitrate transport and assimilation, inflow controller was used to regulate the uptake process, with the help of which a constant nitrate transport rate could be achieved under a limited external nitrate concentration. As regard to nitrate reduction by *NR*, the outflow controller I was chosen to express it. When inflow controller V or VII was introduced, nitrate concentration is always determined by the inflow controller. The condition that outflow defining value is lower or equivalent to inflow defining one always generates a continuously rising concentration of outflow controller *NR*. In order to solve this problem, we used inflow controller II or IV instead of V to express the nitrate uptake process. But this attempt could not always bear fruit. Sometimes a continuously rising *NR* concentration was still observed. The attempt of introducing another E_{set} to expand the degradation step of E_{adapt}^{uptake} is worth doing for exploring the condition in which the phenomenon of a rising *NR* concentration can be avoided.

As regard to plant nitrate transport and assimilation, in order to create a shorter duration of efflux process than the duration of homeostasis for cytosolic nitrate concentration, we introduced a nitrate branching point whose homeostasis could be maintained so long as external nitrate supply was not expended completely. However, we are unable to model a decreasing efflux rate. With this model, we succeed to create the phenomenon that after external nitrate supply was used up, vacuolar nitrate became remobilized for keeping the homeostasis of cytosolic nitrate. In order to make a constant cytoslic nitrate level before and after the remobilization, it is necessary to give the same nitrate defining value for the vacuolar efflux inflow controller E_{adapt}^{efflux} with the outflow controller *NR*.Here we came across the same problem of generating a continuously rising *NR* concentration with fungal model. So we tried to use inflow controller II to regulate the vacuolar efflux, which made it possible to give the same defining concentration for E_{adapt}^{efflux} and *NR* without leading to a rising *NR* level. According to the character of *NR*, we know that its level should be proportional to the speed of inflow nitrate. But we failed to generate the same inflow rate to *NR* before and after the depletion of environmental nitrate. This is the reason why we could not create the same *NR* level when vacuolar stored nitrate became the only nitrate source. Although the physiological mechanisms are still unclear, many reports have shown nitrogen metabolites resulting from nitrate reduction may act as regulatory signals to control the rate of nitrate uptake by roots. This inhibition is not included in our model for plant nitrate transport and assimilation pathway, which needs further investigations.

When it comes to the exploration of circadian oscillation, the *NR* feedback loop was our main concern. We have not found out a method how to determine the expression of period length. According to the influence to [*NR*] and $[NO_3^-]$, we succeeded to term these rate constants inside the *NR* feedback loop into two groups: one causing [*NR*] and $[NO_3^-]$ to change in the opposite direction, the other causing their variation in the same direction. In addition, in our design the effect which can be caused by nitrogen metabolism repression (for *Neurospora crassa*) is just to cause a different transcriptional rate of *nr* mRNA in the final analysis.

Appendix A. Differential equations of the models shown in the thesis

The differential equations of the model in Figure 4.1 are as follows:

1. $\frac{d[nr]}{dt} = k_1 \cdot [NO_3^-] - k_8 \cdot [nr]$
2. $\frac{d[NR]}{dt} = k_2 \cdot [nr] - \frac{k_9 \cdot [NR]}{k_{10} + [NR]}$
3. $\frac{d[NO_3^-]}{dt} = k_{11} - \frac{k_3 \cdot [NR] \cdot [NO_3^-]}{k_4 + [NO_3^-]}$
4. $\frac{d[NO_2^-]}{dt} = \frac{k_3 \cdot [NR] \cdot [NO_3^-]}{k_4 + [NO_3^-]} - k_5 \cdot [NO_2^-]$
5. $\frac{d[NH_4^+]}{dt} = k_5 \cdot [NO_2^-] - k_6 \cdot [NH_4^+]$
6. $\frac{d[Gln]}{dt} = k_6 \cdot [NH_4^+] - k_{14} \cdot [Gln]$
7. $\frac{d[NMR]}{dt} = k_7 \cdot [Gln] - k_{12} \cdot [NMR] - k_{15} \cdot [NMR] \cdot [NIT24] + k_{16} \cdot [NMR \cdot NIT24]$
8. $\frac{d[NIT24]}{dt} = -k_{15} \cdot [NMR] \cdot [NIT24] + k_{16} \cdot [NMR \cdot NIT24]$
9. $\frac{d[NMR \cdot NIT24]}{dt} = k_{15} \cdot [NMR] \cdot [NIT24] - k_{16} \cdot [NMR \cdot NIT24]$

The differential equations of the model in Figure 4.4 are as follows:

1. $\frac{d[nr]}{dt} = k_1 \cdot [NO_3^-] - k_8 \cdot [nr]$
2. $\frac{d[NR]}{dt} = k_2 \cdot [nr] - k_9 \cdot [NR] \cdot [E_{set}] + k_{10} \cdot [NR \cdot E_{set}]$
3. $\frac{d[NO_3^-]}{dt} = k_{17} - \frac{k_3 \cdot [NR] \cdot [NO_3^-]}{k_4 + [NO_3^-]}$
4. $\frac{d[NO_2^-]}{dt} = \frac{k_3 \cdot [NR] \cdot [NO_3^-]}{k_4 + [NO_3^-]} - k_5 \cdot [NO_2^-]$
5. $\frac{d[NH_4^+]}{dt} = k_5 \cdot [NO_2^-] - k_6 \cdot [NH_4^+]$
6. $\frac{d[Gln]}{dt} = k_6 \cdot [NH_4^+] - k_{14} \cdot [Gln]$
7. $\frac{d[NMR]}{dt} = k_7 \cdot [Gln] - k_{12} \cdot [NMR] - k_{15} \cdot [NMR] \cdot [NIT24] + k_{16} \cdot [NMR \cdot NIT24]$
8. $\frac{d[NIT24]}{dt} = -k_{15} \cdot [NMR] \cdot [NIT24] + k_{16} \cdot [NMR \cdot NIT24]$

9. $\frac{d[NMR \cdot NIT24]}{dt} = k_{15} \cdot [NMR] \cdot [NIT24] - k_{16} \cdot [NMR \cdot NIT24]$

10. $\frac{d[E_{set}]}{dt} = -k_9 \cdot [NR] \cdot [E_{set}] + (k_{10} + k_{11}) \cdot [NR \cdot E_{set}]$

11. $\frac{d[NR \cdot E_{set}]}{dt} = -\frac{d[E_{set}]}{dt}$

The differential equations of the model in Figure 4.7 are as follows:
Except the third variable NO_3^-, from the first variable to the eleventh variable, the differential equation is the same with Figure 4.4.

3. $\frac{d[NO_3^-]}{dt} = \frac{k_{17} \cdot [NO_3^-]_{env}}{k_{18} + [NO_3^-]_{env}} - \frac{k_3 \cdot [NR] \cdot [NO_3^-]}{k_4 + [NO_3^-]}$

12. $\frac{d[NO_3^-]_{env}}{dt} = -\frac{k_{17} \cdot [NO_3^-]}{k_{18} + [NO_3^-]}$

The differential equations of the model in Figure 4.9 are as follows:
Except the third variable NO_3^-, from the first variable to the eleventh variable, the differential equation is the same with Figure 4.4.

3. $\frac{d[NO_3^-]}{dt} = \frac{k_{17} \cdot [NO_3^-]_{env} \cdot [E_{adapt}^{uptake}]}{k_{18} + [NO_3^-]_{env}} - \frac{k_3 \cdot [NR] \cdot [NO_3^-]}{k_4 + [NO_3^-]}$

12. $\frac{d[NO_3^-]_{env}}{dt} = -\frac{k_{17} \cdot [NO_3^-]_{env} \cdot [E_{adapt}^{uptake}]}{k_{18} + [NO_3^-]_{env}}$

13. $\frac{d[E_{adapt}^{uptake}]}{dt} = k_{19} - \frac{k_{20} \cdot [NO_3^-] \cdot [E_{adapt}^{uptake}]}{k_{21} + [E_{adapt}^{uptake}]}$

The differential equations of the model in Figure 4.14 are as follows:
Except the third variable NO_3^-, from the first variable to the eleventh variable, the differential equation is the same with Figure 4.4.

3. $\frac{d[NO_3^-]}{dt} = \frac{k_{17} \cdot [NO_3^-]_{env}}{(k_{18} + [NO_3^-]_{env}) \cdot (k_{22} + [E_{adapt}^{uptake}])} - \frac{k_3 \cdot [NR] \cdot [NO_3^-]}{k_4 + [NO_3^-]}$

12. $\frac{d[NO_3^-]_{env}}{dt} = -\frac{k_{17} \cdot [NO_3^-]_{env}}{(k_{18} + [NO_3^-]_{env}) \cdot (k_{22} + [E_{adapt}^{uptake}])}$

13. $\frac{d[E_{adapt}^{uptake}]}{dt} = k_{19} \cdot [NO_3^-] - \frac{k_{20} \cdot [E_{adapt}^{uptake}]}{k_{21} + [E_{adapt}^{uptake}]}$

The differential equations of the model in Figure 4.16 are as follows:
Except the third variable NO_3^-, from the first variable to the eleventh variable, the differential equation is the same with Figure 4.4.

3. $$\frac{d[NO_3^-]}{dt} = \frac{k_{17}\cdot[NO_3^-]_{env}}{(k_{18}+[NO_3^-]_{env})\cdot(k_{20}+[E_{adapt}^{uptake}])} - \frac{k_3\cdot[NR]\cdot[NO_3^-]}{k_4+[NO_3^-]}$$

12. $$\frac{d[NO_3^-]_{env}}{dt} = -\frac{k_{17}\cdot[NO_3^-]_{env}}{(k_{18}+[NO_3^-]_{env})\cdot(k_{20}+[E_{adapt}^{uptake}])}$$

13. $$\frac{d[E_{adapt}^{uptake}]}{dt} = k_{19} - \frac{k_{21}\cdot[E_{adapt}^{uptake}]}{(k_{22}+[E_{adapt}^{uptake}])\cdot(k_{23}+[NO_3^-])}$$

The differential equations of the model in Figure 4.17 are as follows:
Except the third variable NO_3^-, from the first variable to the eleventh variable, the differential equation is the same with Figure 4.4.

3. $$\frac{d[NO_3^-]}{dt} = \frac{k_{17}\cdot[NO_3^-]_{env}\cdot[E_{adapt}^{uptake}]}{k_{18}+[NO_3^-]_{env}} - \frac{k_3\cdot[NR]\cdot[NO_3^-]}{k_4+[NO_3^-]}$$

12. $$\frac{d[NO_3^-]_{env}}{dt} = -\frac{k_{17}\cdot[NO_3^-]_{env}\cdot[E_{adapt}^{uptake}]}{k_{18}+[NO_3^-]_{env}}$$

13. $$\frac{d[E_{adapt}^{uptake}]}{dt} = \frac{k_{19}}{k_{22}+[NO_3^-]} - \frac{k_{20}\cdot[E_{adapt}^{uptake}]}{k_{21}+[E_{adapt}^{uptake}]}$$

The differential equations of the model in Figure 4.18 are as follows:

1. $$\frac{d[nr]}{dt} = k_1\cdot[NO_3^-] - k_7\cdot[nr]$$

2. $$\frac{d[NR]}{dt} = k_2\cdot[nr] - k_8\cdot[NR]\cdot[E_{set}] + k_9\cdot[NR\cdot E_{set}]$$

3. $$\frac{d[NO_3^-]_{cyt}}{dt} = k_{14}\cdot[NO_3^-]_{bra} + 19\cdot k_{20}\cdot[NO_3^-]_{vac}\cdot[E_{adapt}^{efflux}] - \frac{k_3\cdot[NR]\cdot[NO_3^-]_{cyt}}{k_4+[NO_3^-]_{cyt}}$$

4. $$\frac{d[NO_2^-]}{dt} = \frac{k_3\cdot[NR]\cdot[NO_3^-]_{cyt}}{k_4+[NO_3^-]_{cyt}} - k_5\cdot[NO_2^-]$$

5. $$\frac{d[NH_4^+]}{dt} = k_5\cdot[NO_2^-] - k_6\cdot[NH_4^+]$$

6. $$\frac{d[Gln]}{dt} = k_6\cdot[NH_4^+] - k_{11}\cdot[Gln]$$

7. $$\frac{d[E_{set}]}{dt} = -k_8\cdot[NR]\cdot[E_{set}] + (k_9+k_{10})\cdot[NR\cdot E_{set}]$$

8. $$\frac{d[NR\cdot E_{set}]}{dt} = -\frac{d[E_{set}]}{dt}$$

9. $\frac{d[NO_3^-]_{vac}}{dt} = k_{15} \cdot [NO_3^-]_{bra} \cdot [E_{adapt}^{influx}] - k_{20} \cdot [NO_3^-]_{vac} \cdot [E_{adapt}^{efflux}] - k_{19} \cdot [NO_3^-]_{vac}$

10. $\frac{d[NO_3^-]_{bra}}{dt} = \frac{k_{12} \cdot [NO_3^-]_{env} \cdot [E_{adapt}^{uptake}]}{k_{13} + [NO_3^-]_{env}} - \frac{k_{30} \cdot [NAXT1] \cdot [NO_3^-]_{bra}}{k_{31} + [NO_3^-]_{bra}}$
$-19 \cdot k_{15} \cdot [NO_3^-]_{bra} \cdot [E_{adapt}^{influx}] - k_{14} \cdot [NO_3^-]_{bra}$

11. $\frac{d[NO_3^-]_{env}}{dt} = -\frac{k_{12} \cdot [NO_3^-]_{env} \cdot [E_{adapt}^{uptake}]}{k_{13} + [NO_3^-]_{env}}$

12. $\frac{d[E_{adapt}^{influx}]}{dt} = k_{16} - \frac{k_{17} \cdot [NO_3^-]_{vac} \cdot [E_{adapt}^{influx}]}{k_{18} + [E_{adapt}^{influx}]}$

13. $\frac{d[E_{adapt}^{efflux}]}{dt} = k_{21} - \frac{k_{22} \cdot [NO_3^-]_{cyt} \cdot [E_{adapt}^{efflux}]}{k_{23} + [E_{adapt}^{efflux}]}$

14. $\frac{d[E_{adapt}^{uptake}]}{dt} = k_{24} - \frac{k_{25} \cdot [NO_3^-]_{bra} \cdot [E_{adapt}^{uptake}]}{k_{26} + [E_{adapt}^{uptake}]}$

15. $\frac{d[naxt1]}{dt} = k_{27} \cdot [NO_3^-]_{bra} - k_{28} \cdot [naxt1]$

16. $\frac{d[NAXT1]}{dt} = k_{29} \cdot [naxt1] - k_{32} \cdot [NAXT1] \cdot [EF_{set}] + k_{33} \cdot [NAXT1 \cdot EF_{set}]$

17. $\frac{d[EF_{set}]}{dt} = -k_{32} \cdot [NAXT1] \cdot [EF_{set}] + (k_{33} + k_{34}) \cdot [NAXT1 \cdot EF_{set}]$

18. $\frac{d[NAXT1 \cdot EF_{set}]}{dt} = -\frac{d[EF_{set}]}{dt}$

The differential equations of the model in Figure 4.19 are as follows:

1. $\frac{d[NO_3^-]_{cyt}}{dt} = k_1 + k_4 \cdot [NO_3^-]_{vac} \cdot [E_{adapt}^{efflux}] - \frac{k_2 \cdot [NO_3^-]_{cyt}}{k_3 + [NO_3^-]_{cyt}}$

2. $\frac{d[E_{adapt}^{efflux}]}{dt} = k_5 - \frac{k_6 \cdot [NO_3^-]_{cyt} \cdot [E_{adapt}^{efflux}]}{k_7 + [E_{adapt}^{efflux}]}$

3. $\frac{d[NO_3^-]_{vac}}{dt} = -k_4 \cdot [NO_3^-]_{vac} \cdot [E_{adapt}^{efflux}]$

The differential equations of the model in Figure 4.23 are as follows:

1. $\frac{d[NO_3^-]_{cyt}}{dt} = k_1 + \frac{k_4 \cdot [NO_3^-]_{vac}}{k_8 + [E_{adapt}^{efflux}]} - \frac{k_2 \cdot [NO_3^-]_{cyt}}{k_3 + [NO_3^-]_{cyt}}$

2. $\frac{d[E_{adapt}^{efflux}]}{dt} = k_5 \cdot [NO_3^-]_{cyt} - \frac{k_6 \cdot [E_{adapt}^{efflux}]}{k_7 + [E_{adapt}^{efflux}]}$

3. $\frac{d[NO_3^-]_{vac}}{dt} = -\frac{k_4 \cdot [NO_3^-]_{vac}}{k_8 + [E_{adapt}^{efflux}]}$

The differential equations of Figure 4.35

1. $\frac{d[nr]}{dt} = k_1 \cdot [NO_3^-]_{cyt} - k_7 \cdot [nr]$
2. $\frac{d[NR]}{dt} = k_2 \cdot [nr] - k_8 \cdot [NR] \cdot [E_{set}] + k_9 \cdot [NR \cdot E_{set}]$
3. $\frac{d[NO_3^-]_{cyt}}{dt} = k_{14} \cdot [NO_3^-]_{bra} + \frac{19 \cdot k_{20} \cdot [NO_3^-]_{vac}}{k_{24} + [E_{adapt}^{efflux}]} - \frac{k_3 \cdot [NR] \cdot [NO_3^-]_{cyt}}{k_4 + [NO_3^-]_{cyt}}$
4. $\frac{d[NO_2^-]}{dt} = \frac{k_3 \cdot [NR] \cdot [NO_3^-]_{cyt}}{k_4 + [NO_3^-]_{cyt}} - k_5 \cdot [NO_2^-]$
5. $\frac{d[NH_4^+]}{dt} = k_5 \cdot [NO_2^-] - k_6 \cdot [NH_4^+]$
6. $\frac{d[Gln]}{dt} = k_6 \cdot [NH_4^+] - k_{11} \cdot [Gln]$
7. $\frac{d[E_{set}]}{dt} = -k_8 \cdot [NR] \cdot [E_{set}] + (k_9 + k_{10}) \cdot [NR \cdot E_{set}]$
8. $\frac{d[NR \cdot E_{set}]}{dt} = -\frac{d[E_{set}]}{dt}$
9. $\frac{d[NO_3^-]_{vac}}{dt} = k_{15} \cdot [NO_3^-]_{bra} \cdot [E_{adapt}^{influx}] - \frac{k_{20} \cdot [NO_3^-]_{vac}}{k_{24} + [E_{adapt}^{efflux}]} - k_{19} \cdot [NO_3^-]_{vac}$
10. $\frac{d[NO_3^-]_{env}}{dt} = \frac{k_{12} \cdot [NO_3^-]_{env}}{(k_{13} + [NO_3^-]_{env}) \cdot (k_{28} + [E_{adapt}^{uptake}])} - \frac{k_{32} \cdot [NAXT1] \cdot [NO_3^-]_{bra}}{k_{33} + [NO_3^-]_{bra}}$
    $-19 \cdot k_{15} \cdot [NO_3^-]_{bra} \cdot [E_{adapt}^{influx}] - k_{14} \cdot [NO_3^-]_{bra}$
11. $\frac{d[NO_3^-]_{env}}{dt} = -\frac{k_{12} \cdot [NO_3^-]_{env}}{(k_{13} + [NO_3^-]_{env}) \cdot (k_{28} + [E_{adapt}^{uptake}])}$
12. $\frac{d[E_{adapt}^{influx}]}{dt} = k_{16} - \frac{k_{17} \cdot [NO_3^-]_{vac} \cdot [E_{adapt}^{influx}]}{k_{18} + [E_{adapt}^{influx}]}$
13. $\frac{d[E_{adapt}^{efflux}]}{dt} = k_{21} \cdot [NO_3^-]_{cyt} - \frac{k_{22} \cdot [E_{adapt}^{efflux}]}{k_{23} + [E_{adapt}^{efflux}]}$
14. $\frac{d[E_{adapt}^{uptake}]}{dt} = k_{25} \cdot [NO_3^-]_{bra} - \frac{k_{26} \cdot [E_{adapt}^{uptake}]}{k_{27} + [E_{adapt}^{uptake}]}$
15. $\frac{d[naxt1]}{dt} = k_{29} \cdot [NO_3^-]_{bra} - k_{30} \cdot [naxt1]$
16. $\frac{d[NAXT1]}{dt} = k_{31} \cdot [naxt1] - k_{34} \cdot [NAXT1] \cdot [EF_{set}] + k_{35} \cdot [NAXT1 \cdot EF_{set}]$
17. $\frac{d[EF_{set}]}{dt} = -k_{34} \cdot [NAXT1] \cdot [EF_{set}] + (k_{35} + k_{36}) \cdot [NAXT1 \cdot EF_{set}]$
18. $\frac{d[NAXT1 \cdot EF_{set}]}{dt} = -\frac{d[EF_{set}]}{dt}$

Appendix B. Raw data for the graphs and tables shown in the thesis

In the program, all the input data are double precision constants.

The parameter values leading to Figure 3.10:

Rate constant
k_2 = 1.000000000000000
k_3 = 1.000000000000000
k_4 = 2.000000000000000
k_5 = 1.000000000000000
k_6 = $1.000000000000000\times 10^{-6}$

Initial concentration
[A] = 0.000000000000000
[E_{adapt}] = 0.000000000000000

The parameter values leading to Figure 3.13:

Rate constant
k_1 = 1.000000000000000
k_2 = 1.000000000000000
k_3 = 1.000000000000000
k_4 = $1.000000000000000\times 10^{-6}$

Initial concentration
[A] = 1.000000000000000
[E_{adapt}] = 0.000000000000000

The parameter values leading to Figure 4.5 (a) (b):

Rate constant
k_0 = 0.20000000000000
k_2 = 1.00000000000000
k_3 = 22.0000000000000
k_4 = 95.5000000000000
k_5 = 1.00000000000000
k_6 = 1.10000000000000
k_7 = 0.00000000000000
k_8 = 5.00000000000000
k_9 = 5.78750000000000
k_{10} = $1.00000000000000\times 10^{-8}$
k_{11} = 8.00000000000000
k_{12} = 1.50000000000000
k_{13} = 0.10000000000000
k_{14} = 1.90000000000000
k_{15} = 1.00000000000000
k_{16} = 10.0000000000000

Initial concentration
[nr] = 14.0976598922568
[NR] = 8.19689298933763
[NO_3^-] = 681.438860064865
[NO_2^-] = 10.6386968233246
[NH_4^+] = 16.8029636186648
[Gln] = 14.6653538439387
[NMR] = 0.00000000000000
[$NIT24$] = 0.10000000000000
[$NMR{\cdot}NIT24$] = 0.00000000000000

The parameter values leading to Figure 4.5 (c) (d):

Rate constant

k_0 = 0.20000000000000
k_2 = 1.00000000000000
k_3 = 22.0000000000000
k_4 = 95.5000000000000
k_5 = 1.00000000000000
k_6 = 1.10000000000000
k_7 = 0.00000000000000
k_8 = 5.00000000000000
k_9 = $1.00000000000000\times10^{8}$
k_{10} = 0.50000000000000
k_{11} = 0.50000000000000
k_{12} = 1.50000000000000
k_{13} = 0.10000000000000
k_{14} = 1.90000000000000
k_{15} = 1.00000000000000
k_{16} = 10.0000000000000
k_{17} = 8.00000000000000

Initial concentration

[*nr*] = 14.0976598922568
[*NR*] = 8.19689298933763
[NO_3^-] = 681.438860064865
[NO_2^-] = 10.6386968233246
[NH_4^+] = 16.8029636186648
[*Gln*] = 14.6653538439387
[*NMR*] = 0.00000000000000
[*NIT24*] = 0.10000000000000
[*NMR·NIT24*] = 0.00000000000000
[E_{set}] = 11.57500000000000
[$NR{\cdot}E_{set}$] = 0.00000000000000

The parameter values leading to Figure 4.6 (a):

Rate constant

k_0 = 0.50000000000000
k_2 = 1.00000000000000
k_3 = 22.0000000000000
k_4 = 95.5000000000000
k_5 = 1.00000000000000
k_6 = 1.10000000000000
k_7 = 0.00000000000000
k_8 = 5.00000000000000
k_9 = 5.78750000000000
k_{10} = 0.04000000000000
k_{11} = 8.00000000000000
k_{12} = 1.50000000000000
k_{13} = $1.00000000000000\times10^{-4}$
k_{14} = 1.90000000000000
k_{15} = 1.00000000000000
k_{16} = 10.0000000000000

Initial concentration

[*nr*] = 6.04463966075566
[*NR*] = 1.26987129850828
[NO_3^-] = 60.3985502192925
[NO_2^-] = 8.29620853403252
[NH_4^+] = 6.19092634979609
[*Gln*] = 3.33098524095421
[*NMR*] = 0.00000000000000
[*NIT24*] = $1.472925440366243\times10^{-2}$
[*NMR·NIT24*] = 0.00000000000000

The parameter values leading to Figure 4.6 (b):

Rate constant

k_0 = 0.50000000000000
k_2 = 1.00000000000000
k_3 = 22.0000000000000
k_4 = 95.5000000000000
k_5 = 1.00000000000000
k_6 = 1.10000000000000
k_7 = 0.00000000000000
k_8 = 5.00000000000000
k_9 = 100.000000000000
k_{10} = 2.0000000000000
k_{11} = 2.00000000000000
k_{12} = 1.50000000000000
k_{13} = $1.00000000000000\times10^{-4}$
k_{14} = 1.90000000000000
k_{15} = 1.00000000000000
k_{16} = 10.0000000000000
k_{17} = 8.00000000000000

Initial concentration

[*nr*] = 6.04463966075566
[*NR*] = 1.26987129850828
[NO_3^-] = 60.3985502192925
[NO_2^-] = 8.29620853403252
[NH_4^+] = 6.19092634979609
[*Gln*] = 3.33098524095421
[*NMR*] = 0.00000000000000
[*NIT24*] = $1.472925440366243\times10^{-2}$
[*NMR*·*NIT24*] = 0.00000000000000
[E_{set}] = 2.89375000000000
[*NR*·E_{set}] = 0. 00000000000000

The parameter values leading to Figure 4.8:

Rate constant

k_0 = 5.00000000000000
k_2 = 1.00000000000000
k_3 = 12.0000000000000
k_4 = 71.0000000000000
k_5 = 1.00000000000000
k_6 = 1.10000000000000
k_7 = 0.00000000000000
k_8 = 1.00000000000000
k_9 = 100.000000000000
k_{10} = 0.10000000000000
k_{11} = 0.50000000000000
k_{12} = 1.50000000000000
k_{13} = 0.20000000000000
k_{14} = 1.90000000000000
k_{15} = 1.00000000000000
k_{16} = 10.0000000000000
k_{17} = 0.10000000000000
k_{18} = 1000.00000000000

Initial concentration

[*nr*] = 0.00000000000000
[*NR*] = 0.00000000000000
[NO_3^-] = 0.50000000000000
[NO_2^-] = 0.00000000000000
[NH_4^+] = 0.00000000000000
[*Gln*] = 0.00000000000000
[*NMR*] = 0.00000000000000
[*NIT24*] = 0.20000000000000
[*NMR*·*NIT24*] = 0.00000000000000
[E_{set}] = 2.50000000000000
[*NR*·E_{set}] = 0. 00000000000000
[NO_3^-]$_{env}$ = 100.00000000000

The parameter values leading to Figure 4.10:

Rate constant

k_0 = 3.00000000000000
or k_0 = 4.00000000000000
or k_0 = 5.00000000000000
or k_0 = 6.00000000000000
k_2 = 1.00000000000000
k_3 = 12.0000000000000
k_4 = 71.0000000000000
k_5 = 1.00000000000000
k_6 = 1.10000000000000
k_7 = 0.00000000000000
k_8 = 1.00000000000000
k_9 = 100.000000000000
k_{10} = 0.10000000000000
k_{11} = 0.50000000000000
k_{12} = 1.50000000000000
k_{13} = 0.20000000000000
k_{14} = 1.90000000000000
k_{15} = 1.00000000000000
k_{16} = 10.0000000000000
k_{17} = 0.10000000000000
k_{18} = 1000.00000000000
k_{19} = 2000.00000000000
k_{20} = 1000.00000000000
k_{21} = $1.000000000000000 \times 10^{-6}$

Initial concentration

$[nr]$ = 0.00000000000000
$[NR]$ = 0.00000000000000
$[NO_3^-]$ = 2.00000000000000
$[NO_2^-]$ = 0.00000000000000
$[NH_4^+]$ = 0.00000000000000
$[Gln]$ = 0.00000000000000
$[NMR]$ = 0.00000000000000
$[NIT24]$ = 0.20000000000000
$[NMR \cdot NIT24]$ = 0.00000000000000
$[E_{set}]$ = 4.00000000000000
$[NR \cdot E_{set}]$ = 0. 00000000000000
$[NO_3^-]_{env}$ = 5000.00000000000
$[E_{adapt}^{uptake}]$ = 0. 00000000000000

The parameter values generating Figure 4.11:

Rate constant

k_0 = 5.00000000000000
k_2 = 1.00000000000000
k_3 = 12.0000000000000
k_4 = 71.0000000000000
k_5 = 1.00000000000000
k_6 = 1.10000000000000
k_7 = 0.00000000000000
k_8 = 1.00000000000000
k_9 = 100.000000000000
k_{10} = 0.10000000000000
k_{11} = 0.50000000000000
k_{12} = 1.50000000000000
k_{13} = 0.20000000000000
k_{14} = 1.90000000000000
k_{15} = 1.00000000000000
k_{16} = 10.0000000000000
k_{17} = 0.10000000000000
k_{18} = 1000.00000000000
k_{19} = 490.000000000000
k_{20} = 1000.00000000000
k_{21} = $1.00000000000000 \times 10^{-6}$

Initial concentration

$[nr] = 0.00000000000000$
$[NR] = 0.00000000000000$
$[NO_3^-] = 0.50000000000000$
$[NO_2^-] = 0.00000000000000$
$[NH_4^+] = 0.00000000000000$
$[Gln] = 0.00000000000000$
$[NMR] = 0.00000000000000$
$[NIT24] = 0.20000000000000$
$[NMR{\cdot}NIT24] = 0.00000000000000$
$[E_{set}] = 2.50000000000000$
$[NR{\cdot}E_{set}] = 0.\ 00000000000000$
$[NO_3^-]_{env} = 100.000000000000$
$[E_{adapt}^{uptake}] = 0.\ 00000000000000$

The parameter values leading to Figure 4.12:

Rate constant

$k_0 = 2.00000000000000$
$k_2 = 8.00000000000000$
$k_3 = 1.00000000000000$
$k_4 = 20.0000000000000$
$k_5 = 1.00000000000000$
$k_6 = 1.00000000000000$
$k_7 = 0.00000000000000$
$k_8 = 0.50000000000000$
$k_9 = 1.00000000000000\times10^{9}$
$k_{10} = 1.00000000000000\times10^{3}$
$k_{11} = 1.00000000000000$
$k_{12} = 1.50000000000000$
$k_{13} = 0.20000000000000$
$k_{14} = 1.00000000000000$
$k_{15} = 1.00000000000000$
$k_{16} = 10.0000000000000$
$k_{17} = 1.00000000000000$
$k_{18} = 1.00000000000000$
$k_{19} = 300.000000000000$
or $k_{19} = 350.000000000000$
$k_{20} = 1000.00000000000$
$k_{21} = 1.00000000000000\times 10^{-6}$

Initial concentration

$[nr] = 0.00000000000000$
$[NR] = 0.00000000000000$
$[NO_3^-] = 0.30000000000000$
$[NO_2^-] = 0.00000000000000$
$[NH_4^+] = 0.00000000000000$
$[Gln] = 0.00000000000000$
$[NMR] = 0.00000000000000$
$[NIT24] = 0.20000000000000$
$[NMR{\cdot}NIT24] = 0.00000000000000$
$[E_{set}] = 4.00000000000000$
$[NR{\cdot}E_{set}] = 0.\ 00000000000000$
$[NO_3^-]_{env} = 100.000000000000$
$[E_{adapt}^{uptake}] = 0.00000000000000$

The parameter values leading to Figure 4.13:

Rate constant

k_0 = 5.00000000000000
k_2 = 1.00000000000000
k_3 = 12.0000000000000
k_4 = 71.0000000000000
k_5 = 1.00000000000000
k_6 = 1.10000000000000
k_7 = 0.00000000000000
k_8 = 1.00000000000000
k_9 = 1.00000000000000×10^2
k_{10} = 0.10000000000000
k_{11} = 0.50000000000000
k_{12} = 1.50000000000000
k_{13} = 0.20000000000000
k_{14} = 1.90000000000000
k_{15} = 1.00000000000000
k_{16} = 10.0000000000000
k_{17} = 0.10000000000000
k_{18} = 1000.00000000000
k_{19} = 750.000000000000
or k_{19} = 500.000000000000
k_{20} = 1000.00000000000
k_{21} = 1.00000000000000× 10^{-6}

Initial concentration

[nr] = 0.00000000000000
[NR] = 0.00000000000000
[NO_3^-] = 0.75000000000000
[NO_2^-] = 0.00000000000000
[NH_4^+] = 0.00000000000000
[Gln] = 0.00000000000000
[NMR] = 0.00000000000000
[$NIT24$] = 0.20000000000000
[$NMR{\cdot}NIT24$] = 0.00000000000000
[E_{set}] = 4.00000000000000
[$NR{\cdot}E_{set}$] = 0. 00000000000000
[NO_3^-]$_{env}$ = 100.000000000000
[E_{adapt}^{uptake}] = 0. 00000000000000

The parameter values generating Figure 4.15:

Rate constant

k_0 = 5.00000000000000
k_2 = 8.00000000000000
k_3 = 22.0000000000000
k_4 = 90.0000000000000
k_5 = 1.00000000000000
k_6 = 10.0000000000000
k_7 = 0.00000000000000
k_8 = 2.00000000000000
k_9 = 1.00000000000000×10^2
k_{10} = 0.10000000000000
k_{11} = 0.50000000000000
k_{12} = 1.50000000000000
k_{13} = 0.10000000000000
k_{14} = 10.0000000000000
k_{15} = 1.00000000000000
k_{16} = 10.0000000000000
k_{17} = 2.00000000000000
k_{18} = 1.00000000000000
k_{19} = 2500.00000000000
k_{20} = 10000.0000000000
k_{21} = 1.00000000000000× 10^{-6}

Initial concentration
$[nr]$ = 0.498826073061659
$[NR]$ = 2.55718319514992
$[NO_3^-]$ = 0.399060869516096
$[NO_2^-]$ = 0.248350185659299
$[NH_4^+]$ = $2.483504569314989\times 10^{-2}$
$[Gln]$ = $2.483507283786963\times 10^{-2}$
$[NMR]$ = 0.00000000000000
$[NIT24]$ = 0.10000000000000
$[NMR{\cdot}NIT24]$ = 0.00000000000000
$[E_{set}]$ = $1.872671373806222\times 10^{-2}$
$[NR{\cdot}E_{set}]$ = 7.98127328626193
$[NO_3^-]_{env}$ = 150.285779413917
$[E_{adapt}^{uptake}]$ = $1.108213316182029\times 10^{-7}$

The parameter values leading to Figure 4.20:

Rate constant
k_1 = 0.00000000000000
k_2 = 1.50000000000000
k_3 = 1.00000000000000
k_4 = 2.00000000000000
k_5 = 1.00000000000000
k_6 = 1.00000000000000
k_7 = $1.00000000000000\times 10^{-8}$

Initial concentration
$[NO_3^-]_{cyt}$ = 0.999956000000000
$[E_{adapt}^{efflux}]$ = $8.247410000000000\times 10^{-3}$
$[NO_3^-]_{vac}$ = 50.0000000000000

The parameter values leading to Figure 4.21:

Rate constant
k_1 = 0.00000000000000
k_2 = 1.50000000000000
or k_2 = 3.00000000000000
k_3 = 1.00000000000000
k_4 = 2.00000000000000
k_5 = 1.00000000000000
k_6 = 1.00000000000000
k_7 = $1.00000000000000\times 10^{-8}$

Initial concentration
$[NO_3^-]_{cyt}$ = 0.999956000000000
$[E_{adapt}^{efflux}]$ = $8.247410000000000\times 10^{-3}$
$[NO_3^-]_{vac}$ = 50.0000000000000

The parameter values leading to Figure 4.22:

Rate constant
k_1 = 0.00000000000000
k_2 = 1.50000000000000
k_3 = 1.00000000000000
k_4 = 2.00000000000000

Initial concentration
$[NO_3^-]_{cyt}$ = 0.999956000000000
$[E_{adapt}^{efflux}]$ = $8.247410000000000\times 10^{-3}$
$[NO_3^-]_{vac}$ = 50.0000000000000

or k_4 = 20.0000000000000
k_5 = 1.00000000000000
k_6 = 1.00000000000000
k_7 = $1.00000000000000\times 10^{-8}$

The parameter values leading to Figure 4.24:

Rate constant

k_1 = 0.00000000000000
k_2 = 1.50000000000000
k_3 = 1.00000000000000
k_4 = 0.01000000000000
k_5 = 1.00000000000000
k_6 = 1.00000000000000
k_7 = $1.00000000000000\times 10^{-6}$
k_8 = $1.00000000000000\times 10^{-6}$

Initial concentration

$[NO_3^-]_{cyt}$ = 1.00000000000000
$[E_{adapt}^{efflux}]$ = $1.00000000000000\times 10^{-2}$
$[NO_3^-]_{vac}$ = 60.0000000000000

The parameter values leading to Figure 4.25:

Rate constant

k_1 = 0.00000000000000
k_2 = 1.50000000000000
or k_2 = 3.00000000000000
k_3 = 1.00000000000000
k_4 = 0.01000000000000
k_5 = 1.00000000000000
k_6 = 1.00000000000000
k_7 = $1.00000000000000\times 10^{-6}$
k_8 = $1.00000000000000\times 10^{-6}$

Initial concentration

$[NO_3^-]_{cyt}$ = 1.00000000000000
$[E_{adapt}^{efflux}]$ = $1.00000000000000\times 10^{-2}$
$[NO_3^-]_{vac}$ = 200.000000000000

The parameter values leading to Figure 4.26:

Rate constant

k_1 = 0.00000000000000
k_2 = 1.50000000000000
k_3 = 1.00000000000000
k_4 = 0.01000000000000
or k_4 = 0.05000000000000
k_5 = 1.00000000000000
k_6 = 1.00000000000000
k_7 = $1.00000000000000\times 10^{-6}$
k_8 = $1.00000000000000\times 10^{-6}$

Initial concentration

$[NO_3^-]_{cyt}$ = 1.00000000000000
$[E_{adapt}^{efflux}]$ = $1.00000000000000\times 10^{-2}$
$[NO_3^-]_{vac}$ = 60.0000000000000

The parameter values leading to Figure 4.27:

Rate constant

k_1 = 1.00000000000000
k_2 = 1.00000000000000 (a)
or k_2 = 0.00000000000000 (b)
k_3 = 12.0000000000000
k_4 = 71.0000000000000
k_5 = 1.00000000000000
k_6 = 1.10000000000000
k_7 = 0.00000000000000
k_8 = 100.000000000000
k_9 = 0.10000000000000
k_{10} = 0.50000000000000
k_{11} = 1.90000000000000
k_{12} = 0.10000000000000
k_{13} = 1000.00000000000
k_{14} = 0.01000000000000
k_{15} = 0.10000000000000
k_{16} = 100.000000000000
k_{17} = 2.00000000000000
k_{18} = $1.00000000000000\times10^{-6}$
k_{19} = 0.00000000000000
k_{20} = 0.00000000000000
k_{21} = $5.00000000000000\times 10^{3}$
k_{22} = $1.00000000000000\times 10^{4}$
k_{23} = $1.00000000000000\times 10^{-6}$
k_{24} = $1.00000000000000\times 10^{3}$
k_{25} = $1.00000000000000\times 10^{3}$
k_{26} = $1.00000000000000\times 10^{-6}$
k_{27} = 1.00000000000000
k_{28} = 0.50000000000000
k_{29} = 1.00000000000000
k_{30} = 1.00000000000000
k_{31} = 20.0000000000000
k_{32} = $1.00000000000000\times 10^{9}$
k_{33} = $1.00000000000000\times 10^{3}$
k_{34} = 1.00000000000000

Initial concentration

[*nr*] = 0.00000000000000
[*NR*] = 0.00000000000000
$[NO_3^-]_{cyt}$ = 0.00000000000000
$[NO_2^-]$ = 0.00000000000000
$[NH_4^+]$ = 0.00000000000000
[*Gln*] = 0.00000000000000
$[E_{set}]$ = 10.0000000000000
$[NR\cdot E_{set}]$ = 0.00000000000000
$[NO_3^-]_{vac}$ = 50.0000000000000
$[NO_3^-]_{bra}$ = 1.00000000000000
$[NO_3^-]_{env}$ = 1000.00000000000
$[E_{adapt}^{influx}]$ = 0.00000000000000
$[E_{adapt}^{efflux}]$ = 0.00000000000000
$[E_{adapt}^{uptake}]$ = 0.00000000000000
[*naxt1*] = 0.00000000000000
[*NAXT1*] = 0.00000000000000
$[EF_{set}]$ = 4.00000000000000
$[NAXT1\cdot EF_{set}]$ = 0.00000000000000

The parameter values leading to Figure 4.28:

Rate constant

k_1 = 1.00000000000000
k_2 = 1.00000000000000
k_3 = 12.0000000000000
k_4 = 71.0000000000000
k_5 = 1.00000000000000
k_6 = 1.10000000000000
k_7 = 0.10000000000000
k_8 = 100.000000000000
k_9 = 0.10000000000000
k_{10} = 0.50000000000000
k_{11} = 2.00000000000000
k_{12} = 1.00000000000000
k_{13} = 1.00000000000000
k_{14} = 3.00000000000000
k_{15} = 1.00000000000000
k_{16} = 100.000000000000
k_{17} = 2.00000000000000
k_{18} = $1.00000000000000\times10^{-6}$
k_{19} = 0.00000000000000
k_{20} = 0.01000000000000
k_{21} = $5.00000000000000\times 10^{3}$
k_{22} = $1.00000000000000\times 10^{4}$
k_{23} = $1.00000000000000\times 10^{-6}$
k_{24} = $5.00000000000000\times 10^{3}$
k_{25} = $5.00000000000000\times 10^{3}$
k_{26} = $1.00000000000000\times 10^{-6}$
k_{27} = 1.00000000000000
k_{28} = 0.50000000000000
k_{29} = 1.00000000000000
k_{30} = 1.00000000000000
k_{31} = 20.0000000000000
k_{32} = $1.00000000000000\times 10^{9}$
k_{33} = $1.00000000000000\times 10^{3}$
k_{34} = 1.00000000000000

Initial concentration

$[nr]$ = 8.89181001831743
$[NR]$ = 41.7359887485820
$[NO_3^-]_{cyt}$ = 0.50000000000000
$[NO_2^-]$ = 8.00573777151832
$[NH_4^+]$ = 7.29852248309812
$[Gln]$ = 4.23793355971440
$[E_{set}]$ = 8.00000000000000
$[NR{\cdot}E_{set}]$ = 2.00000000000000
$[NO_3^-]_{vac}$ = 50.0000000000000
$[NO_3^-]_{bra}$ = 1.00000000000000
$[NO_3^-]_{env}$ = 1000.00000000000
$[E_{adapt}^{influx}]$ = 0. 00000000000000
$[E_{adapt}^{efflux}]$ = 0. 00000000000000
$[E_{adapt}^{uptake}]$ = 0. 00000000000000
$[naxt1]$ = 0.00000000000000
$[NAXT1]$ = 0.00000000000000
$[EF_{set}]$ = 4.00000000000000
$[NAXT1{\cdot}EF_{set}]$ = 0.00000000000000

The parameter values leading to Figure 4.30:

Rate constant

k_1 = 1.00000000000000
k_2 = 1.00000000000000
k_3 = 12.0000000000000
k_4 = 71.0000000000000
k_5 = 1.00000000000000
k_6 = 1.10000000000000
k_7 = 0.10000000000000
k_8 = 100.000000000000
k_9 = 0.10000000000000
k_{10} = 0.50000000000000
k_{11} = 2.00000000000000
k_{12} = 0.10000000000000
k_{13} = 1000.00000000000
k_{14} = 0.01000000000000
k_{15} = $8.00000000000000\times10^{-3}$
k_{16} = 100.000000000000
k_{17} = 2.00000000000000
k_{18} = $1.00000000000000\times10^{-6}$
k_{19} = 0.00000000000000
or k_{19} = $1.00000000000000\times 10^{-3}$
or k_{19} = $5.00000000000000\times 10^{-3}$
or k_{19} = $1.00000000000000\times 10^{-2}$
k_{20} = 0.01000000000000
k_{21} = $5.00000000000000\times 10^{3}$
k_{22} = $1.00000000000000\times 10^{4}$
k_{23} = $1.00000000000000\times 10^{-6}$
k_{24} = $5.00000000000000\times 10^{3}$
k_{25} = $5.00000000000000\times 10^{3}$
k_{26} = $1.50000000000000\times 10^{-6}$
k_{27} = 1.00000000000000
k_{28} = 0.50000000000000
k_{29} = 1.00000000000000
k_{30} = 1.00000000000000
k_{31} = 20.0000000000000
k_{32} = $1.00000000000000\times 10^{9}$
k_{33} = $1.00000000000000\times 10^{3}$
k_{34} = 1.00000000000000

Initial concentration

[*nr*] = 5.00018092419815
[*NR*] = 72.6987450482467
$[NO_3^-]_{cyt}$ = 0.500000228072364
$[NO_2^-]$ = 6.10054542184316
$[NH_4^+]$ = 5.54590658434945
[*Gln*] = 3.05023513117952
$[E_{set}]$ = $8.252556284676702\times10^{-4}$
$[NR\cdot E_{set}]$ = 9.99917474437158
$[NO_3^-]_{vac}$ = 45.9873343966219
$[NO_3^-]_{bra}$ = $4.063583076111295\times10^{-18}$
$[NO_3^-]_{env}$ = 0.00000000000000
$[E_{adapt}^{influx}]$ = 111.424888692423
$[E_{adapt}^{efflux}]$ = 0.698201022610504
$[E_{adapt}^{uptake}]$ = 83847.2349577894
[*naxt1*] = $9.425975652532770\times10^{-4}$
[*NAXT1*] = $4.715379735819632\times10^{-10}$
$[EF_{set}]$ = 3.99811568380348
$[NAXT1\cdot EF_{set}]$ = $1.884316196543005\times10^{-3}$

The parameter values leading to Figure 4.31, 4.32:

Rate constant

k_1 = 1.00000000000000
k_2 = 1.00000000000000
k_3 = 12.0000000000000
k_4 = 71.0000000000000
k_5 = 1.00000000000000
k_6 = 1.10000000000000
k_7 = 0.10000000000000
k_8 = 100.000000000000
k_9 = 0.10000000000000
k_{10} = 0.50000000000000
k_{11} = 2.00000000000000
k_{12} = 1.00000000000000
k_{13} = 1.00000000000000
k_{14} = 3.00000000000000
k_{15} = 1.00000000000000
k_{16} = 100.000000000000
k_{17} = 2.00000000000000
k_{18} = $1.00000000000000\times10^{-6}$
k_{19} = 0.00000000000000
k_{20} = 0.01000000000000
k_{21} = $5.00000000000000\times 10^{3}$
k_{22} = $1.00000000000000\times 10^{4}$
k_{23} = $1.00000000000000\times 10^{-6}$
k_{24} = $5.00000000000000\times 10^{3}$
k_{25} = $5.00000000000000\times 10^{3}$
k_{26} = $1.00000000000000\times 10^{-6}$
k_{27} = 1.00000000000000
k_{28} = 0.50000000000000
k_{29} = 1.00000000000000
k_{30} = 1.00000000000000
k_{31} = 20.0000000000000
k_{32} = $1.00000000000000\times 10^{9}$
k_{33} = $1.00000000000000\times 10^{3}$
k_{34} = 1.00000000000000

Initial concentration

$[nr]$ = 8.89181001831743
$[NR]$ = 41.7359887485820
$[NO_3^-]_{cyt}$ = 0.50000000000000
$[NO_2^-]$ = 8.00573777151832
$[NH_4^+]$ = 7.29852248309812
$[Gln]$ = 4.23793355971440
$[E_{set}]$ = 8.00000000000000
$[NR{\cdot}E_{set}]$ = 2.00000000000000
$[NO_3^-]_{vac}$ = 50.0000000000000
$[NO_3^-]_{bra}$ = 1.00000000000000
$[NO_3^-]_{env}$ = 1000.00000000000
$[E_{adapt}^{influx}]$ = 0. 00000000000000
$[E_{adapt}^{efflux}]$ = 0. 00000000000000
$[E_{adapt}^{uptake}]$ = 0. 00000000000000
$[naxt1]$ = 0.00000000000000
$[NAXT1]$ = 0.00000000000000
$[EF_{set}]$ = 4.00000000000000
$[NAXT1{\cdot}EF_{set}]$ = 0.00000000000000

The parameter values leading to Figure 4.33:

Rate constant

k_1 = 1.00000000000000
k_2 = 1.00000000000000
k_3 = 12.0000000000000
k_4 = 71.0000000000000
k_5 = 1.00000000000000
k_6 = 1.10000000000000
k_7 = 0.10000000000000
k_8 = 100.000000000000
k_9 = 0.10000000000000
k_{10} = 0.50000000000000
k_{11} = 2.00000000000000
k_{12} = 1.00000000000000
k_{13} = 1.00000000000000
k_{14} = 3.00000000000000
k_{15} = 1.00000000000000
k_{16} = 100.000000000000
k_{17} = 2.00000000000000
k_{18} = $1.00000000000000\times10^{-6}$
k_{19} = 0.00000000000000
k_{20} = 0.01000000000000
k_{21} = $5.50000000000000\times 10^{3}$
k_{22} = $1.00000000000000\times 10^{4}$
k_{23} = $1.00000000000000\times 10^{-6}$
k_{24} = $5.00000000000000\times 10^{3}$
k_{25} = $5.00000000000000\times 10^{3}$
k_{26} = $1.00000000000000\times 10^{-6}$
k_{27} = 1.00000000000000
k_{28} = 0.50000000000000
k_{29} = 1.00000000000000
k_{30} = 1.00000000000000
k_{31} = 20.0000000000000
k_{32} = $1.00000000000000\times 10^{9}$
k_{33} = $1.00000000000000\times 10^{3}$
k_{34} = 1.00000000000000

Initial concentration

$[nr]$ = 8.89181001831743
$[NR]$ = 41.7359887485820
$[NO_3^-]_{cyt}$ = 0.50000000000000
$[NO_2^-]$ = 8.00573777151832
$[NH_4^+]$ = 7.29852248309812
$[Gln]$ = 4.23793355971440
$[E_{set}]$ = 8.00000000000000
$[NR{\cdot}E_{set}]$ = 2.00000000000000
$[NO_3^-]_{vac}$ = 50.0000000000000
$[NO_3^-]_{bra}$ = 1.00000000000000
$[NO_3^-]_{env}$ = 3000.00000000000
$[E_{adapt}^{influx}]$ = 0. 00000000000000
$[E_{adapt}^{efflux}]$ = 0. 00000000000000
$[E_{adapt}^{uptake}]$ = 0. 00000000000000
$[naxt1]$ = 0.00000000000000
$[NAXT1]$ = 0.00000000000000
$[EF_{set}]$ = 4.00000000000000
$[NAXT1{\cdot}EF_{set}]$ = 0.00000000000000

The parameter values leading to Figure 4.34:

Rate constant

k_1 = 1.00000000000000
k_2 = 1.00000000000000
k_3 = 12.0000000000000
k_4 = 71.0000000000000
k_5 = 1.00000000000000
k_6 = 1.10000000000000
k_7 = 0.10000000000000
k_8 = 100.000000000000
k_9 = 0.10000000000000
k_{10} = 0.50000000000000
k_{11} = 2.00000000000000
k_{12} = 1.00000000000000
k_{13} = 1.00000000000000
k_{14} = 0.01000000000000
k_{15} = $8.00000000000000\times10^{-3}$
k_{16} = $2.00000000000000\times10^{6}$
k_{17} = $4.00000000000000\times10^{4}$
k_{18} = $1.00000000000000\times10^{-6}$
k_{19} = 0.00000000000000
k_{20} = 1.00000000000000
k_{21} = $2.00000000000000\times 10^{4}$
k_{22} = $1.00000000000000\times 10^{5}$
k_{23} = $1.00000000000000\times 10^{-6}$
k_{24} = $5.00000000000000\times 10^{3}$
k_{25} = $5.00000000000000\times 10^{3}$
k_{26} = $1.00000000000000\times 10^{-3}$
k_{27} = 1.00000000000000
k_{28} = 0.50000000000000
k_{29} = 1.00000000000000
k_{30} = 1.00000000000000
k_{31} = 20.0000000000000
k_{32} = $1.00000000000000\times 10^{9}$
k_{33} = $1.00000000000000\times 10^{3}$
k_{34} = 1.00000000000000

Initial concentration

$[nr]$ = 8.89181001831743
$[NR]$ = 41.7359887485820
$[NO_3^-]_{cyt}$ = 0.50000000000000
$[NO_2^-]$ = 8.00573777151832
$[NH_4^+]$ = 7.29852248309812
$[Gln]$ = 4.23793355971440
$[E_{set}]$ = 8.00000000000000
$[NR{\cdot}E_{set}]$ = 2.00000000000000
$[NO_3^-]_{vac}$ = 50.0000000000000
$[NO_3^-]_{bra}$ = 1.00000000000000
$[NO_3^-]_{env}$ = 70.0000000000000
$[E_{adapt}^{influx}]$ = 0. 00000000000000
$[E_{adapt}^{efflux}]$ = 0. 00000000000000
$[E_{adapt}^{uptake}]$ = 0. 00000000000000
$[naxt1]$ = 0.00000000000000
$[NAXT1]$ = 0.00000000000000
$[EF_{set}]$ = 4.00000000000000
$[NAXT1{\cdot}EF_{set}]$ = 0.00000000000000

The parameter values leading to Figure 4.36:

Rate constant

k_1 = 1.00000000000000
k_2 = 1.00000000000000
k_3 = 1.00000000000000
k_4 = 200.000000000000
k_5 = 1.00000000000000
k_6 = 1.10000000000000
k_7 = 0.50000000000000
k_8 = $1.00000000000000\times10^{9}$
k_9 = $1.00000000000000\times10^{3}$
k_{10} = 1.00000000000000
k_{11} = 1.00000000000000
k_{12} = 1.00000000000000
k_{13} = 1.00000000000000
k_{14} = 0.10000000000000
k_{15} = 1.00000000000000
k_{16} = 100.000000000000
k_{17} = 2.00000000000000
k_{18} = $1.00000000000000\times10^{-6}$
k_{19} = 0.00000000000000
k_{20} = 1.50000000000000
k_{21} = 500.000000000000
k_{22} = $1.00000000000000\times 10^{3}$
k_{23} = $1.00000000000000\times 10^{-6}$
k_{24} = 2.00000000000000
k_{25} = $5.00000000000000\times 10^{2}$
k_{26} = $1.50000000000000\times 10^{3}$
k_{27} = $1.00000000000000\times 10^{-6}$
k_{28} = 1.00000000000000
k_{29} = 0.50000000000000
k_{30} = 0.50000000000000
k_{31} = 1.00000000000000
k_{32} = 1.00000000000000
k_{33} = $2.00000000000000\times 10^{3}$
k_{34} = $1.00000000000000\times 10^{9}$
k_{35} = 100.000000000000
k_{36} = 1.00000000000000

Initial concentration

$[nr]$ = 0.00000000000000
$[NR]$ = 0.00000000000000
$[NO_3^-]_{cyt}$ = 4.00000000000000
$[NO_2^-]$ = 0.00000000000000
$[NH_4^+]$ = 0.00000000000000
$[Gln]$ = 0.00000000000000
$[E_{set}]$ = 4.00000000000000
$[NR{\cdot}E_{set}]$ = 0.00000000000000
$[NO_3^-]_{vac}$ = 50.0000000000000
$[NO_3^-]_{bra}$ = 2.00000000000000
$[NO_3^-]_{env}$ = 200.000000000000
$[E_{adapt}^{influx}]$ = 0.00000000000000
$[E_{adapt}^{efflux}]$ = 0.00000000000000
$[E_{adapt}^{uptake}]$ = 0.00000000000000
$[naxt1]$ = 0.00000000000000
$[NAXT1]$ = 0.00000000000000
$[EF_{set}]$ = 4.00000000000000
$[NAXT1{\cdot}EF_{set}]$ = 0.00000000000000

The parameter values generating Figure 4.37:

Rate constant

k_1 = 0.10000000000000
k_2 = 1.00000000000000
k_3 = 22.0000000000000
k_4 = 1.10000000000000
k_5 = 1.00000000000000
k_6 = 1.10000000000000
k_7 = 0.00000000000000
k_8 = 1.00000000000000
k_9 = 1.00000000000000
k_{10} = 1.00000000000000×10^{-2}
k_{11} = 8.00000000000000
k_{12} = 1.00000000000000
k_{13} = 1.00000000000000×10^{-3}
k_{14} = 1.50000000000000
k_{15} = 1.00000000000000×10^{3}
k_{16} = 100.000000000000

Initial concentration

[*nr*] = 1.47652918132859
[*NR*] = 0.379889888499067
[NO_3^-] = 23.4004494072504
[NO_2^-] = 3.37608001531119
[NH_4^+] = 2.24487626354991
[*Gln*] = 2.02792260287317
[*NMR*] = 0.00000000000000
[*NIT24*] = 3.680981595092126×10^{-3}
[*NMR·NIT24*] = 0.00000000000000

When t = 29.53, the calculation is terminated. Starting from the concentration of every variable at this point, we increase the concentration of nitrate by one-fold. Below is this new set of concentration:

[*nr*] = 1.47119165750123
[*NR*] = 0.372616466040261
[NO_3^-]$_{cyt}$ = 46.7980525005934
[NO_2^-] = 3.30962766092717
[NH_4^+] = 2.23206724623582
[*Gln*] = 2.03648362730474
[*NMR*] = 0.000000000000000
[*NIT24*] = 3.680981595092126×10^{-3}
[*NMR·NIT24*] = 0.000000000000000

The parameter values leading to Figure 4.38:

Rate constant

k_1 = 0.50000000000000
k_2 = 1.00000000000000
k_3 = 22.0000000000000
k_4 = 95.5000000000000
k_5 = 1.00000000000000
k_6 = 1.10000000000000
k_7 = 0.00000000000000
k_8 = 5.00000000000000
k_9 = 5.78750000000000
k_{10} = 1.00000000000000×10^{-2}
k_{11} = 8.00000000000000 or k_{11} = 12.0000000000000
k_{12} = 1.50000000000000
k_{13} = 1.00000000000000×10^{-3}
k_{14} = 1.90000000000000
k_{15} = 1.00000000000000
k_{16} = 10.0000000000000

Initial concentration
when k_{11} = 8.0
[*nr*] = 5.52022356855451
[*NR*] = 1.25092925568653
[NO_3^-] = 58.3934073511144
[NO_2^-] = 10.5670153073971
[NH_4^+] = 8.74157906371040
[*Gln*] = 4.66833383308026
[*NMR*] = 0.000000000000000
[*NIT24*] = $1.472925440366243\times10^{-2}$
[*NMR·NIT24*] = 0.000000000000000

when k_{11} = 12.0
[*nr*] = 5.14413111453449
[*NR*] = 1.56903117080545
[NO_3^-] = 54.6307044806988
[NO_2^-] = 15.2349321463566
[NH_4^+] = 14.0748049697252
[*Gln*] = 7.88223484726116
[*NMR*] = 0.000000000000000
[E_{set}] = $1.472925440366243\times10^{-2}$
[*NMR·NIT24*] = 0.000000000000000

The parameter values leading to Figure 4.39

Rate constant
k_1 = 0.20000000000000
k_2 = 1.00000000000000
k_3 = 22.0000000000000
k_4 = 95.5000000000000
k_5 = 1.00000000000000
k_6 = 1.10000000000000
k_7 = 0.00000000000000
k_8 = $5.00000000000000\times10^{-2}$
k_9 = 10.0000000000000
or k_9 = 1.00000000000000
or k_9 = 0.10000000000000
or k_9 = 0.01000000000000
k_{10} = 0.80000000000000
k_{11} = 0.20000000000000
k_{12} = 1.50000000000000
k_{13} = 0.20000000000000
k_{14} = 1.90000000000000
k_{15} = 1.00000000000000
k_{16} = 10.0000000000000
k_{17} = 0.01000000000000
or k_{17} = 0.10000000000000
or k_{17} = 1.00000000000000
or k_{17} = 10.0000000000000
or k_{17} = 100.000000000000

Initial concentration
[*nr*] = 0.00000000000000
[*NR*] = 0.00000000000000
[NO_3^-] = 0.00000000000000
[NO_2^-] = 0.00000000000000
[NH_4^+] = 0.00000000000000
[*Gln*] = 0.00000000000000
[*NMR*] = 0.000000000000000
[*NIT24*] = 0.200000000000000
[*NMR·NIT24*] = 0.000000000000000
[E_{set}] = 10.00000000000000
[$NR{\cdot}E_{set}$] = 10.00000000000000

The parameter values leading to Figure 4.40:

Rate constant
k_1 = 0.50000000000000
k_2 = 1.00000000000000
k_3 = 22.0000000000000
k_4 = 95.5000000000000
k_5 = 1.00000000000000
k_6 = 1.10000000000000
k_7 = 0.00000000000000
k_8 = 0.10000000000000
or k_8 = 0.40000000000000
or k_8 = 0.70000000000000
or k_8 = 1.00000000000000
k_9 = 5.78750000000000
k_{10} = 1.00000000000000×10^{-2}
k_{11} = 8.00000000000000
k_{12} = 1.50000000000000
k_{13} = 1.00000000000000×10^{-4}
k_{14} = 1.90000000000000
k_{15} = 1.00000000000000
k_{16} = 10.0000000000000

Initial concentration
[*nr*] = 6.00010634825910
[*NR*] = 16.9281299719988
[NO_3^-] = 2.414898498274519×10^{-2}
[NO_2^-] = 8.00173681435889
[NH_4^+] = 7.27908433914891
[*Gln*] = 4.21706880611559
[*NMR*] = 0.000000000000000
[*NIT24*] = 1.472925440366243×10^{-2}
[*NMR*·*NIT24*] = 0.00000000000000

The parameter values leading to Figure 4.41 (a)(b)(c):

Rate constant
k_0 = 0.50000000000000
k_2 = 1.00000000000000
k_3 = 22.0000000000000 (ref)
or k_3 = 33.0000000000000
k_4 = 95.5000000000000
k_5 = 1.00000000000000
k_6 = 1.10000000000000
k_7 = 0.00000000000000
k_8 = 5.00000000000000
k_9 = 5.78750000000000
k_{10} = 1.00000000000000×10^{-2}
k_{11} = 8.00000000000000
k_{12} = 1.50000000000000
k_{13} = 1.00000000000000×10^{-4}
k_{14} = 1.90000000000000
k_{15} = 1.00000000000000
k_{16} = 10.0000000000000

The parameter values leading to Figure 4.41 (d)(e)(f):

Rate constant
k_0 = 0.50000000000000
k_2 = 1.00000000000000
k_3 = 22.0000000000000
k_4 = 45.5000000000000
or k_4 = 95.5000000000000 (ref)
k_5 = 1.00000000000000
k_6 = 1.10000000000000
k_7 = 0.00000000000000
k_8 = 5.00000000000000
k_9 = 5.78750000000000
k_{10} = 1.00000000000000×10^{-2}
k_{11} = 8.00000000000000
k_{12} = 1.50000000000000
k_{13} = 1.00000000000000×10^{-4}
k_{14} = 1.90000000000000
k_{15} = 1.00000000000000
k_{16} = 10.0000000000000

The data generating Figure 4.41 (g)(h)(i):

Rate constant
k_0 = 0.50000000000000
k_2 = 1.00000000000000
k_3 = 22.0000000000000
k_4 = 95.5000000000000
k_5 = 1.00000000000000
k_6 = 1.10000000000000
k_7 = 0.00000000000000
k_8 = 5.00000000000000
k_9 = 5.78750000000000
k_{10} = $1.00000000000000\times10^{-2}$
k_{11} = 8.00000000000000 (ref)
or k_{11} = 12.0000000000000
k_{12} = 1.50000000000000
k_{13} = $1.00000000000000\times10^{-4}$
k_{14} = 1.90000000000000
k_{15} = 1.00000000000000
k_{16} = 10.0000000000000

The parameter values leading to Figure 4.42 (a)(b)(c):

Rate constant
k_0 = 0.50000000000000 (ref)
or k_0 = 0.60000000000000
k_2 = 1.00000000000000
k_3 = 22.0000000000000
k_4 = 95.5000000000000
k_5 = 1.00000000000000
k_6 = 1.10000000000000
k_7 = 0.00000000000000
k_8 = 5.00000000000000
k_9 = 5.78750000000000
k_{10} = $1.00000000000000\times10^{-2}$
k_{11} = 8.00000000000000
k_{12} = 1.50000000000000
k_{13} = $1.00000000000000\times10^{-4}$
k_{14} = 1.90000000000000
k_{15} = 1.00000000000000
k_{16} = 10.0000000000000

The parameter values leading to Figure 4.42 (d)(e)(f):

Rate constant
k_0 = 0.50000000000000
k_2 = 1.00000000000000 (ref)
or k_2 = 1.20000000000000
k_3 = 22.0000000000000
k_4 = 95.5000000000000
k_5 = 1.00000000000000
k_6 = 1.10000000000000
k_7 = 0.00000000000000
k_8 = 5.00000000000000
k_9 = 5.78750000000000
k_{10} = $1.00000000000000\times10^{-2}$
k_{11} = 8.00000000000000
k_{12} = 1.50000000000000
k_{13} = $1.00000000000000\times10^{-4}$
k_{14} = 1.90000000000000
k_{15} = 1.00000000000000
k_{16} = 10.0000000000000

The parameter values leading to Figure 4.42 (g)(h)(i):

Rate constant
k_0 = 0.50000000000000
k_2 = 1.00000000000000
k_3 = 22.0000000000000
k_4 = 95.5000000000000
k_5 = 1.00000000000000
k_6 = 1.10000000000000
k_7 = 0.00000000000000
k_8 = 3.00000000000000
or k_8 = 5.00000000000000 (ref)
k_9 = 5.78750000000000
k_{10} = 1.00000000000000×10^{-2}
k_{11} = 8.00000000000000
k_{12} = 1.50000000000000
k_{13} = 1.00000000000000×10^{-4}
k_{14} = 1.90000000000000
k_{15} = 1.00000000000000
k_{16} = 10.0000000000000

The parameter values leading to Figure 4.42 (j)(k)(l):

Rate constant
k_0 = 0.50000000000000
k_2 = 1.00000000000000
k_3 = 22.0000000000000
k_4 = 95.5000000000000
k_5 = 1.00000000000000
k_6 = 1.10000000000000
k_7 = 0.00000000000000
k_8 = 5.00000000000000
k_9 = 5.78750000000000 (ref)
or k_9 = 7.78750000000000
k_{10} = 1.00000000000000×10^{-2}
k_{11} = 8.00000000000000
k_{12} = 1.50000000000000
k_{13} = 1.00000000000000×10^{-4}
k_{14} = 1.90000000000000
k_{15} = 1.00000000000000
k_{16} = 10.0000000000000

The initial concentration leading to Figure 4.41 and 4.42 are based on the same condition:
[*nr*] = 6.04463966075566
[*NR*] = 1.26987129850828
[NO_3^-] = 60.3985502192925
[NO_2^-] = 8.29620853403252
[NH_4^+] = 6.19092634979609
[*Gln*] = 3.33098524095421
[*NMR*] = 0.000000000000000
[*NIT24*] = 1.472925440366243×10^{-2}
[*NMR·NIT24*] = 0.000000000000000

(This reference condition is refer to the data set k_0 = 0.5, k_2 = 1.0, k_3 = 22.0, k_4 = 95.5, k_8 =5.0, k_9=5.7875, k_{11} = 8.0. When one of these rate constants is changed, a new oscillation is generated. Through extending the simulation time and putting the final concentration got from the last calculation as the initial concentration of the current one, stable oscillation can be obtained)

The parameter values leading to Figure 4.44:

Rate constant
k_1 = 1.00000000000000
k_2 = 1.00000000000000
k_3 = 2.00000000000000
k_4 = 6.00000000000000
k_5 = 10.0000000000000
k_6 = 1.00000000000000
k_7 = 0.00000000000000
k_8 = 60.0000000000000
k_9 = 1.55000000000000
k_{10} = 0.25000000000000
k_{11} = 8.00000000000000
(k_{12} and k_{13} are not included in the program here, which will not affect the result)

Initial concentration

when $[E_{set}]_{tot}$ = 20.0
$[nr]$ = 5.61220553818555
$[NR]$ = 0.898077917540093
$[NO_3^-]$ = 6.77683843624619
$[NR \cdot NO_3^-]$ = 0.743767579234977
$[NO_2^-]$ = 6.76844391411598
$[E_{set}]$ = 0.650159419046311
$[NR \cdot E_{set}]$ = 19.3498405809534

when $[E_{set}]_{tot}$ = 70.0
$[nr]$ = 21.0065356341892
$[NR]$ = 0.217193319755617
$[NO_3^-]$ = 24.4138872593054
$[NR \cdot NO_3^-]$ = 0.634850102797655
$[NO_2^-]$ = 4.39755363565126
$[E_{set}]$ = 8.84080735104096
$[NR \cdot E_{set}]$ = 61.1591926489570

The parameter values leading to Figure 4.45:

Rate constant

k_1 = 0.50000000000000
k_2 = 1.00000000000000
k_3 = 22.0000000000000
k_4 = 95.5000000000000
k_5 = 1.00000000000000
k_6 = 1.10000000000000
k_7 = 0.00000000000000 (*nmr* mutant)
or k_7 = 1.00000000000000 (wild type)
k_8 = $5.00000000000000 \times 10^{-2}$
k_9 = 5.78750000000000
k_{10} = $1.00000000000000 \times 10^{-2}$
k_{11} = 8.00000000000000
k_{12} = 1.50000000000000
k_{13} = 1.00000000000000
k_{14} = 1.90000000000000
k_{15} = 1.00000000000000
k_{16} = 10.0000000000000

Initial concentration

$[nr]$ = 0.00000000000000
$[NR]$ = 0.00000000000000
$[NO_3^-]$ = 0.00000000000000
$[NO_2^-]$ = 0.00000000000000
$[NH_4^+]$ = 0.00000000000000
$[Gln]$ = 0.00000000000000
$[NMR]$ = 0.000000000000000
$[NIT24]$ = 0.20000000000000
$[NMR \cdot NIT24]$ = 0.000000000000000

The parameter values leading to Figure 4.46, 4.47 (they are done at the same time):

Rate constant
k_0 = 2.50000000000000
k_2 = 1.00000000000000
k_3 = 22.0000000000000
k_4 = 95.5000000000000
k_5 = 1.00000000000000
k_6 = 1.10000000000000
k_7 = 0.00000000000000
or k_7 = 1.00000000000000
or k_7 = 2.00000000000000
or k_7 = 3.00000000000000
k_8 = 3.00000000000000
k_9 = 5.78750000000000
k_{10} = 1.00000000000000×10^{-2}
k_{11} = 8.00000000000000
k_{12} = 1.50000000000000
k_{13} = 1.00000000000000×10^{-2}
k_{14} = 1.90000000000000
k_{15} = 1.00000000000000
k_{16} = 10.0000000000000

Initial concentration
[*nr*] = 5.14012482062873
[*NR*] = 1.53277707430467
[NO_3^-] = 50.7031481406050
[NO_2^-] = 13.1483714402261
[NH_4^+] = 10.8944945851868
[*Gln*] = 5.64887856853552
[*NMR*] = 0.000000000000000
[*NIT24*] = 1.431569254068703×10^{-2}
[*NMR*·*NIT24*] = 0.000000000000000

The parameter values leading to Table 4.1:

Rate constant
k_1 = 0.10000000000000
k_2 = 1.00000000000000
k_3 = 22.0000000000000
k_4 = 1.10000000000000
k_5 = 1.00000000000000
k_6 = 1.10000000000000
k_7 = 0.00000000000000
k_8 = 5.00000000000000×10^{-2}
k_9 = 10.0000000000000
or k_9 = 1.00000000000000×10^2
or k_9 = 10.0000000000000×10^3
or k_9 = 10.0000000000000×10^4
or k_9 = 10.0000000000000×10^5
or k_9 = 10.0000000000000×10^6
or k_9 = 10.0000000000000×10^7
or k_9 = 10.0000000000000×10^8
k_{10} = 0.50000000000000
k_{11} = 0.50000000000000
k_{12} = 1.50000000000000
k_{13} = 0.20000000000000
k_{14} = 1.90000000000000
k_{15} = 1.00000000000000
k_{16} = 10.0000000000000
k_{17} = 10.0000000000000

Initial concentration
[*NIT24*] = 0.20000000000000
$[E_{set}]_{tot}$ = 11.5750000000000

The parameter values leading to Table 4.2:

The reference condition:
Rate constant

k_0 = 0.50000000000000
k_2 = 1.00000000000000
k_3 = 22.0000000000000
k_4 = 1.10000000000000
k_5 = 1.00000000000000
k_6 = 1.10000000000000
k_7 = 0.00000000000000
k_8 = $5.00000000000000\times10^{-2}$
k_9 = 5.78750000000000
k_{10} = $1.00000000000000\times10^{-2}$
k_{11} = 8.00000000000000
k_{12} = 1.50000000000000
k_{13} = $1.00000000000000\times10^{-4}$
k_{14} = 1.90000000000000
k_{15} = 1.00000000000000
k_{16} = 10.0000000000000

Initial concentration
[*NIT24*] = $1.472925440366243\times10^{-2}$
The parameter values leading to Table 4.3:

The reference condition:
Rate constant

k_0 = 0.50000000000000
k_2 = 1.00000000000000
k_3 = 22.0000000000000
k_4 = 1.10000000000000
k_5 = 1.00000000000000
k_6 = 1.10000000000000
k_7 = 0.00000000000000
k_8 = $5.00000000000000\times10^{-2}$
k_9 = 5.78750000000000
k_{10} = $1.00000000000000\times10^{-2}$
k_{11} = 8.00000000000000
k_{12} = 1.50000000000000
k_{13} = 0.20000000000000
k_{14} = 1.90000000000000
k_{15} = 1.00000000000000
k_{16} = 10.0000000000000

Initial concentration
[*NIT24*] = 0.20000000000000

The parameter values leading to Table 4.4:

The reference condition:
Rate constant

k_0 = 1.00000000000000
k_2 = 1.00000000000000
k_3 = 20.0000000000000
k_4 = 50.0000000000000
k_5 = 1.00000000000000
k_6 = 1.10000000000000
k_7 = 0.00000000000000
k_8 = 5.00000000000000
k_9 = 5.00000000000000
k_{10} = 1.00000000000000
k_{11} = 8.00000000000000
k_{12} = 1.00000000000000
k_{13} = 0.20000000000000
k_{14} = 1.00000000000000
k_{15} = 1.00000000000000
k_{16} = 10.0000000000000

Initial concentration
[*nr*] = 0.000000000000000
[*NR*] = 0.000000000000000
[NO_3^-] = 0.000000000000000
[NO_2^-] = 0.000000000000000
[NH_4^+] = 0.000000000000000
[*Gln*] = 0.000000000000000
[*NMR*] = 0.000000000000000
[*NIT24*] = 0.200000000000000
[*NMR·NIT24*] = 0.000000000000000

The parameter values leading to Table 4.5:

The reference condition:
Rate constant
k_0 = 2.50000000000000
k_2 = 1.00000000000000
k_3 = 22.0000000000000
k_4 = 95.5000000000000
k_5 = 1.00000000000000
k_6 = 1.10000000000000
k_7 = 5.00000000000000
k_8 = 3.00000000000000
k_9 = 5.78750000000000
k_{10} = $1.00000000000000\times10^{-2}$
k_{11} = 8.00000000000000
k_{12} = 1.50000000000000
k_{13} = $1.00000000000000\times10^{-2}$
k_{14} = 1.90000000000000
k_{15} = 1.00000000000000
k_{16} = 10.0000000000000

Initial concentration
[*NIT24*] = $7.89183494592240\times10^{-3}$
[*NMR·NIT24*] = $6.423862046095593\times10^{-3}$

In Table 4.1, 4.2, 4.3 and 4.5, so as to determine the period length in oscillation mode, we need to put the final concentrations of every variable obtained from the last calculation as a new set of initial concentration. Repeating the process is helpful to get an accurate period length. It is a heavy assignment to repeat every calculation by this method for several times. Listing the concentrations used in one given calculation is not necessary since this set of concentration is always not the “best” one. For the sake of simplicity, when exhibiting the data for the generation of Table 4.1, 4.2, 4.3 and 4.5,. I only give the concentration of those variables whose variation can give a different result and the reason for causing such a difference is nothing to do with the “concentration repeating” process.

List of Figures

List of Tables

References

1. Redinbaugh, M. G., and Campbell, W. H. 1991. Higher plant responses to environmental nitrate. ***Physiologia Plantarum*** 82:640–650.
2. Crawford, N. M., 1995. Nitrate: nutrient and signal for plant growth. ***Plant Cell*** 7:859–868.
3. Miller, A. J., Fan, X. R., Orsel, M., Smith, S. J., Wells, D. M. 2007. Nitrate transport and signalling. ***Journal of Experimental Botany*** 58:2297–2306.
4. Crawford, N. M., Glass, A. D. M. 1998. Molecular and physiological aspects of nitrate uptake in plants. ***Trends in Plant Science*** 3:389–395.
5. Lillo, C., 2008. Signalling cascades integrating light-enhanced nitrate metabolism. ***Biochemical Journal*** 415:11–19.
6. Krouk, G., Crawford, N. M., Coruzzi, G. M., Tsay, Y. F. 2010. Nitrate signaling: adaptation to fluctuating environments. ***Current Opinion in Plant Biology*** 13: 266–273.
7. Dechorgnat, J., Nguyen, C. T., Armengaud, P., Jossier, M., Diatloff, E., Filleur, S., Daniel-Vedele, F. 2010. From the soil to the seeds: the long journey of nitrate in plants. ***Journal of Experimental Botany*** 62: 1349–1359.
8. Miller, A. J., Cookson, S. J., Smith, S. J., Wells, D. M. 2001. The use of microelectrodes to investigate compartmentation and the transport of metabolized inorganic ions in plants. ***Journal of Experimental Botany*** 52:541–549.
9. Miller, A. J., and Smith, S. J. 2008. Cytosolic nitrate ion homeostasis: could it have a role in sensing nitrogen status? ***Annals of Botany*** 101:485–489.
10. Van der Leij, M., Smith, S. J. and Miller, A. J. 1998. Remobilisation of vacuolar stored nitrate in barley root cells. ***Planta*** 205:64–72.
11. Jia, L. J., Fan, X. R., Yin, X. M., Cao, Y., Shen. Q. R., 2005. Remobilisation of nitrate in rice leaf vacuoles measured with double-barrelled nitrate-selective microelectrodes. ***Scientia Agricultura Sinica*** 38:1379–1385.
12. Fan, X. R., Jia, L. J., Li, Y. L., Smith, S. J., Miller, A. J., Shen, Q. R. 2007. Comparing nitrate storage and remobilization in two rice cultivars that differ in their nitrogen use efficiency. ***Journal of Experimental Botany*** 58:1729–40.
13. Aslam, M., Travis, R. L., Rains, D. W. 1996. Evidence for Substrate lnduction of a Nitrate Efflux System in Barley Roots. ***Plant Physiology*** 112: 1167–1175.
14. Segonzac, C., Boyer, J. C., Ipotesi, E., Szponarski, W., Tillard, P., Touraine, B., Sommerer, N., Rossignol, M., Gibrat, R. 2007. Nitrate efflux at the root plasma membrane: identification of an Arabidopsis excretion transporter. ***Plant Cell*** 19:3760–77.
15. Schumaker, K. S., Sze, H. 1987. Decrease of pH Gradients in Tonoplast Vesicles by NO_3^- and Cl^-: Evidence for H^+-Coupled Anion Transport. ***Plant Physiology*** 83:490–496.
16. Miller, A. J., Smith, S. J. 1992. The mechanism of nitrate transport across the tonoplast of barley root cells. ***Planta*** 187:554–557.
17. Harada, H., Kuromori, T., Hirayama, T., Shinozaki, K., Leigh, R. A. 2004. Quantitative trait loci analysis of nitrate storage in *Arabidopsis* leading to an investigation of the contribution of the anion channel gene, *AtCLC-c*, to variation in nitrate levels. ***Journal of Experimental Botany*** 55:2005–2014.
18. De Angeli, A., Monachello, D., Ephritikhine, G., Frachisse, J. M., Thomine, S., Gambale, F., Barbier-Brygoo, H. 2006. The nitrate/proton antiporter AtCLCa mediates nitrate accumulation in plant vacuoles. ***Nature*** 442:939–942.
19. Zifarelli, G., Pusch, M. 2010. CLC transport proteins in plants. ***FEBS Letteers*** 584:2122–2127.
20. Schumacher, K., Krebs, M. 2010. The V-ATPase: small cargo, large effects. ***Current Opinion in Plant Biology*** 13:724–730.
21. Krebs, M., Beyhl, D., Gorlich, E., Al-Rasheid, K. A. S., Marten, I., Stierhof, Y. D., Hedrich, R., Schumacher, K. 2010. *Arabidopsis* V-ATPase activity at the tonoplast is required for

efficient nutrient storage but not for sodium accumulation. ***Proceedings of the National Academy Sciences of the United States of America*** 107:3251–3256.
22. Yang, Z. J. And David, J. M. 2005. A Model for the Circadian Oscillations in Expression and Activity of Nitrate Reductase in Higher Plants. ***Annals of Planta*** 96: 1019–1026.
23. Bijlsma, R. J., Lambers, H. and Kooijman, S. A. L. M. 2000. A dynamic whole-plant model of integrated metabolism of nitrogen and carbon. 1. Comparative ecological implications of ammonium-nitrate interactions. ***Plant and Soil*** 220: 49–69.
24. Rufty, T. W., Thomas, J. F., Remmler, J. L., Campbell, W. H., Volk, R. J. 1986. Intercellular localization of nitrate reductase in roots. ***Plant Physiology*** 82:675–680.
25. Unkles, S. E., Wang, R. C., Wang, Y., Glass, A. D. M., Crawford, N. M., Kinghorn, J. R. 2004. Nitrate reductase activity is required for nitrate uptake into fungal but not plant cells. ***Journal of Biological Chemistry*** 279:28182–28186.
26. Lillo, C., Meyer, C. and Ruoff, P. 2001. The nitrate reductase circadian system. The central clock dogma contra multiple oscillatory feedback loops. ***Plant Physiology*** 125: 1544–1557.
27. Stitt, M., Müller, C., Matt, P., Gibon, Y., Carillo, P., Morcuenda, R., Scheible, W. R. and Krapp, A. 2002. Steps towards an integrated view of nitrogen metabolism. ***Journal of Experimental Botany*** 53: 959–970.
28. Scheible, W. R., Gonzlez-Fontes, A., Morcuende, R., Lauerer, M., Geiger, M., Glaab, J., Gojon, A., Schulze, E. D. and Stitt, M. 1997. Tabacco mutants with a decreased number of functional *nia* genes compensate by modifying the diurnal regulation of transcription, post-translational modification and turnover of nitrate reductase. ***Planta*** 203: 304–319.
29. Geiger, M., Walch-Lin, P., Engels, C., Harnecker, J., Schulze, E. D., Ludewig, F., Sonnewald, U., Scheible, W. R. and Stitt, M. 1998. Enhacned carbon dioxide leads to a modified diurnal rhythm of nitrate reductase activity in older plants, and a large stimulation of nitrate reductase activity and higher levels of amino acids in young tobacco plants. ***Plant, Cell and Environmen*** 21: 253–268.
30. Matt, P., Geiger, M., Walch-Liu, P., Engels, C., Krapp, A. and Stitt, M. 2001. The immediate cause of the diurnal changes of nitrogen metabolism in leaves of nitrate-replete tobacco: a major imbalance between the rate of nitrate reduction and the rates of nitrate uptake and ammonium metabolism during the first part of the light period. ***Plant, Cell and Environment*** 24: 177–190.
31. Marzluf, G. A., 1997. Genetic regulation of nitrogen metabolism in the fungi. ***Microbiology and Molecular Biology Reviews*** 61: 17–32.
32. Christensen, M. K., Falkeid, G., Falkeid, G., Loros, J. J., Dunlap, J. C., Lillo, C. and Ruoff, P., 2004. A Nitrate-Induced *frq*-Less Oscillator in *Neurospora crassa*. ***Journal of Biological Rhythms*** 19: 280–286.
33. Jolma, I. W., Laerum. O. D., Lillo, C and Ruoff, P., 2010. Circadian oscillators in eukaryotes. ***Wiley Interdisciplinary Reviews: Systems Biology and Medicine*** 2: 533–549.
34. Fu, Y. H., Kneesi, J. Y., Marzluf, G. A. Isolation of *nit-4*, the minor nitrogen regulatory gene which mediates nitrate induction in *Neurospora crassa*. ***Journal of Bacteriology*** 171: 4067–4070.
35. Burger, G., Strauss, J., Scanocchio, C. 1991. Molecular cloning and functional-characterization of the pathway-specific regulatory gene *nirA*, which controls nitrate assimilation in *Aspergillus nidulans*. ***Molecular and Cellular Biology*** 11: 795–802.
36. Burger, G., Strauss, J., Scanocchio, C., Lang, B. F. 1991. *nirA*, the pathway-specific regulatory gene of nitrate assimilation in *Aspergillus nidulans*, encodes a putative GAL4-type zinc finger protein and contains four introns in highly conserved regions. ***Molecular and Cellular Biology*** 11: 5746–5755.
37. Fu, Y. H., Marzluf, G. A. 1990. *nit-2*, the major nitrogen regulatory gene of *Neutuspora crassa*, encodes a protein with a putative zinc finger DNA-binding domain. ***Molecular and Cellular Biology*** 10: 1056–1065.
38. Fu, Y. H. and Marzluf, G. A. 1990. *nit-2*, the major positive-acting nitrogen regulatory gene of

Neuropora crassa, encodes a sequence specific DNA-binding protein. ***Proceedings of the National Academy Sciences of the United States of America*** 87: 5331–5335.

39. Kudla, B., Caddlck, M. X., Langdon, T., Martlnez-Roasl, N. M., Bennett, C. F., Slbley, S., Davies, R.W., Arst, H.N., Jr. 1990. The regulatory gene *areA* mediating nitrogen metabolite repression in *Aspergillus nidulans*: Mutations affecting specificity of gene activation alter a loop residue of a putative zinc finger. ***EMBO Journal*** 9: 1355–1364.
40. Xiao, X. D., Fu, Y. H. and Marzluf, G. A. 1995. The Negative-Acting *NMR* Regulatory Protein of *Neurospora crassa* Binds to and Inhibits the DNA-Binding Activity of the Positive-Acting Nitrogen Regulatory Protein *NIT2*. ***Biochemistry*** 34: 8861–8868.
41. Pan, H., Feng, B. and Marzluf, G. A. 1997. Two distinct protein-protein interactions between the *NIT2* and *NMR* regulatory proteins are required to eastablish nitrogen metabolite repression in *Neurospora crassa*. Molecular Microbiology 26: 721–729.
42. Stelling, J., Sauer, U., Szallasi, Z. and Doyle, F. J. and Doyle. J. 2004. Robustness of Cellular Functions. ***Cell*** 118: 675–685.
43. Kitano, H. 2007. Towards a theory of biological robustness. ***Molecular Systems Biology*** 3: 1–7.
44. Lewis, F. L., 1992. Applied Optimal Control & Estimation. Prentice Hall, Englewood Cliffs, NJ.
45. Wilkie, J., Johnson, M., Reza, K. 2002. Control Engineering. An Introductory Course. Palgrave, New York.
46. Yi, T. M., Huang, Y., Simon, M. I., Doyle, J. 2000. Robust perfect adaptation in bacterial chemotaxis through integral feedback control. ***Proceedings of the National Academy Sciences of the United States of America*** 97:4649–4653.
47. Ni, X. Y., Drengstig, T. and Ruoff, P. 2009. The Control of the Controller: Molecular Mechanisms for Robust Perfect Adaptation and Temperature Compensation. ***Biophysical Journal*** 97: 1244–1253.
48. Jolma, I. W., Ni, X. Y., Jensen, K. J., Kjosmoen, T., Drengstig, T., Ruoff, P. 2011. Core topologies of homeostatic networks. ***Proceedings of the National Academy Sciences of the United States of America***, submitted.
49. Gao-Rubinelli, F. and Marzluf, G. A. 2004. Indentification and Characterization of a Nitrate Transporter Gene in *Neurospora crassa*. ***Biochemical Genetics*** 42: 21–34.
50. Blumwald, E. and Poole, R. J. 1986. Kinetics of Ca^{2+}/H^{+} Antiport in Isolated Tonoplast Vesicles from Storage Tissue of *Beta vulgaris* L. ***Plant Physiology*** 80: 772–731.
51. Kabala, K., Klobus, G. and Janicka-Russak, M. 2003. Nitrate transport across the tonoplast of *Cucumis sativus* L. root cells. ***Plant Physiology*** 160: 523–530.
52. Dunn-Coleman, N. S., Tomsett, A. B. and Garrett, R. H. 1981. The Regulation of Nitrate Assimilation in *Neurospora crassa*: Biochemical Analysis of the nmr-1 Mutants. ***Molecular and General Genetics*** 182: 234–239.